

ABSTRACT

Title of Thesis: SECOND WAVE MECHANICS

Anthony Fabbri, Master of Science in Reliability
Engineering, 2024

Thesis Directed By: Professor Jeffrey W. Herrmann, Dept. of
Mechanical Engineering

The COVID-19 pandemic experienced very well-documented "waves" of the virus's progression, which can be analyzed to predict future wave behavior. This thesis describes a data analysis algorithm for analyzing pandemic behavior and other, similar problems. This involves splitting the linear and sinusoidal elements of a pandemic in order to predict the behavior of future "waves" of infection from previous "waves" of infection, creating a very long-term prediction of a pandemic. Common wave shape patterns can also be identified, to predict the pattern of mutations that have recently occurred, but have not become popularly known as yet, to predict the remaining future outcome of the wave. By only considering the patterns in the data that could possibly have acted in tandem to generate the observed results, many false patterns can be eliminated, and, therefore, hidden variables can be estimated to a very high degree of probability. Similar mathematical relationships can reveal hidden variables in other underlying differential equations.

SECOND WAVE MECHANICS

by

Anthony Fabbri

Thesis submitted to the Faculty of the Graduate School of the
University of Maryland, College Park, in partial fulfillment
of the requirements for the degree of
Master of Science
2024

Advisory Committee:

Professor Jeffrey W. Herrmann (Chair)

Professor M. Coleman Miller

Associate Professor Yi Xu

Table of Contents

1. Introduction.....	1
1.1 Purpose	1
1.2 Overview	2
1.3 Use of covid-19 virus data	3
1.4 Outline	5
2. Prior work	6
2.1 Virology background	6
2.2 Flow method.....	8
2.3 Predator-prey model	9
2.4 Current CDC method.....	10
2.5 Chaotic methods	12
2.6 Next	14
3. Approach.....	16
3.1 Big picture	16
3.2 Similar Flow method	21
3.3 Similar Waves method	25
3.4 Reverse Chaos: Theory	30
3.5 Reverse Chaos: in use	32
3.6 Putting it together	34
3.7 Data cleaning.....	35
3.8 Experimental Procedure	35
4. Results	41
4.1 Similar Flow method	41
4.2 Similar Waves method	45
4.3 Reverse Chaos	48
4.4 What was learned?	52
5. Summary and conclusions, Similar work	54
5.1 Conclusions	54
5.2 Summary	55
5.3 Difficult Physics Simulations	58
5.4 Economic modeling	59
6. Code Appendix and References	63

List of Figures

Figure 1, $X(n+1) = R * \sin(X_n)$... Pg. 15

Figure 2, Pyramid of infectivity ... Pg. 15

Figure 3, Flowchart of method steps ... Pg. 16

Figure 4: New cases in DC and Virginia on a logarithmic scale. ... Pg. 43

Figure 5: New cases in New York City on a logarithmic scale, by week ... Pg. 45

Figure 6: New cases in New York City, including waves, on a log scale, by week ... Pg. 48

Figure 7: New cases in the entire USA on a logarithmic scale. Spikes occur of different amplitudes around weeks 50 and 100. Reverse spikes occur around weeks 50, 100, and 112 ... Pg. 49

Figure 8: Absolute value of error in new cases in the entire USA using all methodologies, in weeks of interpolating new data ... Pg. 52

List of Tables

Table 1, Arbitrary data used for flow example step-through ... Pg. 22

Table 2: The x vector coefficients from the state of Colorado ... Pg. 41

Table 3: Output of the computed wavelengths and amplitudes for arbitrary states ... Pg. 45

1. Introduction

1.1 PURPOSE

The problem of predicting the progress of epidemics has been studied, however much of the base numerical data underlying the actual real-world numbers can be missing, or contains junk data fabricated by intermediaries. This provides challenges that are not present in more theoretical mathematics. This thesis documents a way of overcoming this problem by measuring not only the data, but connections and correlations the data represents, and therefore maximizing the amount of useful actionable information that can be derived from the data, even in ultra-sparse or very noisy data sets.

A series of data points that begins $\{1, 2, 3, 4, 5, 6, 7\}$ does not gain much additional explanatory power by also then including data points $\{8, 9, 10\}$. The pattern recognition has been achieved, and increasing amounts of data do not necessarily lead to similarly increasing amounts of conceptual understanding of that data.

Pandemics, and other mathematical structures, have similar hidden variables which influence the underlying function, but are not directly obtainable from that function. Previous attempts to derive such 'paradigm variables,' or meta-variables, rely on numerical methods, statistical techniques, machine learning, and/ or Bayesian inference to estimate the values, where such values cannot be exactly calculated analytically. These methods frequently rely on intense computational calculation. However, such 'brute force' methods are wasteful, as they do not take into account that only some explanations for the data have any feasible likelihood of providing contributory power to the model. By first analyzing the data for such bottlenecks, the solution space can be greatly reduced beforehand, putting less burden on the later computational methods, especially by separating useful from non-useful information, before going through with the effort of deriving the non-useful information, which is especially useful for such noisy data sources.

Historically, the measurement of systems of flows has assumed some type of conservation law, implying a source or sink of some finite value, that can be depleted, consumed, or refilled. However,

some flows, such as pandemics, do not obey a conservation law; a second person getting sick does not somehow cause the first person to become less sick, so the flow of the pandemic is not conserved. This requires a different flow methodology than the classical differential equations involving water pipe flows, electrical current flows, traffic flow, and other systems that do obey a conservation law. While people move about, the general “contagiousness” of a population can vary wildly, for example during the winter, and cannot be tracked by calculating in-minus-out, as a conserved flow would.

This expands the solution set drastically. For example, an infinite number of sine waves of different amplitudes can be described that all have the same wavelength. Sine waves of that wavelength may be described by an amplitude of 5 or an amplitude of 1,000,000; the size of the amplitude of that source does not in this way necessarily aid in the measurement of that wavelength. If the size of multiple synchronous wave sources are completely unknown, such wavelengths would be difficult, if not impossible, to solve for analytically, using classical methods. New methods that economize on the obtainable information are necessary.

1.2 OVERVIEW

This thesis describes a brief introduction and summary background in the relevant points of virology and virus data retrieval. And how these new methods can be used to solve such a problem.

This work describes three methodologies operating in tandem to solve certain types of problems that have historically been difficult to solve. While prior works touch on portions of the three methods, by combining all three in tandem, each method can “gold mine” nuggets useful information units, in a vast field of nonuseful information. The different methodologies tend to find completely different units of information first, so by uniting all three methodologies simultaneously, most of the “essence” of the pandemic’s underlying function can be ascertained more elegantly. The methods are as follows: 1. the similar waves method, 2. The similar flow method, and 3. the reverse chaos method, each of which will be discussed in turn separately, and then unified into one algorithm. Further, this

describes previous attempts to solve similar problems mathematically, including the predator-prey model and previous flow methods, and what the current algorithm takes from these methods and where they diverge.

There is an emphasis of the wave behavior of the COVID-19 virus as a case study, which has a good conceptual model, as well as a great deal of numerical data documenting its spread; but these methodologies can also be used for other types of differential equations that behave in similar ways, such as physics simulations that include real-world noise, the propagation of pricing and consumer behavior data, tourism flow, and other nonconservative flows.

The COVID-19 virus's behavior occurs with a wave-like pattern. The number of infected people rises to some peak, and then declines to some trough, before rising in a second peak, and then declining in a second trough, etc. An instance of the virus stopping the decline, rising to an arbitrary peak, and then sliding down to the arbitrary trough as commonly termed a "second wave" of the virus, similar to parlance for ocean waves. As such, other terms used in waves can also be used, for example each individual wave instance has an amplitude, which is the height of the peak for that one wave instance. And a given wave instance has a wavelength, which is the time it takes to go from trough, to the peak, and then back to trough again. A single wave instance of one wavelength from trough to peak amplitude, back to trough will be called a single "wave" of the virus. A pandemic or outbreak, then, would consist of many waves. Note that the individual waves/wave instances will each have slightly different amplitudes and lengths of time, even if they occur in the same area.

1.3 USE OF COVID-19 VIRUS DATA

The COVID-19 virus's spread is exceptionally well-documented in several countries, to a very high degree of precision. The CDC in the United States, for example, has publicly available data sets for populations and sub-populations of various kinds, which provided a robust publicly-accessible data

source. The currently used data source is the CDC report of weekly COVID-19 infections by state or region. The regions the CDC tracked include the 50 States of the US, The District of Columbia as a 51st "state", New York City as its own region, and eight additional territories and principalities that are similarly tracked, forming a time-series data for all 60 regions that are so tracked by the CDC. This tracks the pandemic from the 1st week the pandemic was declared until the 173rd week when the pandemic was officially declared resolved.

Using this data, the virus's propagation can be analyzed to predict future wave behavior that would be in line with previous waves' behavior. Future waves statistically have features in common with past waves. In addition, sudden deviational wave shape shifts, that were later found to be the result of mutations, can be found embedded in real-time data to predict mutations that must have recently occurred, but have not yet become popularly known. This allows unearthing of hidden information, that can be used to predict the different future outcome of the wave as a result of this new information, even if the hidden information itself can not be known.

The basic idea of the analysis is being able to tell what hidden variables are present, and whether or not the variables are changing over time. If the shape function remains exactly the same, but the intensity factor changes dramatically after a known mutation, this provides further confidence in several derivative conclusions: For example, when the shape itself of the function is not changing as greatly, but the intensity factor is changing greatly, one can determine a value of the intensity factor that matches very well to the old data, and a higher intensity factor that matches very well to the new data; this allows information that is derived from the previous wave features to be applied to predictions of the next wave without having to explicitly calculate them. This can be seen as analogous to similar triangles in geometry; by maintaining such a two-system correlation, this allows each cross-correlation to inform, but not contaminate the results of, the other. Additionally, good-quality leading indicators, for example of a mutation, can be used to predict with good accuracy indicators of a new infection.

1.4 OUTLINE

Chapter 2 describes previous work in virology and in epidemiology, as well as the conceptual basis for later improvements. Chapter 3 discusses the logic and algorithms of a new method that can predict sudden changes in outbreaks with far less time-series data than previous methods, allowing problems to be discovered much earlier in the chain. Chapter 4 discusses actual results with current COVID-19 data at the CDC. Chapter 5 discusses uses of the method with other types of ultra-sparse problems such as physics simulations, or adversarial math problems where noise has been introduced, such as pricing data; for example, gas prices are “contagious” to other, nearby gas stations. And customer service improves when a nearby competitor drastically increases its customer service.

2. Prior work

2.1 VIROLOGY BACKGROUND

Under the prevailing Viral Load theory of virus propagation [1], a given infection requires the presence of some approximate number of virite particles to achieve symptomatic infection. If a few virite particles slip into the body, the immune system has a high probability of destroying the virites before too much damage is done. However, if a “critical mass” beachhead is established by the virus, it is much more difficult for the body to prepare a response. Those with compromised immune systems and/or elderly persons thus have a lower viral load required, whereas young children can have a much higher viral load necessary, to achieve symptomatic infection.

The model of how much virus a person sheds to those around them is a function of the amount of virus present in the person, as well as the level of contact between that person has with other people. Those with a high number of virite particles tend to shed more virus, and those who interact frequently with another person tend to have a higher number of virus-shedding events with that other individual. This provides for a differential equation between the two individuals, or any other groups that the first individual happens to meet. However, the number of virite particles a person possesses at a particular time is not directly measurable. The fact that the person contains ANY virite particles only becomes revealed when the person starts showing symptoms and gets tested for the virus, having already exceeded the viral load threshold, when it is far too late to do anything about it.

In addition, the viral load ceiling to achieve symptomatic infection is, itself, always changing; as the person is further exposed to non-symptomatic numbers of virite particles. As the person experiences symptomless infection, the ceiling goes up slightly, depending upon the immune system of that one individual, the viral load that person currently possesses, and other factors outside of the experimenters' control. As the ceiling goes up, the "average" apparent breakthrough infection rate in society proportionally goes down, as fewer and fewer people now have a near-100% viral load rate,

due to the increasing ceiling required to achieve symptomatic infection. As the threshold is now much higher, their current viral load is no longer sufficient to achieve symptomatic infection, with the now-higher threshold. This provides a dampening effect on the visibility of the virus, even though the number of virites in circulation has not diminished. The result of this effect is a second-order differential equation; as the number of virites goes up, the number of virites needed to achieve visibility also goes up, so the number of apparent infections goes down, causing people to interact more, causing people to spread an even higher number of virite particles, which finally exceeds the new, higher threshold, causing the number of apparent infections to go up again. This explains the "wave" nature of the infection.

Additionally, the virus can suddenly, and unexpectedly, mutate, suddenly crashing the viral load threshold to a much, much lower value. This causes a large number of breakthrough cases to simultaneously suddenly become visibly emergent. Or, similarly, the virus can drastically increase the replication rate, leading to a similar outcome from the other direction, by more quickly achieving the current ceiling.

The time between outbreaks can tell us the "depth" of each wave in a locality, which tells us hidden variables, such as the number of virite particles a given sub-population must necessarily have as a fraction of threshold, regardless of what that threshold's value actually is; we can determine how much of the wavelength is being consumed per day. This predicts the time to next outbreak, and its severity, giving us access to previously invisible information. This also informs how much the population is shedding, which can give a good idea of what facilities should be open or closed in key places in the wave. Additionally, the long-term trends of the virus's waves tells us when the virus suddenly deviates, for example, during mutation. This provides for early notification of the mutation, before it becomes readily visible, and allows steps to be taken to mitigate and observe the new strain before the new strain becomes even more problematic, leading to advance notice of problems.

2.2 FLOW METHOD (PRECURSOR TO SIMILAR FLOW METHOD)

The flow method works for measuring non-conserved flows moving from one location to another to create a flow diagram of the flow of contagion from one node to another. There are numerous ways of measuring human contact and travel flows in this way, however, Schlundt et al. [7], teaches that zoonotic origins are the prime spreader in foodborne illnesses, which means that current methods that primarily track human contagion will not provide much insight when the primary contagion process is caused by animal-to-animal transmission, outside of observation. New methodologies are required to offset this.

Nohara et al. [2] teaches using an effective distance approach combined with time-to-onset for each graph node. This allows for correlation even among 'invisible' nodes, such as would be encountered for a zoonotic origin or contagion, as is described by Schlundt et al. [7]

Brockmann et al. [3] shows that a distance/correlation constant can be used to simplify the $n!$ graph edges, overcoming overcomplexity and allowing for a pulling of the actionable information out of the graph as a series of outward flow functions. Nodes with a high correlation to each other, but are separated in time, are likely logically nearby on the flow graph, but with several invisible nodes in between, taking up time in propagation delay.

Jacobs et al. [4] suggests that a node's flux can be exceptionally well documented by a number of biggest contributors. If there are n neighbor nodes, branches with flux much less than $1/n$ of the total flux are usually not applicable. The analogy is used that in electric circuits, "the smallest resistor is the biggest contributor to the current" [4]. This lowers the solution set significantly. In real life processes, the flow tends to be mostly determined by a few biggest contributors, and the remaining $n!$ nodes can safely be ignored.

Pastore et al. [5] shows that a least spanning tree can be used to parse out a path to the origin of contamination from a nodal network. This can be combined with the above references to form a back-in-time path, and extrapolate a forward-in-time path from a given snapshot state of the nodes.

Pinto et al. [6] describes accounting for invisible nodes along a flow trajectory. It does this by estimating a source, by sorting by propagation time, and then filling in invisible nodes, as needed.

The disadvantage of the previous methods is the assumption of burst behavior on the part of the virus; that the progression of the virus is monotonically increasing, and all the nodes gradually go from 0% virus to 100% virus over some period of time. However, long-term trends don't support this assumption. Even factoring in mutations, the relative prevalence of different strains go up and down several times over the course of several years, accounting for things such as population movement, local holidays, and seasonal variations. The downforce of virus must be accounted for along with upwards force in virus propagation.

2.3 PREDATOR-PREY MODEL (PRECURSOR TO SIMILAR WAVES)

The predator-prey model is a classic two-population model in differential equations: predator and prey. [9] A population of predators (Y) can be supported by a given population of prey (X). If the prey becomes more numerous, it can support more predators. If the population of prey becomes less numerous, it can now support a lower population of predators, putting a downward pressure on the predator population; for some constants C_1 , C_2 , time t :

$$Y'(t) = C_1 Y(t) + C_2 X(t) \quad 1$$

However, the new, lower population of predators catches less of the prey, causing more prey to escape and reproduce, causing the population of prey to rebound in the absence of predators; for some constants C_3 , C_4 , time t :

$$X'(t) = C_3 X(t) - C_4 Y(t) \quad 2$$

The new, higher population of prey can support a higher population of predators, leading the predators to also then rebound at a later time t , which, in turn, causes the population of prey to crash again. This combination forms a second-order differential equation. The population of prey is continuously rising and falling.

To determine the exact equation of the populations of predator and prey, a number of snapshots of the estimated predator and prey population are captured, and the values for $C_1, C_2, X(t=0)$ and $Y(t=0)$ can be solved for, using differential equations. However, this methodology requires knowing the populations of X and Y under consideration, and also doesn't account for predators or prey moving on to a different location not under observation. This type of methodology quickly breaks down when the number of unknowns drastically outnumber the amount of knowns. This makes it difficult to "mine" sparse data, or data that may contain erroneous entries.

2.4 CURRENT CDC METHOD

The CDC currently analyzes long-term virus propagation using R_0 and R_t . [10] R_t can also be notated as $R(t)$ as a function of t . The value R_0 represents, generally speaking, how many new people a given patient should infect. R_t is used similarly, but is a better estimate because it is time-varying, and therefore generally represents whether the population of infected is increasing or decreasing. The formula for the number infected at any given time is therefore a straightforward exponential of R_0 (or R_t) raised to the power of t , representing time; the Number infected N at time t , is therefore:

$$N(t) = R_0^t$$

3

While R_t makes for a really good paradigm variable, it necessarily limits the amount of information it can represent. The CDC also acknowledges that it is a trailing indicator, in that this

information only becomes evident after a given process has already completed. Whereas a more helpful function, such as the one being proposed, represents a leading indicator, which enables better predictive methodology of what is going to happen in the immediate future. It is an improvement to acknowledge not only that something has happened, but as a result of the new difference, exactly what new changes will occur, as a consequence.

During the COVID-19 pandemic, many other models were experimented on to attempt to determine a long-range planning model. However, the further out from the training data the models went, the more wildly divergent they became. "some early models predicted millions of deaths during the first few months in the United States ... while others expected an end to the pandemic by May 2020" (Rahmandad et al.) [18]. Further, Cramer et al. [16] describe a "naive baseline" with which to compare models. In this study, only a single, complex ensemble model performed better than the naive baseline in all such cases. Cramer additionally discusses other problems the further out from the training data a prediction attempts to infer, leaving most of the models incapable of predicting a great degree of time in one go, instead continuously updating with recent data to get predictions distant in time by slowly catching up to them. The naïve baseline in Cramer was the predicted number of reported deaths in the next week is equal to the number of reported deaths in the previous week. Similarly, in the current study, the number of reported cases' naïve baseline is based on a function of the number of expected cases in the previous week. This similar naïve baseline prediction, for comparison, is being made using the CDC's methodology of R_0^t by taking the number of infected in the previous week times R_0 , taking the number of infected in the training data and interpolating it forward in time. This creates an exponential growth, which registers as a line on a logarithmic plot. This created an empirical $R(t=53)$ for each state, and a sum combined $R(t=53)$ for the USA as a whole, and interpolates it forward using R_0^t . This baseline is compared to the new methodologies in a manner similar to the CDC comparison. Using the current $R(53)$ data for reference, the R_0 is determined to be

1.005 per week, extended forward in time from week 53's value $R(53)$, multiplying this value by 1.005 every week forward after this time.

2.5 CHAOTIC METHODS

Many systems in nature are Chaotic, for example the famous Mandelbrot set, and other fractally-nested problems. A sine wave can be nested within another sine wave, creating Beat Notes. That second sine wave can then be nested within a third, fourth, etc. indefinitely. For example, the following equation (See figure 1 for plot) iterates the next step by taking a Rate of growth R times the sine of the previous iteration. For a rate of growth R (especially with $R > \pi$) :

4

$$X_{(n+1)} = R * \sin(X_n)$$

Nested sine waves must inherit some of the properties of the parent sine waves, regardless of the viewing scale; for example, the ratio of the second to the third is the same as the ratio of the third to the fourth; the ratio of the 1st and 10th is necessarily the same as the 10th and 19th, by the properties of logarithms. The use of such nested fractals is already well understood, even if difficult to decode. [8]

A solving methodology commonly used to break very strong encryption problems is the use of Rainbow Tables, [19] discussed next. In a strongly one-way encryption algorithm or hash function, a problem that is easy to solve one way but difficult to reverse is used, for example multiplying two numbers is trivial, however factoring large numbers is numerically difficult by brute force. If a hash method is sufficiently punishing to reverse, it would be easier to perform multiple iterations of the original, easy function. For example, encryption of the number 1, then the number 2, then 3, ... through one million, using the easy half of the one-way function, and outputting the results in a table of the hashes of the first million integers, called a Rainbow Table. Then, the target's encrypted traffic is

scanned over a large period of time. If any of the transmitted numbers provided by the scanned target match any of the hashed numbers in the Rainbow Table, the original key that was used to encrypt that message might be revealed.

For example, say 65 hashed to 1,234,567,890,123,456,789. Reversing the function of such a huge number back to 65 might be nearly impossible. However, that very long number would appear in our Rainbow Table as $f(65) = 1,234,567,890,123,456,789$, right between $f(64)$ and $f(66)$. Then, at a later time, if the number “1,234,567,890,123,456,789” is observed in a target, one can recognize the values from the table, and realize the original password, before encryption, was “65”. This is commonly how very unsecure passwords are mined from exposed password databases, even if the passwords were stored in an encrypted format.

One can make a similar Rainbow Table for the nested sine waves, knowing that below the resolution of the current scale of observation, the underlying mini-waves must be following the same pattern as the ones under observation by the rules of logarithms, above. One can then find the chaotic value of the function by using the Rainbow Table previously calculated for the coarsest level of precision, then adding to this a multiple of the logarithm of the next closest level of precision, and repeating to the desired level of precision. This is similar to how long division divides, for example $1/7$ by first dividing by 10 and finding the next level of precision to the first numeral after the decimal point, (1) then dividing by 10 (30) and using a multiplication table to get the next numeral after the decimal point (4, because $4*7=28$), then dividing by 10 and getting the next numeral (20, and $2*7 = 14$) and so forth to a desired level of precision. Similarly, one can solve a fractal wave to an arbitrary level of precision by finding the outermost wave, and then the next outermost wave, and then so forth to an arbitrary level of precision. After all, any estimation of an outbreak wave on a ridiculously fine resolution, say from a second-to-second basis, is below the threshold of observation and is likely empirically meaningless.

This process is more numerically-based than the other two, rather than being as empirically based. Snapshots of all of the waves can be compared for key features, which can, in other embodiments, include machine learning. The first, second, and third derivatives of the running average can be analyzed as features to determine whether hidden patterns can be found that affect the remainder of the wave, forming a table of new, unexpected paradigm variables of the form ‘when X is observed to happen, Y is also observed to happen’. A given wave can be divided into a number of wavelets, wherein each wavelet’s behavior predicts certain aspects of the behavior of the remainder of the wave.

Validation is critical to this method because spurious correlations and machine hallucination is common. Even among human beings, superstitious behavior can easily arise when things happen around other things, by mere chance. However, sub-wavelet behavior that does predict future events can be analyzed, and the exact connection between the wavelet behavior and the future even can be registered and future events can be decomposed to a linear combination of the contributions of each sub-behavior. As each sub-behavior is deducted from the noisy whole, it is expected that future patterns might be found that are orthogonal to the current patterns, which can also be used to predict.

2.6 NEXT

Chapter 3 discusses how this method may be improved to predict sudden changes in outbreaks with far less time-series data than previous methods, allowing problems to be discovered earlier in time, and therefore reacted to, before the predicted consequences fully occur.

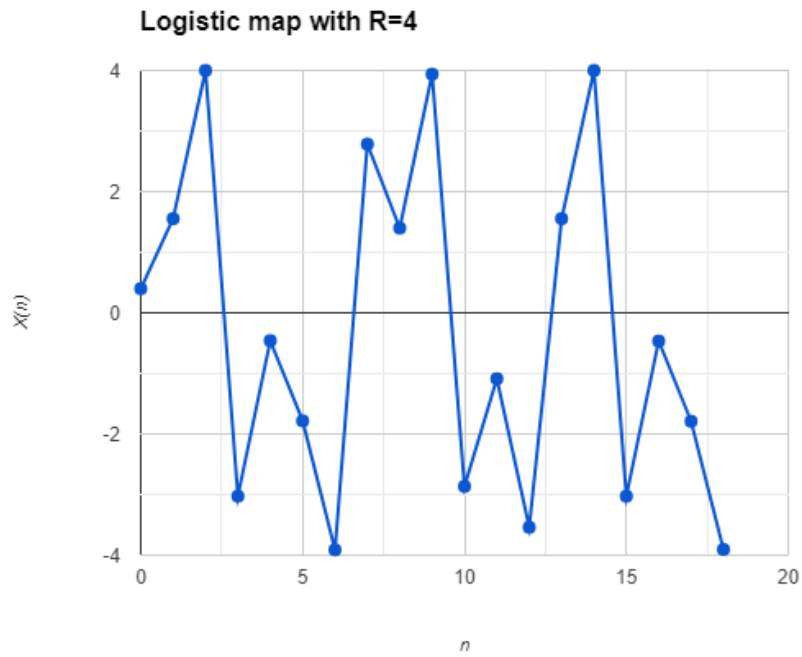


Figure 1, $X_{(n+1)} = R * \text{Sin}(X_n)$, (Note the nested wavelets inside a larger wave)

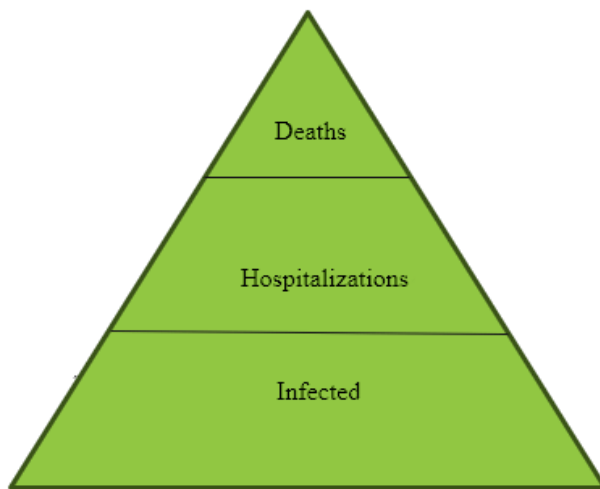


Figure 2, Pyramid of infectivity

3. Approach

3.1 BIG PICTURE

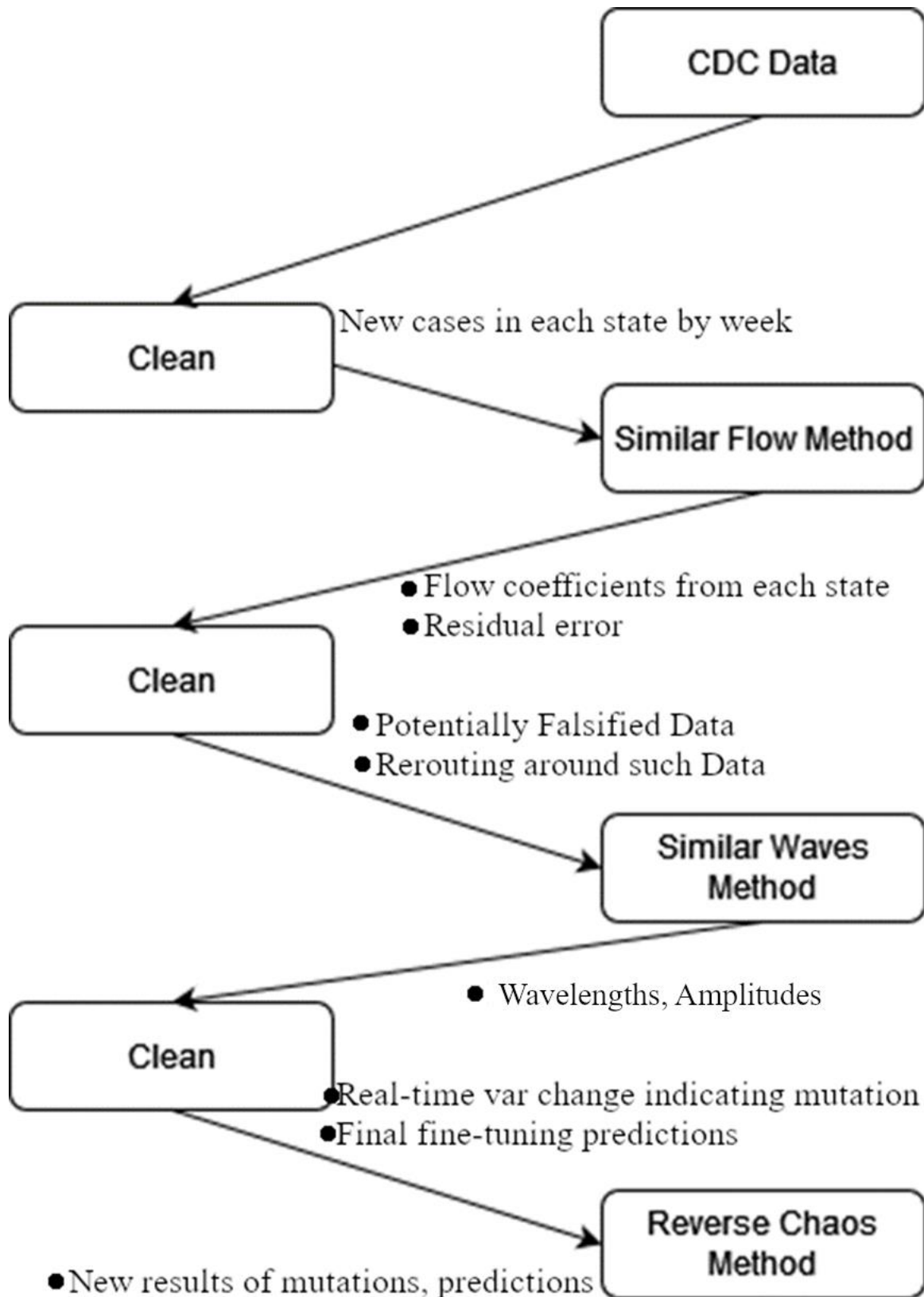


Figure 3, Flowchart of method steps

This algorithm evolves from an input data source (such as CDC data) to establish further data that is invisible from a single data measurement, by collating together several snapshots of data from the same locations over time, and several times at the same location. While random variation would, of course, cause each iteration of the wave to be slightly different, the shape of the wave, in general, should be similar, in many ways, from one wave to another, since they were caused by certain initial conditions. Therefore, we treat observations from the same place in multiple different waves as observations of a similar event. Additionally, we can gather observations from several different places at similar times as observations of what is occurring at that moment in time. This allows for interpolation of multiple dimensions of data. This can generate knowledge of movement through space vs. movement through time, which allows for the mapping of the “contagiousness” of an outbreak, and the overall orthogonality of the generic data.

Each state’s flow mechanics (in this case) is based on internal infection, with a modifier for importing of virus from the global society. Other methodologies presume infection increases to be a function of the current local or global infection rate, but that doesn’t take into account external infection “popping” a bubble of an uninfected city, sparking a local massive uptick at a given arbitrary time. It is the combination of multiple aspects of the method that lends its strength.

Figure 3 is a flowchart describing the overall procedure of the method. The CDC (Center for Disease Control) has pandemic data available to a very high degree of precision. It has daily population and heat maps available for various states, cities, ethnic groups, and age partitions, telling us the number of documented, visible positive cases on a day-to-day basis. The current analysis is using time-series data from the 50 US states as well as Washington, DC to create a 51-element array. Additionally, the CDC added NYC as a 52nd "state", as well as 8 territories or regions, making 60 total locations. I added an additional trivial, fictional state of “Outside” to estimate inflow from the global

population in that step. This creates a time-series array with 61 location entries, and weekly data from each state for time entries.

First, trailing indicators can be used to verify the veracity of data from municipal agencies. For example, the "excess mortality" is a very unalterable measure of the disease's progression. One takes the number of deaths from any cause, whatsoever, in a community over several years running. Then, this 'average mortality' is subtracted from the mortality in that community that occurred during the pandemic. The result is the 'excess mortality' that is assumed to be caused by the pandemic. If one area, for example Florida, suddenly shows a quite large number of deaths simultaneously with a precisely zero reported covid rate, this provides a strong indicator that the numbers being reported by Florida have perhaps been massaged too heavily, and should be relied upon with lesser confidence than data from more verifiable sources. Especially for the first few iterations, only highly trusted data is used in the method. Optionally, less-trusted data can be used later to interpolate future results once the baseline values are discovered analytically. However, less-trusted data is preferably not used to derive those values as this could skew the analysis. Further description of the data cleaning and filtering protocol will be discussed in the relevant section. This limits the data under review to a smaller number of 'trusted' states along one axis, currently 51, and a number of entries representing weeks along the time axis, creating a 2-dimensional array. Further details of this cleaning of data are defined in section 3.7, below.

The data is first fed into the Similar Flow method discussed in section 3.2, next section. The Similar Flow method's algorithm is directed towards discovering the inflow of each state based upon the current values of all the other states at a given moment in time. The increase due to external contagion in a state is based not only on the neighboring states, but can also include one-time events, such as Mardi Gras, as well as the current infectivity of major population centers, such as New York City. The similar flow method aims to discover by how much a given state increases its infectivity by

including importing infection from the other states in a given time period. The internal flow data from the Similar Flow method can then be used in the next algorithm.

The Similar Flow method takes in the 2-dimensional array from the cleaning step. Each state has an amount of “contagiousness” assigned to every week, which is number of newly infected from one week. Those people, who caught the virus, received the virus from one of two sources: internal or external infection. If they received it from internal infection, the amount by which the infection has increased from the previous week should be roughly proportional to the contagiousness of that state, as it represents some function of the spread inter-among the state of people who were previously infected. If they have received it from external infection, that portion of new infection must have come from contagiousness of another state or from the “outside” state. (The Outside state simply means it has come from outside the system as it has been measured, whether from outside the US, a heretofore unobserved pocket inside the US, or from a noncompliant state whose data was removed from consideration.)

The Similar Flow method determines what fraction of the contagiousness comes from within the state, which should be based on the previous contagiousness of that particular state, and what fraction comes from other places, which is the portion which is not based on the previous contagiousness of that particular state, but should be based on the contagiousness of each of the other states and the Outside state. The Similar Flow method’s algorithm is set up to determine this partition, and thereby outputs a connected network graph that identifies the inward/outward flow between the various states, and from each state to itself; see section 3.2 for details on the algorithm.

The data from the first iteration of the Similar Flow method is then fed into a second algorithm, the Similar Waves method, that aims to show purely internal infection, independent of outward importation of infection. Recall the concept of the viral load ceiling upon which an individual shows symptomatic infection, creating a second-order differential equation, that can be solved for.

The resulting data points of purely internal infection, derived from the previous method, can be placed in a Markov Chain, differential equation solver, or other, similar methodology, for example using the Python programming language. This allows multiple waves to be evaluated for shape parameters and magnitude parameters, where the shape parameters should be similar between waves of the same virus in the same location, however magnitude parameters can be wildly divergent. By measuring the behavior of the virus under different types of stresses, an acceleration factor can be derived to determine that types of forces that determine the wavelength of the wave and the amplitude of the resulting wave under various historically-known initial conditions, and how they affect the shape of the wave. The exact algorithm for finding this differential equation is described in section 3.3, further below.

Additionally, this information would allow the determination of a given wave's new hidden variables, such as historical knowledge of a mutation, by recognizing the sudden change in shape very early in the wave, as soon as it occurs, using the Reverse Chaos method, mentioned in section 3.4, below. Once the new variables are determined, whether through Reverse Chaos or Similar Waves, the algorithm can thereby extrapolate the remainder of the wave. In addition, if the wave's behavior changes suddenly mid-wave, this provides new information that the underlying hidden variables have suddenly changed and what they might now be; for example, a mutation causing increased replication and/or evasion of the patients' immune systems. The new hidden variables will allow for a new interpolation of how the remainder of the wave will now play out, accounting for this mutation's change in parameters.

For example, a large increase in replication or evasion will both cause the wave's amplitude to increase, however if evasion lowers the inhibitory threshold, the change becomes more obvious sooner, and makes changes to the wavelength that may cause it to burn out sooner. This changes the shape and wavelength of the wave in ways that a simple increase in replication does not. If the increase in replication is not caused by, for example, Christmas travel, this may provide early warning of mutation, especially when accompanied by new evasion markers. Otherwise, the Christmas increase in

replication can be added into the model as an acceleration factor, and predict hospital occupancy in the weeks following Christmas based on the rates immediately preceding it and the estimated acceleration factor generated by holiday travel in previous years, thereby modifying the current wave's trajectory by that holiday multiplier/acceleration factor, allowing multiple factors to be extrapolated simultaneously.

The amount of internal infection can be fed back into the Similar Flow algorithm to adjust the amount of external infection variables, and the loop repeats until the change in the variables so derived no longer changes by a significant amount. The resulting predictions can then be extrapolated forward in time to "future" data and compared to the CDC's estimation of the future and actual data that occurred later in the epidemic to validate the methodology.

3.2 SIMILAR FLOW METHOD

The Similar Flow method works for measuring the effects of a node on its neighbors, creating a "ripple in a pond" effect. For each change made to a node, the "ripple" of that change will create measurable propagation results on the remaining nodes. The change the other nodes experience can be triangulated to compute the location and intensity of the original "splash".

A dripping faucet takes longer to fill up a cup than one going full blast. In the same way, the inflow rate to any node (cup) is proportional to the time until a given threshold is infected in the node. In this way, the flow rate into the node can be calculated. Once calculated, the inflow of a node is equal to the flow input from all nodes. Therefore, once the flow rate for a node is calculated as a delta, a contribution flow can be calculated from its neighbors (and itself) as shares of the incoming flow. ("inflow" from a node's self represents internal spread of the virus.)

Each "link" between given nodes A and node B has a value denoting the population travel dispersal/flux along that path from A to B. This is basically the contagion flow from A to B, and is

roughly proportional to $\Pr(B \text{ is infected})$, given $\Pr(A \text{ is infected})$. Each link is then assigned a link weight depending on the flow along that link. The weight of each link can be used to calculate a minimum spanning tree using well-known methods of solving the resulting linear equations. It can then be extrapolated forward into the future to determine the outcome of the outbreak if nothing is done to contain it. This methodology can also be used as a validation technique for the method; can be used with “future” data from historical outbreaks to verify whether the predicted outcome matches the actual, historical outcome. Similarly, the original point of the spanning tree can be extrapolated backward into the past to identify the origin point of outbreaks to see if it agrees with the generally accepted value for historical outbreaks, and then again as a practical use, especially to track the origin of foodborne illnesses.

An example step-through of the process will now be performed with arbitrary data.

Table 1: Arbitrary data used for flow example step-through

Infected	Week 1	Week 2	Week 3	Week 4
Node 1	4.5	14.5	21	22
Node 2	3.2	5.1	6.4	7
Node 3	2	2.5	2.7	2.8
Node 4	1.7	2.2	3.7	7

Node1(1,2) is defined as change in Node 1’s infected value from Week 1 to Week 2, so the change is Week 2’s value minus Week 1’s value.. In this case, it is $14.5 - 4.5 = 10$. Now that we know the incoming flow is 10 at this time, we need to find what share of that 10 should be attributed to each of the incoming links. Note that this includes a node pipe to itself, for contagion spreading within a place node. Node 1’s internal infection is denoted x_1 . Node 1’s inflow from node 2 is denoted x_2 . Node

1's inflow from node 3 is denoted x_3 , and node 1's inflow from node 4 is denoted x_4 . We can then solve for x_1 through x_4 using linear algebra, with a line of best fit for overconstrained values: (these X_n are other day 1 values for node1's potential neighbors)

5

$$\begin{aligned} \text{Day 1:} \quad 10 &= x_1 \times 4.5 + x_2 \times 3.2 + x_3 \times 2 + x_4 \times 1.7 \\ \text{Day 2: } (21 - 14.5) &= x_1 \times 14.5 + x_2 \times 5.1 + x_3 \times 2.5 + x_4 \times 2.2 \\ \text{Day 3: } (22 - 21) &= x_1 \times 21 + x_2 \times 6.4 + x_3 \times 2.7 + x_4 \times 3.7 \end{aligned}$$

Now with these equations, node 1's weights to nodes 2, 3, and 4 can be calculated. However, this is only for node 1. The process repeats for nodes 2, 3, and 4 to find their weights to the other nodes.

Once each nodal weight is calculated, this immediately describes some patterns. Some places may have mostly internal infection, especially at earlier or later stages of the outbreak, however some high-tourist/ high-travel areas may have inflow infection all the way through the outbreak. Places with high internal infection have more internal disease travel than places with low internal infection, and may not be behaving appropriately. Similarly, if a line of best fit for a node is exceptionally poor, whereas all of its neighbors are not, this raises concerns that this specific node may be fabricating data, since it does not appear to be correlated with any travel from any of its neighbors in a consistent way. However, the system can 'repair' around this. Since the node with fabricated data is not contributing consistent flow to its neighbors, the flow contribution from second-most-nearby neighbors will show a better line of best fit than the immediate neighbors, thereby drawing some information out of the flow network despite one misbehaving node. For example, if Node3 is fabricating data, Node4's input from x_1 and x_2 for Node1 and Node2 would be different in the line of best fit, as they would have a more consistent correlation with the results of node4 than the fictional data from Node3.

The final diagram can provide value, in that the effects of one area can then be extrapolated to other areas forward in time, also proving validation for the method by comparing predictions to "future" data that was recorded after.

Overall, this routine takes in 61 sets of weekly time series data and outputs a link diagram yielding each state's average contagion to each other state, and an additional link to self-contagion in the next week. This predicts that the contagion in a given state in the next week is a linear function of: the contagion of each of the states this week, and a global "Outside" parameter. The self-contagion will be further tweaked in the next functions, but for the first iteration will be assumed to be linear. After the first iteration of all three functions is complete, the process can also repeat this routine with a time-based independent function, instead of a purely linear self-contagion parameter, yielding more precise results, until the results are not changed significantly.

A number of states and/or metropolitan areas can be connected together in a flow diagram to determine how the effects of one influences the spread to the remainder. For example, during Spring Break and holiday travel, the effects on each state is very dependent on the effects of key other states that are common travel destinations, and states and municipalities that are close to each source. For example, a high number of virites in Chicago can affect the outbreak in Michigan, Indiana, and greater Illinois in the immediate future, even during non-holiday times. This causes high population areas to radiate contagion to all of the other nodes to a greater or lesser degree and to absorb contamination to a greater or lesser degree. Additionally, nearby areas may radiate and absorb non-trivial amounts of contagion even if they are not high-travel or high-population areas, for example again North Dakota to South Dakota. Originally, all possible locations can be made nodes, and then nodes with trivial contagion links can be eliminated as inefficient. Historically, most of the contagion comes from a finite number of links that are either culturally important or geographically nearby, so that the final network can be solved with much, much fewer links. A perfectly naive way would be to try every node and every day connecting with every other node in every week, along every possible chain through every possible week for 100 nodes and 100 weeks, crating 100! links. Thankfully, only a handful are actually nontrivial, at least for the states of the US. It is cautioned however, that locations that have different

geographical needs may experience a much different final flow diagram, for example nations that have most of their population in a single capital city, with a very sparse population in other districts. Those populations may wind up looking more similar to a hub-and-spoke diagram when trivial connections are severed.

3.3 SIMILAR WAVES METHOD

The immunity ceiling continuously increases by an amount proportional to (the current viral load * time), excepting artificial increases, such as vaccination, suddenly increasing the ceiling drastically. Therefore, the ceiling an individual possesses right now is necessarily proportional to the sum of all previous viral loads through all of time to $t = 0$, because on Day 1 the ceiling was increased by some x based on day 1's viral load, and then on Day 2, it was increased again by an amount proportional to Day 2's viral load, etc. A given individual will start somewhere at their 'natural immunity' point, and then travel 'uphill' based on the new viral load received, granting them additional immunity. Someone with absolutely no immunity has a probability of 1 of showing symptoms (ceiling = 0 virites); regardless of the probabilistic 'roll of the dice' of the number of virites obtained, the number of virites will always be above such a low ceiling (for example, those with compromised immunity).

The number of VISIBLE cases is therefore proportional to the number of virites, minus the immunity ceiling of the sum/integral of the number of virites in the past through time. The result is a differential equation that is solved to use the number of visible cases to derive the average amount of virites through finding the probability of infection (number of visible cases/population = probability of that population being visibly infected at that time), and from that deriving the average amount of virites in circulation, taking into account that some people, especially the elderly, have a very low amount of natural immunity to infection.

First will be the mathematical background of the solving of the underlying equations, followed by a more procedural description outlining the method steps.

The visible data of breakthrough-threshold cases from a single wave's window of time can be analyzed. The rate of rise and fall in the wave informs how "deep" the wave is allowed to be. The replication of the virus, reduced by the population's immunity raising the threshold ceiling, must necessarily limit the options of the shape and scale parameters of the resulting equation. Other waves have similar shape parameters/ disease models of propagation, but may have a vastly different scale/ intensity factor, from viral load/evasion mutation, as well as replication on the part of the virus.

Additionally, the release of various vaccines will drastically raise the viral threshold, whereas a documented mutation will drastically lower it. The effects of these numbers on the resulting waves provide valuable insights into how changing one parameter alone changes the values, independent of other parameters, such as how people travel. Similarly, tracking the waves that occur after major travel holidays provide additional insights of the increase in replication, independent of mutation, if a major mutation was not simultaneously documented in that area. This allows multiple paradigm variables to be analyzed independent of the others, in a more controlled environment.

A single wave has an amplitude A and a wavelength λ . The first iteration can be solved empirically by taking the ratio of children, basic adults, and elderly in the population of, for example, a state, and the number proven infected (over threshold ceiling) in each sub-population of the state. Similarly, a running average of total hospitalizations, releases, and excess mortality can cross-verify the wave data as likely to be verifiable. The states with least opaque data make a good benchmark for the first iteration. The wavelength and amplitude of several waves adjacent in time and adjacent in space can then be measured, for example, North Dakota vs. South Dakota for the same time period, and a given wave compared to the wave immediately before it and after it.

A number of paradigm variables can be determined once a good baseline is found across many areas and time periods. The baseline variables are then validated by taking data early in the pandemic and then extrapolating them into the “future” to historical data that was recorded later in the pandemic. The later-pandemic data matches those that would be expected from the paradigm variables observed earlier in the pandemic. Further, when the virus has been observed to mutate at known dates, the paradigm variables change drastically coming off of those dates. Similarly, when patients have disobeyed no-travel orders during popular holiday times such as Christmas (and early in the pandemic, Mardi Gras especially), the paradigm variable for contagion increases drastically for a limited period afterwards. Even if some of these paradigm variables aren’t directly alterable (one cannot make people travel or not travel), the predictive capacity still provides value. For example, many hospitals are again seeing a resurgence around the holiday season, and foresight that contagion is likely to increase by around a known percentage can inform staffing levels and possible postponement of elective surgeries. Whereas, especially early in the pandemic, panicking hospitals postponed elective surgeries in some areas over and over, anticipating a resurgence that never came. Knowing when to predict the resurgence and capping a high likelihood upper and lower limit on the strength of the resurgence allows such resources to be redeployed elsewhere.

Once the effects of changes on paradigm variables are better known, combined paradigm variables can be used to predict and interpolate multiple variables simultaneously, for example a mutation that occurs during Christmastime. The Mutation meta-variable can be deduced from the change in wave behavior immediately preceding the holidays, and the Christmastime travel behavior can be inferred from previous and next years’ data. The interaction therebetween can then be deduced from each contribution separately, and the additional contribution to each other. Eventually, the values of several paradigm variables can be deduced, for example those that are unique to one geographical area such as Mardi Gras, or a particularly unlucky random event, or New York City’s first outbreak, as a deviation from a standardized wave for that time period. The inertia of purely exponential growth is

$x(t+1)=R_0 \times x(t) + \text{Neighboring add-ins}(t) \text{ from Outside (denoted } O(t) \text{)}$, for some infectivity increase R_0 , and the neighboring add-ins from phase 1 are deducted to calculate purely internal spread. But this is not a constant R_0 ; it goes up and down. So we have the goal of minimizing epsilon, ε , in:

$$x(t + 1) = \varepsilon + O(t) + R_0 \times x(t) - \text{Ceiling}(Z_{pop}) \quad 6$$

The R_0 can be calculated from very early in the pandemic, when virtually no one is hitting the ceiling naturally. The ceiling ratio can be best calculated when the second derivative switches from positive to negative, meaning that more people are being saved by the ceiling than getting new cases. Z_{pop} is a normal distribution of the natural immunity ceiling, ex. 1,000 virites for adults, 500 for elderly, 1500 for children. This can be modeled loosely as a normal distribution. In addition, the immunity for each step is indicative of a higher level of infection. Ex. People who are very affected are hospitalized, and people that are even further infected cannot be saved. This means the ratio of cases of infections to hospitalization to deaths provides a good indicator of the “depth” of the curve, whereas the gain or loss over time gives a good indication of the “width” of the curve.

The curve can be difficult to solve analytically, however, a table can be made for varying height and width values, and the table entry that most closely matches the curve can be used to define close height and width vales that must have created a similar curve to the one observed.

This is especially true as Z_{pop} changes over time proportionally with the integral of all the asymptomatic virites an individual has ever come into contact with, so both the mean and standard deviation go up over time, resulting in an expanded Z_{pop} of the original $Z_{pop} + \text{integral}(x(t)) \, dx$:

$$x(t + 1) = \varepsilon + O(t) + R_0 \times x(t) - \text{Ceiling} \times Z_{pop} \int x(t) \, dx \quad 7$$

Turning the difference equation into a differential equation as follows:

$$x'(t) = \varepsilon + x(t) + O(t) + R_0 \times x(t) - Ceiling \times Z_{pop} \int x(t) dx \quad 8$$

Taking the derivative of the whole equation with respect to x gives us the following second order differential equation:

$$x''(t) = x'(t) + O'(t) + R_0 \times x'(t) - C (Z_{pop} + x(t)) \quad 9$$

Rearranging gives us a very solvable equation, for some constants C_1, C_2 , where C_1 is $1 + R_0$ and C_2 the old C times Z_{pop} :

$$x''(t) - C_1 x'(t) + C_2 x(t) = O'(t) \quad 10$$

C_1 and C_2 can be solved for by the computer; in this embodiment, by the Python Solve and Fast Fourier Transform functions, and the results can be used to modulate the internal contagion from a node to itself in the Similar Flow method, fine-tuning the parameters for $O(t)$, which can then, in turn, fine-tune the parameters for the Similar Waves/Reverse Chaos methods.

The procedure of the method steps will now be described. The first step is to take the purely internal contagion from the states' time-series data, which is the amount of contagion each state has to itself in the future, after the outside contagion has been subtracted, so there will be 60 differentials between each state at week t and week $t+1$ that cannot be explained by external effects. This sets the “outside” of the above equation (10) to zero.

We can then take the grid of the 61 states under consideration by the number of weeks under observation for analysis. In this embodiment, since we are attempting to measure R_0 especially, the first wave is measured in the first year. The resulting 61 state by 53 week grid is run through a differential equation solver in Python (although other solvers can be used such as MATLAB or R) to

solve for the constants in equation (10). The result is a single sinusoid up and down with $1 + R_0 = C_1$ and C_2 being the mean of the distribution of the viral load ceiling.

If the wave under consideration contains no sub-waves, for example in the first wave ever of the COVID-19 pandemic, this completely describes the internal contagion. The internal numbers of infection from each state to itself is replaced by the numbers from the differential equation and recorded.

However, sometimes a single wave contains one or more sub-waves, especially later in the pandemic, as travel restrictions are relaxed and mutations occur, leading to a messier model. This is taken into account by the Reverse Chaos method, below in section 3.4.

3.4 REVERSE CHAOS: THEORY

Some variables are deeply time-based, not simply travel behavior, but also seasonal changes in virus behavior. For example, during Winter, the air is very dry, the virites tend to not experience de-aerosolization.

Normally, in the Summer, virite particles are encased in water droplets spread by coughing or sneezing, and stay in the air much like motes in a sunbeam. Such water droplets encounter and absorb water in the atmosphere, gradually becoming heavier, and no longer able to maintain their status as aerosol particles. This causes the droplets to fall to earth in a process known as de-aerosolization.

In the dry air of Winter, this process is much less effective at naturally removing contaminants from the air, so the temperature and internal humidity has a great effect on the spread of disease completely independently of travel or accumulation of persons together. Even such places as grocery stores can more readily spread such droplets, which can “hang” in the air for a protracted time, infecting other individuals. Thereby an additional paradigm variable for seasonality should be applied. Such a paradigm variable can be unmasked by comparing similar states close together that experience

the same temperature swings, and by the termination shock during spring, when the effects begin to vanish.

During the Similar Waves method, an occurrence may arise where one or more sub-waves are spotted inside of another wave, creating a wavelet with a much smaller amplitude and wavelength than the parent wave under observation. This implies that some occurrence has caused a deviation in the trajectory of the wave. The wavelets cannot be simply subtracted from the parent wave, as the wavelet and parent experience synergies; by having an increase in contagion, for example, a smooth line or curve can experience a jump to a suddenly higher value, reaching the peak much earlier than would otherwise be the case, affecting not only the amplitude, which could easily be subtracted out as $F_{TOTAL} = F_1(t) - F_2(t)$, but also affects the wavelength, so the resulting double-wave equation would appear more like as follows, with both X_1 and X_2 being variables, or even functions, that must be solved for:

$$F_{TOTAL} = e^{it(x_1-x_2)} \quad 11$$

A variation on Rainbow Tables can use pre-solving for a handful of known problems, and then recognize when these problems occur, and make adjustments in real-time.

For example, the change in amplitude and wavelength after a known mutation can be recorded, as well as changes after the onset of cold weather, holiday travel, as an offset from the amplitude and wavelength of a baseline immediately before the mutation or travel at each location. Then, for example during holiday travel, that offset can be applied at known times in the future, as an additional increase. For events such as mutations or cold snaps that do not occur at preset times, a running predication window of multiple potential events can be run concurrently. For example, a prediction of the future n weeks with no events, and a secondary or tertiary predication of the future n weeks if a mutation were to occur right now, or a cold snap were to occur right now. As the trajectory continues for the next several weeks, if it suddenly deviates from a baseline trajectory and starts to very closely match an

alternate trajectory, the system can conclude that a mutation might have occurred at the crucial point and then emphasize the remainder of the trajectory of that wave cycle with that in mind, giving feedback to the operator of future events before the mutation has even been isolated in a medical laboratory.

In this way, one or more side-windows can run concurrently with the Similar Wave method and the algorithm can modify predicted outcomes if certain patterns are realized. The modified prediction is then fed forward to the next iteration of Similar Flow and Similar Wave methods until concurrence is reached, same as the iterations of Similar Waves in isolation.

3.5 REVERSE CHAOS: IN USE

The procedure will now be described in some detail, repeating equation (10), with the additional modification that the outside amount O (for outside) has already been subtracted, and therefore is always equal to 0, along with its derivatives O' :

$$x''(t) - C_1 x'(t) + C_2 x(t) = 0 \quad 11$$

This is a very classical homogenous differential equation, and therefore should exhibit very classical wave-like behavior. However, frequently, something will occur mid-wave that changes the complete trajectory of the remainder of the wave, leading to a one or more sub-waves or wavelets. However, these wavelets must be created because either C_1 or C_2 has changed mid-wave. Either the virus has become more contagious, either through excess travel or replication mutation, or the ceiling has changed up or down, because of vaccination or evasion mutation, or possibly both, such as an evasion mutation followed by a vaccination for that mutation, or by vaccination followed by travel or mutation.

Because of the fact that classical differential equations with different values of C_1 or C_2 are well understood, waves with many different values of C_1 and C_2 can be pre-computed. After the very first wave is computed in a more simple mode, waves with different values of C_1 and C_2 can be extrapolated out and stored as virtual expected states alongside the “real life” states, with rising and falling values, alongside the actual measured outcomes of the actual “real life” state data of the various states. For example, C_1 (AKA R_0) and a C_2 of 1 through 10 can be pre-computed and the results populating 100 (10X10) virtual states' data.

If these values change mid-wave, the values will be similar to one of these 100 waves for a period of time and then suddenly deviate at some time t , mid-wave, to a different prerecorded value. Additionally, in an alternative embodiment, the R-squared values of the equation solver for the Similar Waves method will be much higher than it ordinarily is, as it does not precisely match any single-wave situation. Additionally, when a change occurs mid-wave, a wavelet will be observed in the graph of the wave near the point of change. All three of these features, in tandem, can be used for validation of the Reverse Chaos method, as they should always be found together.

The Reverse Chaos method, as explained previously, can keep a running tally of, for example, all 100 possibilities to compare a given state to. If the C_1 and C_2 values do not change mid-wave, a state should, very roughly, follow a standard wave trajectory. The reverse Chaos subroutine matches the values of the state in question versus the expected values of the virtual state table, which should roughly measure the final outcome of C_1 and C_2 measured by the solver in the Similar Waves method. When this does not happen, the wave is halved and measured again. If convergence is still not reached, the halving may be repeated until it is. This results in at least one section that does match a wave, and has a valid single solution to the differential equation under the similar waves method, successfully completing that portion of the similar waves method. However, this leaves another section of $\frac{3}{4}$, $\frac{1}{2}$, etc. of the wave that does not match the current solution and requires one or more additional solutions. The remaining portion of the wave, after a pause of one week, can then be compared against the 99

remaining virtual waves to see if one follows the remainder of the wave more closely. If not, there are two sub-waves and the halving process is repeated to create a third section of the wave. After the sectioning is completed, the second section only (followed by the third section only, if any) is then fed into the Similar Waves equation solver and new C_1 and C_2 are derived for the remainder of the wave.

The reverse Chaos method is expected to be relatively rare, compared to the Similar Waves method and only handles outliers, where a major event happens mid-wave. Numerous waves may come and go before a large change in the C_1 and C_2 values become necessary. However, even though they are rare, it is expected to be the best source of data when measuring a pandemic in real time, as a change mid-wave gives an indication that the underlying event has occurred, and if it is a mutation, provides insight that a mutation has occurred before it is generally known, and additionally, what the nature of that mutation might be.

While the real strength in the Reverse Chaos method is in real-time data, it can also be used to lookback to previous training data and find a nexus where a variable has changed suddenly, implying a mutation. If one is found, the second "real-time" algorithm can be run on each half of the state so found, one pre-mutation, and one post-mutation.

3.6 PUTTING IT TOGETHER

Once concurrence is reached, in that none of the three methodologies add meaningful changes to the predicted behavior in a cycled iteration, the resulting prediction can be compared against the CDC's predictions and the actual observed data of what historically occurred after that point in time. A graph is displayed of the CDC prediction, actual results, and newly predicted results, and the similarities therebetween can be described.

As a possible embodiment, if the results are changed significantly, for example by more than 1% over the previous results, the process repeats instead of terminates. Thereby the function as a whole must necessarily run at least twice, but further runs of this routine are data-dependent, and depend on the time to convergence for a given data set.

The sum of the results from the similar waves method that is subtracted from the total in all 50 states is compared to the total infections. If the subtraction amount in all states is less than 1% of the total infection in all states, convergence is presumed to have been achieved, and further looping is not necessary.

3.7 DATA CLEANING

Certain states are removed from the variable calculation phase as potentially falsified data. States with such data can still have some of the calculations performed, but not all. Besides the effect of "healing" around missing data, as elaborated on in section 4.1, states with no wave behavior may also contain falsified data, and so no wave processing is performed under the Reverse Chaos method. Because any falsified data would not follow any particular pattern, any attempt to incorporate such patternless data would be more likely to introduce random noise than actionable insight.

3.8 EXPERIMENTAL PROCEDURE

This section describes what was done to generate the results that are presented in Chapter 4 and presents the pseudocode for those algorithms. Appendix A contains the entire Python notebook.

The first step generated the linear model for the Similar Flow approach, which was done using Algorithm 1. The matrix X is created by using the first 53 weeks of data to predict the values for weeks 2 to 54. This was done for each state, and the results were combined into the matrix X . The matrix Z contains the predictions for each state for the weeks 54 to 173.

The following pseudocode describes the process:

Let s_{it} be the number of actual COVID-19 cases for state i in week t .

Let z_{it} be the predicted number of COVID-19 cases for state i in week t .

Algorithm 1. SIMILAR FLOW

Given: for $i = 1, \dots, 60, t = 1, \dots, 173$.

1. Set $s_{it} = 1000$ for $i = 61, t = 1, \dots, 173$. // "Outside" Row
2. For $i = 1$ to 60 // loop over states
3. Set $y = [s_{i2}, \dots, s_{i54}]$
4. Using y , for $i = 1, \dots, 61, t = 1, \dots, 53$, and y , use linear regression to determine a vector of coefficients x used for predicting the values for state i .
5. Form the matrix X from the $i = 1, \dots, 60$ of each individual x vector.
6. Form the column vector $[z_{1,53}, \dots, z_{61,53}] = [s_{1,53}, \dots, s_{61,53}]$ // the last week of the training data
7. Set $[z_{1..53},] = [s_{1..53}]$ // "Predict" the current training data
8. For $t = 53$ to 173 // loop over remaining weeks in time horizon
9. Calculate $[z_{1,t}, \dots, z_{60,t}] = X[z_{1,t-1}, \dots, z_{61,t-1}]$
10. Set $z_{61,t} = 1000$
11. Form the matrix $Z = [z_{1,54}, \dots, z_{60,173}]$ and the matrix $S = [s_{1,54}, \dots, s_{60,173}]$
12. Calculate $[deltas] = Z - S$ // Calculate prediction error

The next step determined the one-dimension discrete Fourier transforms for each state, which generated amplitudes and wavelengths for each state. This was done using Algorithm 2.

Algorithm 2. SIMILAR WAVES

Given: $deltas_{it}$, for $i = 1, \dots, 60, t = 1, \dots, 53$ // prediction error from algorithm 1

X , the matrix of regression coefficients

S , the matrix $[s_{1,54}, \dots, s_{61,173}]$

// s_{it} = internal + external + sinusoidal, so we

// increment each state's remaining error by the purely internal contagion so that

// the final prediction = all minus external contagion from any other state, as in equation [10].

1. Set $D = [X_{1,1}, \dots, X_{61,61}]$ // the diagonal of X

2. Calculate $T = S - DS$ // prediction errors and purely internal contagion, from the X matrix, which is the internal contagion to itself in the next t increment.

3. For $i = 1$ to 60 // loop over states

Determine the one-dimension discrete Fourier transforms of $[s_{i,54}, \dots, s_{i,173}]$,

which returns a set of frequencies F_i and amplitudes A_i for state i .

Calculate adjusted amplitudes $A_i^* = \frac{2}{54} |A_i|$ and wavelengths λ_i

(the reciprocals of the frequencies).

For New York City, we used the first three amplitudes (1100, 800, and 1400) and wavelengths (54, 27, and 18) to create a sinusoidal model that was added to the predictions in the matrix Z , as shown in Algorithm 3, to create new predictions W .

Algorithm 3. [for state i]

Given:

z_{it} for $t = 54, \dots, 173$ // Predicted cases for state i .

$A_{i,1}^*, A_{i,2}^*$, and $A_{i,3}^*$ // adjusted amplitudes for state i .

$\lambda_{i,1}, \lambda_{i,2}$, and $\lambda_{i,3}$ // wavelengths for state i .

1. For $t = 66$ to 173 // loop over weeks

2. Calculate $w_{it} = z_{it} + 2A_{i,1}^* \sin\left(\frac{2\pi t}{\lambda_{i,1}}\right) - 2A_{i,2}^* \sin\left(\frac{2\pi t}{\lambda_{i,2}}\right) - 2A_{i,3}^* \sin\left(\frac{2\pi t}{\lambda_{i,3}}\right)$

For the entire county and selected jurisdictions (the District of Columbia (DC), Virginia, and New York City), we used the CDC's exponential model to create a baseline prediction B , as shown in Algorithm 4. We used the following basic reproduction numbers: DC: 1.005; Virginia: 1.0036; New York City: 1.008; all of the USA: 1.00451355. The value for the USA was found by fitting an exponential curve to the nationwide totals from weeks 40 to 100.

Algorithm 4. [for state i]

Given:

$s_{i,53}$ // Actual cases for state i .

$R_{0,i}$ // Basic reproduction number for state i .

1. Set $B_{i,54} = R_{0,i}s_{i,53}$
2. For $t = 55$ to 173 // loop over weeks
3. Calculate $B_{it} = R_{0,i}B_{i,t-1}$

For the entire country, we included a sinusoidal model (using the sums of the states' amplitudes and the wavelengths 54, 27, and 18) and a factor for the impact of the vaccinations starting at week 112, as shown in Algorithm 5, which yielded the national prediction U . The amplitudes were rounded to the nearest thousands, so the values used were 101,000, 150,000, and 184,000.

Algorithm 5.

Given:

z_{it} for $i = 1, \dots, 60$; $t = 54, \dots, 173$ // Predicted cases for state i and week t .

$A_{i,1}^*$, $A_{i,2}^*$, and $A_{i,3}^*$ for $i = 1, \dots, 60$ // adjusted amplitudes for state i .

λ_1 , λ_2 , and λ_3 // Wavelengths

$v = -10000$ // constant for impact of vaccination

1. For $a = 1$ to 3

2. Calculate $A_a^U = A_{1,a}^* + \dots + A_{60,a}^*$ // sum of the amplitudes (rounded)

3. For $t = 54$ to 173 // loop over weeks

4. If $t < 112$

5. $u_t = \sum_{i=1}^{60} z_{it} - 2A_1^U \sin\left(\frac{2\pi t}{\lambda_1}\right) - 2A_2^U \sin\left(\frac{2\pi t}{\lambda_2}\right) - 2A_3^U \sin\left(\frac{2\pi t}{\lambda_3}\right)$

6. Else

7. $v = 61v$

8. $u_t = \sum_{i=1}^{60} z_{it} - 2A_1^U \sin\left(\frac{2\pi t}{\lambda_1}\right) - 2A_2^U \sin\left(\frac{2\pi t}{\lambda_2}\right) - 2A_3^U \sin\left(\frac{2\pi t}{\lambda_3}\right) + v$

Algorithm 6. REVERSE CHAOS (embodiment 1: lookback to previous predictions)

Given: $deltas_{it}$, s_{it} , z_{it} for $i = 1, \dots, 60$, $t = 1, \dots, 173$, // deltas, z, s states from SIMILAR WAVES

1. For $i = 1$ to 60 // loop over states

2. Fit z_{it} to a single sinusoid $y(t) = A \sin(bt) + c$

errorBaseline = 2 * Average($error_i$) from above fit.

3. if ($error_i$) > errorbaseline)

4. perform two one-state half-time REVERSE CHAOS:

5. REVERSE CHAOS ($s[i, 0 \dots (53 / 2)]$)

6. REVERSE CHAOS ($s[i, (53 / 2) \dots 53]$)

7. Print results for manual look

Algorithm 7. REVERSE CHAOS (embodiment 2: Real-time analysis)

Given: $deltas_{it}, s_{it}, z_{it}$ for $i = 1, \dots, 60, t = 1, \dots, 173$, // deltas, z, s states from SIMILAR WAVES

1. For $t = \{\text{current week}\}$ down to 1, step by -1 // count backwards from now to beginning of pandemic

// populate [A], a $10 \times 10 \times \{\text{current } t\}$ table of errors

2. For $C_1 = .5$ to 1.5, step by 0.1

3. For $C_2 = .5$ to 1.5, step by 0.1

4. $A_{C1,C2} = \text{Solve } x''(t) - C_1 x'(t) + C_2 x(t) = 0, x(t) = \text{sum}(s(t))$

5. For $t = \{\text{current week}\}$ down to 1, step by -1 // count backwards to beginning of pandemic

6. Let k_j = lowest errored column, the minimum value.

7. if ($k_j \neq \text{previous_kj}$) AND ($\text{previous_kj} \neq 0$)

// if the lowest errored C1 and C2 is different, mutation has occurred

// if $\text{previous_kj} = 0$, then the variable hasn't been set yet. (first iteration)

8. Print("mutation at time:" t "of strength:" k, j)

9. Return t

10. $\text{previous_kj} = k_j$

11. Print "no mutation found"

4. Results

4.1 SIMILAR FLOW METHOD

Table 2: The x vector coefficients from the state of Colorado:

1	0	2	0	3	0	4	0	5	0	6	0
7	0.3357675	8	0	9	0	10	0	11	0	12	0
13	0	14	0	15	0	16	0.13530653	17	0	18	0
19	0	20	0	21	0	22	0	23	0	24	0
25	0	26	0	27	0	28	0	29	0	30	0
31	0	32	0	33	0.08497	34	0	35	0	36	0
37	0	38	0	39	0	40	0.01574976	41	0	42	0
43	0	44	0	45	0	46	0	47	0	48	0
49	0	50	1.08451019	51	0	52	0	53	0	54	0
55	0	56	0	57	0	58	0	59	0	60	1.97079
61	0										

The Similar Flow method reduces the calculation, as expected, to a small number of either neighboring states or other high-value sources. Much of the infectivity of a given week can be predicted using the infectivity of these "friend" states to each given state, that have a nonzero coefficient. Because of this, the baseload of infection can be estimated out to a very high margin for many states, as a linear combination of their previous week's infectivity and the Friend States' previous week infectivity. Colorado's results are posted above as exemplary. In this table, Colorado, for example, has no contribution from states 1- 6, a contribution from state 7 (itself), state 16 (Iowa), and a small contribution from states 33 (North Dakota) and 40 (NY City), with a larger share coming from state 50, (South Dakota), and state 60 (Wyoming). So the result at $t+1$ is predicted to be roughly this linear coefficient times the values of these states at time t , for each such state.

Maryland and Virginia, unsurprisingly, both have most of their external contribution only from DC. DC has almost all of its infectivity from within DC and from "Outside", one of the few states to receive a contribution from Outside. This, again, makes logical sense, in that DC has a large amount of

international travel and so would acquire most of its infectivity from Outside, especially early in the pandemic, which is the training data currently under consideration. Both NY and DC, additionally, had externally-acquired outbreaks very early in the pandemic, so that in this particular case, most of the contagion was imported into international cities, and then spread to the rest of the US. Contrast to states that mostly generated their own internal contagion, and then became a net exporter of contagion to the world, such as Florida, which is a common source of contagion, but not a common sink of contagion.

It is noted that Puerto Rico's contagion did not seriously affect, or be affected by, any other area. All of its contagion seemed to be internal. As a result, its waves may not provide meaningful insight into the waves of any other states.

This model forced a y-intercept of zero for three reasons. First, an attempt using a very small y-intercept led to drastically, obviously spurious results, secondly because the infectivity was indeed 0 at the beginning of the pandemic so it makes sense that the logical outcome would follow from the mathematical, and finally, because any infectivity that would normally be carried independent of other states is handled by the "outside" factor, which, strangely enough, wasn't used in all of the states; mostly New York, DC, Nevada (Las Vegas), and to a lesser extent, South Carolina, had significant contribution from "Outside", likely because these are good tourist areas, and therefore with a larger contribution unaccounted for from the other states' general travels within the US.

An additional requirement made to the model was that all infectivity coefficients must be non-negative, one because this makes logical sense that there are no anti-infected spreading anti-contagion, and when it was allowed, the system allowed states to have billions infected to compensate for "negative" billions infected elsewhere, which while being technically tighter to the training data, represents an overfit, and is useless at predicting realistic outcomes, since a state cannot realistically have negative infected.

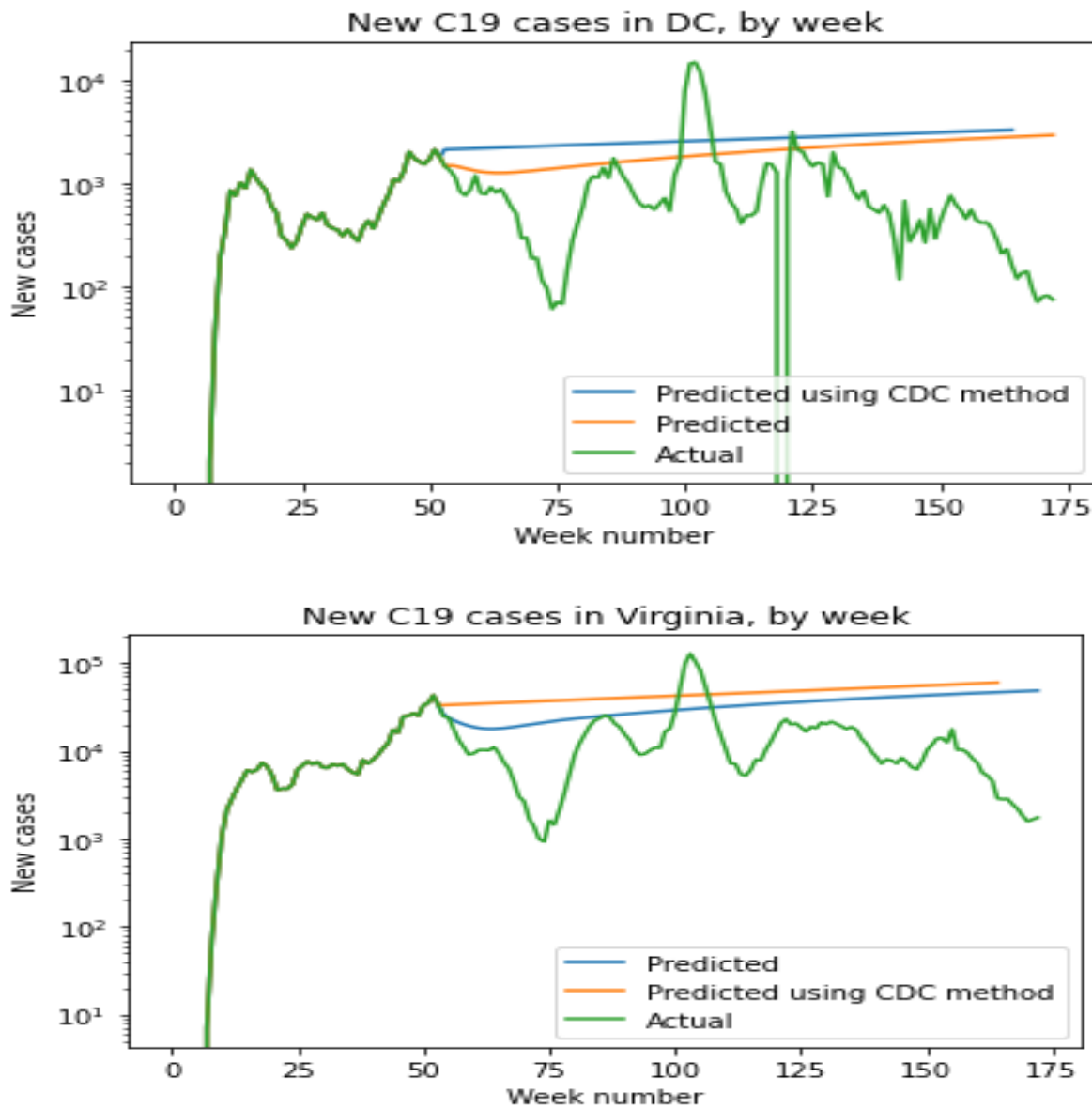


Figure 4: New cases in DC and Virginia on a logarithmic scale.

Colorado is chosen as exemplary in this section for ability to "heal" around any potential false data, for example by Wyoming. If Wyoming's reported data does not form a good linear combination of any other states because it contains false data, the genuine contagion would still grow and decline corresponding to reality, regardless of any fictitious reporting. The actual, genuine contagion will show correlation with other features, for example North and South Dakota. Fictitious Wyoming data will

start to see less and less linear correlation with the other states, such as North and South Dakota, as well as Colorado here, who is importing contagion from Wyoming. However, since the genuine contagion of Wyoming shows a strong linear correlation with North and South Dakota and also with Colorado, the genuine measurement of Colorado will also start to see a large correlation with North and South Dakota, that is not explained by any apparent correlation with Wyoming. Therefore, the randomized, potentially falsified data will see less and less importance, and be less strongly linearly correlated with the genuine data. Instead, the genuine data will show a stronger correlation with other genuine data, one step removed, in this case. This shows an impressive ability for the system to "heal" around sparse or false data by gathering much of the information from the genuine data it does have. In this way, the extrapolation has healed around any falsification by Wyoming by also including some factors from some of Wyoming's own factors directly: North and South Dakotas. In this way, the prediction for Colorado stayed accurate, even though some of the input data may have been falsified.

The Similar Flow method thus used more states' data points if sourcing from one of these states that were later disqualified for possibly having bad data, essentially attempting to correlate instead with the states that the disqualified states **should** have logically been correlating with, but instead the disqualified states were later to be found to be correlating with nothing in particular/randomness. As a result, the states that were trying to import contagion correlation from the states that would later be disqualified, instead imported contagion correlation from the states that the disqualified states should have properly been correlated with.

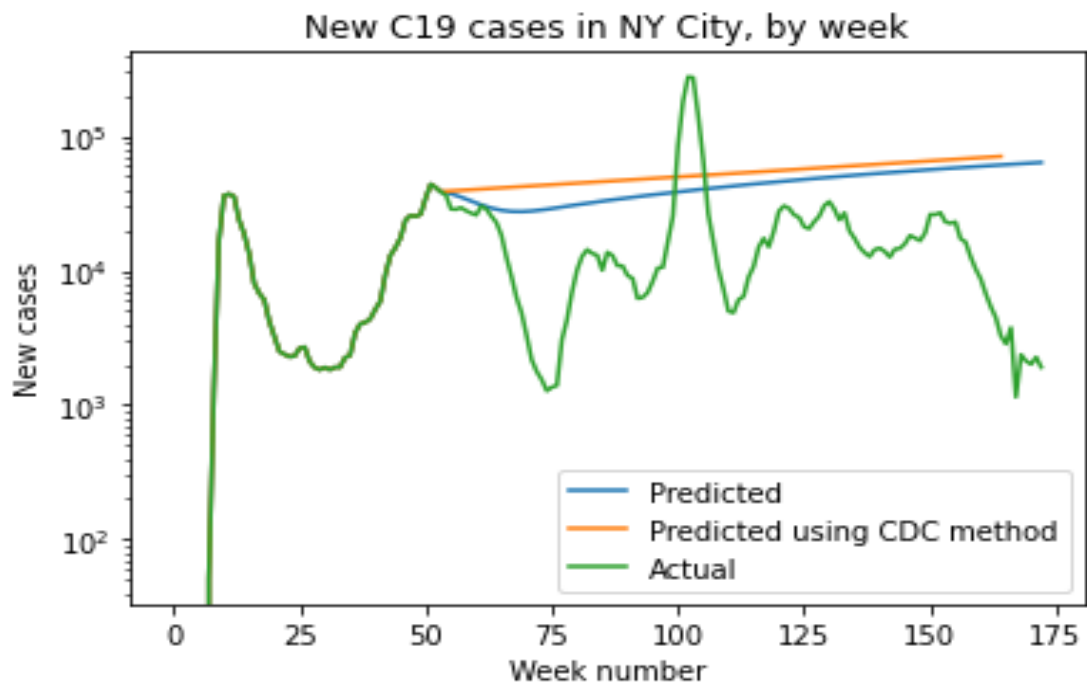


Figure 5: New cases in New York City on a logarithmic scale, by week

4.2 SIMILAR WAVES METHOD

Table 3: Output of the computed wavelengths and amplitudes for arbitrary states: (note the wavelengths are the same)

California (CA) Wavelengths:				
54	27	18	13.5	10.8
California (CA) corresponding Amplitudes:				
37005.9392	40317.6563	29671.2868	18941.71288	13437.72134
Colorado(CO) Wavelengths:				
54	27	18	13.5	10.8
Colorado(CO) corresponding Amplitudes:				
6505.13957	5252.29222	3137.15396	1430.489556	1139.572272

A vast majority of the states exhibited very similar wave behavior. The error and the internal contagion were fit to sinusoids to find the wavelength and amplitude of the waves using the Fast

Fourier Transform function to find the frequencies. This model found that nearly all the states had a wavelength of approximately 1 year, which is logically expected because of the effects of deaerosolization. This predicts that the pandemic will become more extreme in winter months and less extreme in summer months. Further waves are found at the half-year mark, and these are likely due to contagion vs. immunity itself. Temporary sub-waves by state are also created, as vaccinations occur and the virus mutates, changing wave behavior somewhat, but this is discussed in the reverse chaos method, below.

Interestingly enough, all of these states still under consideration exhibited very similar wavelength and amplitude variations (shape), differing only in the time to onset (phase). This makes sense in the case of COVID-19, because of the early-contagion lockdowns resulted in less cross-national travel. Because of this, most contagion sources were from within the state itself once its bubble had been sufficiently "popped". The state would then go on to follow the "standard" wave once this had occurred, with only minor variation from the input from other states, accounted for in the Similar Flow method. The primary state exceptions were Florida and DC, which were tourist areas which saw significant traffic from other states or regions, which could, theoretically have varied their wave mid-wave with an onslaught of new cases that was not grown internally. However, contrariwise, these are also some of the very first states to be infected, so they were responsible for infecting other states, rather than being the states infected themselves, and none of the other states had their bubble affected significantly after it had already been popped. As a result, while these states had tourists that could theoretically have suddenly raised their contagion rates in violation of the model, these areas instead saw well tourists that then became sick on vacation, and then went home to infect their home states. As a result, these states did not see sudden upticks mid-wave, but instead caused other places to increase their infectivity mid-wave. However, since each state had a relatively small proportional population from that other state on vacation at any time, this did not suddenly uptick the other states either, but was instead folded into, as a continuous value in the "regular" wave, which is much easier to

model. As a result, the only changes in wave shape come from mutations and vaccinations, which are accounted for in the reverse chaos method, below.

A few of the states did not exhibit good wave behavior and had to be removed from consideration in the Reverse Chaos method for different reasons. Some states had effectively zero amplitude in their frequency of occurrence at any wavelength whatsoever, and therefore could not be solved nontrivially: Florida and Arkansas. Further, Wyoming had a suspiciously low amplitude, but was still solvable. After subtracting the linear coefficients from the Similar Flow method, the rate of occurrence of these states did not further go up and down significantly, but were always effectively anchored to some arbitrary value, with a very small random deviation, completely independent of any initial conditions whatsoever. The values reported from these states followed a trajectory that was essentially anchored to a linear value with a minor random variation on top, instead of forming a wave of any possible wavelength, giving a high indication for randomness. These two states' lack of any solvable wavelength makes it likely that some of their data might be falsified, so their predictions were not considered in the third phase (Reverse Chaos Method) as they are therefore likely to contain false data input and, therefore, output.

Additionally, Alaska and Rhode Island suffered similar problems, likely because of the low number of infected. The very low amplitude of the signal made it difficult to discern a pattern.

The number of iterations required to form convergence to a single value for these states was increased to 1000 and then 2000 iterations, but Python was still unable to converge on a value. Upon manual inspection of the raw data for these states, the noise apparent exceeded signal for these values. It was therefore considered unlikely that these numbers would ever converge on a single, true value for these states, so Reverse Chaos was not performed on the states of Florida, Arkansas, Alaska, and Rhode Island.

The states can then have their predictions moderated by the largest waves discovered in that states' numbers. Again, this effect is attenuated the further from the training data the line gets.

This portion of the algorithm as a whole is especially strong if there is a lot of raw data, allowing the system to discount uncorrelated data and magnify data that fits a particular pattern, and is therefore best-suited for large data sets of potentially noisy data, even with very sparse real data. It doesn't work as well in very small data sets, or with very small populations.

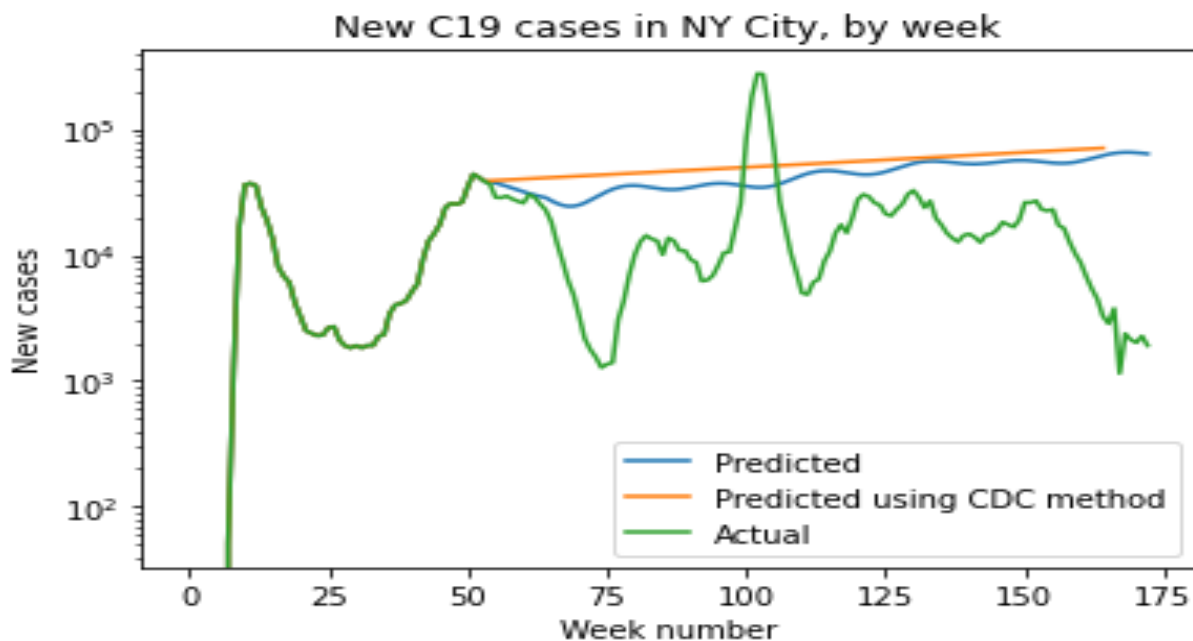


Figure 6: New cases in New York City, including waves, on a log scale, by week

4.3 REVERSE CHAOS METHOD

There were two major wavelength swings. The first swing is around week 50 when, first, the vaccine was distributed, severely increasing the ceiling. However, at about the same time, the Delta variant mutation occurred, drastically raising propagation, as well as evasion in removing some of the

newfound ceiling. This might also have been cause of the rapid displacement of one strain over another in that the old strain now had a drastically higher ceiling than the new strain.

The second major swing was just before week 100 when the Omicron variant suddenly spiked cases by some orders of magnitude. Even though a follow-up vaccine was introduced to combat this strain as well, it and future vaccines were not taken by the public as readily as the first, and so other vaccines had far more diminutive effects. The predictions are moderated to account for pre-planned vaccines' effects at week 112 by adding a one-time vaccine impulse downwards of strength 10,000.

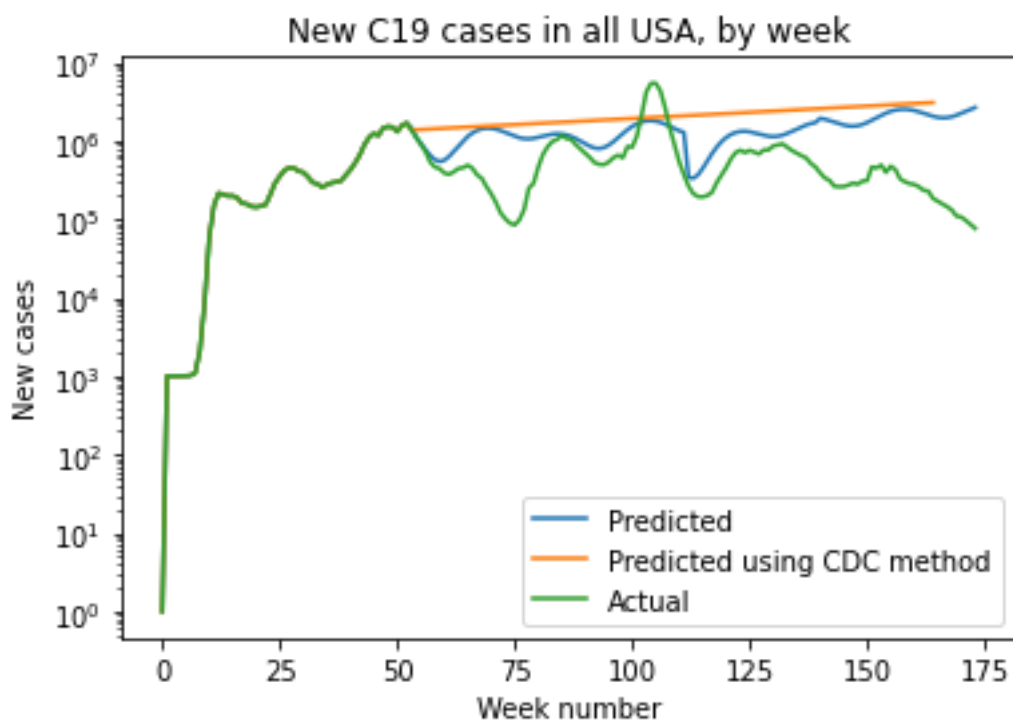


Figure 7: New cases in the entire USA on a logarithmic scale. Spikes occur of different amplitudes around weeks 50 and 100. Reverse spikes occur around weeks 50, 100, and 112.

The reverse chaos method is most useful when a mutation takes place that changes a value mid-wave. There are two main reasons for this to happen: Vaccination, which drastically cuts the wave downward and mutation, which drastically cuts upward. Vaccination doesn't really need to be predicted, since it is known ahead of time, so the only values that really need to be tracked are when the upward force of the virus that increases suddenly mid-wave. When this happens, a second mini-wave occurs within the bounds of the "regular" wave, and can be tracked with multiple methodologies.

In the current data set, the first instance is vaccination halting the upward flow of the wave, wherein the wave begins to curve downwards, immediately followed by the Delta mutation which halts the downward flow as well. This leads to a flat-top wave plateau, where the upward and downward forces on the wave are roughly equal until the downward force begins to "win" at the end of the wave.

The second instance is the Omicron mutation, where the downward trend suggested by the wavelength, is instead replaced with a drastic upward trend of several thousand percent, completely restarting this wave. However, the same wavelength resumes after this uptick, suggesting the same factors are at play, but simply with a larger number of units of amplitude. This implies that such changes can be modeled very well as a one-time bump to the process.

Multiple embodiments and methodologies can be used when a sub-wave exists in the regular wave. The easiest to program is a sudden uptick in error in the one-wave model; the one-wave model will suddenly see a much worse fit than the model did previously, however this requires setting a baseline of a level of acceptable error, which might not be useful in regions where the data is less complete as it was for COVID-19 in the United States, as some error would be generated by the nature of the incomplete data, leading to false positives.

If viewing the data for only a few regions visually, the easiest way is to simply observe a visual mini-wave, or alternatively, sudden jump in wave intensity (depending on if the mutation occurred at the downhill or uphill portion of the wave, respectively). This works very well if the mutation happens on a single graph of time-series data, however is not practical when measuring input interactions from

multiple regions over multiple timelines, (ex. The 60 X 53 matrix creates over 3180 visual-mathematical calculations) however could be done with a large enough workforce or a well-trained machine-learning model.

If such a beat note is found in real-time in "this week's" data, this can provide for a very good opportunity for staying ahead of the mutation and identifying the states where the mutation was present in significant quantities. Because the mutation can be modeled as having occurred identically in all 51 states at different times, the algorithm is agnostic to where the mutation actually occurred for COVID-19, since mutations for this particular virus tended to very quickly become the dominant strain after mutation, displacing other strains of COVID-19; different behavior might be observed for other diseases. Because of this, the disease progression can be modeled such that, at a specific point in time, all copies of the virus in a given state suddenly become copies of a different virus with a better bandwidth, independent of whether the mutation actually happened in that state or whether the mutation was imported from elsewhere.

In the current non-real time data, when a mutation is identified in a state, the state is divided into a pre-mutation and a post-mutation time zone. Since the transposition from a pre-mutation to a post-mutation state takes several weeks while one strain displaces another, there is no focus on attempting to discover "which" week in particular was responsible after the fact. Instead, the wave is cleanly divided into two halves. One of the halves will be "standard", without mutation, and one of the halves will feature the mutation. It was not found necessary in the current data set, but theoretically this process would be repeated to subdivide into quarters, or technically even further. Further subdivisions might not actually create more knowledge, however; it would probably create more accurate predictions of COVID-19 spread to treat two mutations happening back-to-back as a single mutation, mathematically, as any mathematical operation about only one would quickly be drowned out by the propagation of the second since, again, COVID-19 quickly displaces previous iterations of itself in a population. More granular subdivision might produce greater insight for other viruses.

4.4 WHAT WAS LEARNED

Because the current CDC model treats contagion as a logit-like function with exponential growth the new method leads to more accurate leading predications as a quasi-sinusoid, since it predicts what the future R_0 might be, instead of having it need to be updated after-the-fact to fit previous data. As a result, the deviations in the graph can be predicted ahead of time, instead of retrofit to existing data. Here, number of infected = R_0^t with R_0 generally around 1.005, as derived at the moment of $R(1 \text{ year})$ for units of $t = 1 \text{ week}$. This implies for each newly infected, the number of infected in one week will be 1.005 times that. This is the long-form predictive model used by the CDC, as mutations change the amount of contagion frequently throughout the outbreak, so numerical predictions are not published by the CDC that far out. [13]

The figures below describe covid data for the entire US using both the CDC's methodology and the new methodology. The CDC methodology has the additional problem that the values were calculated after the fact, instead of before. Because it does not have that advantage, the new methodology begins to drift further away from actual results as it interpolates more and more beyond its training data. In the first year of interpolation especially, the new method sees much less error than the CDC's method, but decays from this the further it must interpolate.

The cumulative absolute error for the CDC method for 100 weeks of interpolation was 147 million. The cumulative absolute value error for 100 weeks of interpolation for the new method was 89 million, a difference of about 58 million less error. Neither method predicted how severe the Omicron variant spike would be, but the new method was much more accurate for most other times.

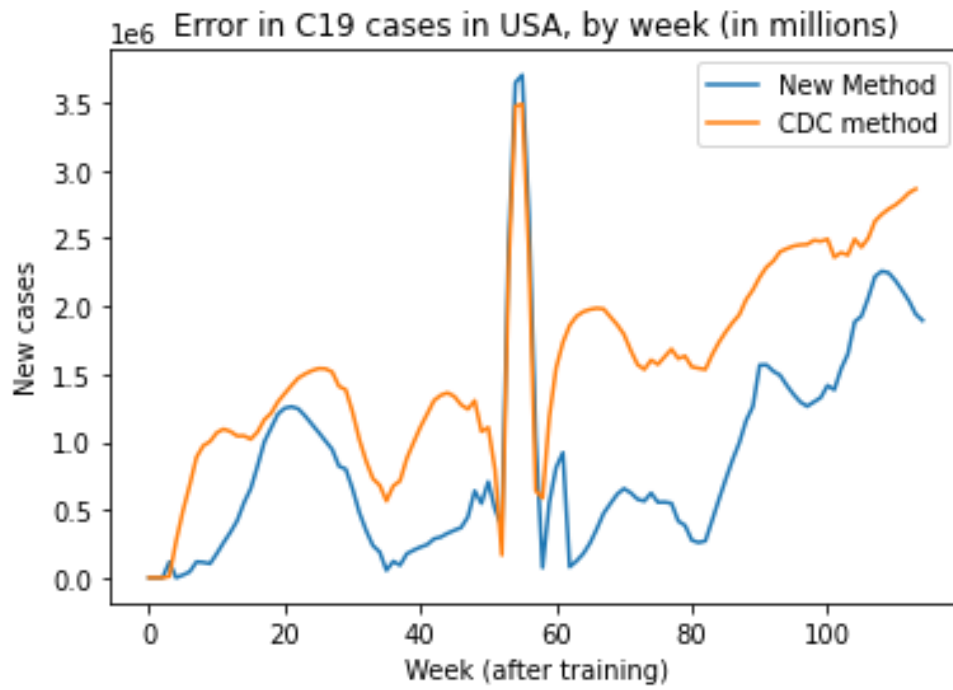


Figure 8: Absolute value of error in new cases in the entire USA using all methodologies, in weeks of interpolating new data. The sum of the absolute value of this error is 147 Million for the CDC method, and 89 million for the new method.

5. Summary and Conclusions, Similar work

5.1 CONCLUSIONS

Because the current CDC model treats contagion as a logit-like function with exponential growth, the new method leads to more accurate leading predications as a quasi-sinusoid, since it predicts what the future R_0 might be, instead of having it need to be updated after-the-fact to fit previous data. As a result, the curves in the graph can be predicted ahead of time, instead of retrofit to existing data. The figures describe covid data for the entire US using both the CDC's methodology and the new methodology. The new methodology begins to drift further away from actual results as it interpolates more and more beyond its training data. In the first year of interpolation especially, the new method sees much less error than the CDC's method, but decays from this, the further it must interpolate.

A continuous look-ahead model might have even greater predictability. If all past data is used as training data and the algorithm is asked to look no more than 25 weeks ahead, a more accurate model could result. However, part of the purpose currently is to form a better long-term prediction method, which is a different methodology than those used currently.

There are a few other limitations of the new methodology. As mentioned earlier, the methodology takes a little bit of information from many, many data points. This works very well even if the real data is relatively sparse in a large amount of noise, but does not work if there are few data points to begin with. This means that a very, very low granularity is not optimal, and works better with bins that are relatively large in comparison to the whole.

This work was done with US data and not global data, but there is no reason a larger data set cannot be used. There may be a problem in places where a significant portion of the population is

located in a single capital city or a small number of hub cities, as the remainder of the area might take up most contagion from those areas and not from within or nearby neighbors.

There are many benefits of the new methodology beyond simply a more precise estimate. The algorithm's ability to "heal" around potentially falsified data can be used in data sets where much of the data is similarly incomplete or falsified. The data that is correct will show linear correlations with other data that is also correct. Data that does not linearly correlate with anything will remain an "island" of data and will be shut off from contaminating future results as much as in some other models. This is also a type of drawback with the methodology in that unrecoverable data is instead dropped and "healed around", rather than attempting to brute-force it. Regions where almost all of the data is fabricated will not be able to make very accurate predictions,. Even though the data will not contaminate the data for other, more trustworthy, regions.

An unexpected benefit is the similarity of the waves. Because the wave shapes are similar differential equations among the many states, and both before and after key events, this greatly simplifies the calculations that need to be performed. The wave shape can be isolated and the effects of events can be simple permutations or acceleration factors that can be applied to an individual wave. This benefit may not exist in all possible data sets, however, leading to states with different wavelengths and drastically different phases in some implementations.

5.2 SUMMARY

Pandemics and other natural forces can be modeled with a distinct wave behavior. This wave can be modeled as a second-order differential equation, creating a sinusoid with a repeating pattern. Early sections can allow for a good mapping of the sinusoid, as they are more free of sub-waves that interfere with computation. Once the easy parameters are solved for, the remaining parameters can be solved with this extra information in mind. This sinusoid mapping can then be applied to nonsmooth,

chaotic sections, which can be difficult to find a straightforward solution for without the foresight of the easy, smoother section first. Once the chaotic features are determined, the controlling variables can be solved for to a desired level of precision.

Falsified information can be treated as noise, and can be accounted for by determining which features of the data are commonly found in tandem and which features are not in tandem with any other features. Features that show no correlation to anything else in the data might be either random noise or fabricated data. Data points that "play well with others" can be separated from data points that follow a completely different function or rule. In this way, genuine data can be solved for independently of noisy or false data. This allows for an empirical methodology of finding outliers that may not represent actionable information and excluding them early in the calculation, so the remainder of the calculation can be routed around such outliers when a pattern is found. This enables the algorithm to "heal" around missing or false data.

A method of finding such noise is to separate each dependency of the data into different bins. Genuine correlations should be common to many of the bins. Noise should not be common to other noise or genuine data, except extremely rarely. As a result, the genuine data patterns becomes increasingly emergent as correlations between data builds up, and noise can be dropped from the pattern.

This is especially useful in "real-time" data where a number of measurements are seen as signal, and are then suddenly dropped all at once in favor of a new set of measurements that is seen as the new second signal, and the old signal is dropped as noise. This implies that two signals are present in the data and the second signal has recently become more powerful than the original signal, and can be the result of an invisible factor in the data that has recently changed, a change that could not be seen directly, but can be seen in the drastic change in behavior of its dependencies. In analyzing the results of the dependencies, situations that cause such behavior change can be predicted, even if the nature of the behavior change itself is not known.

The number of new cases of COVID-19, by week, by state, from the CDC were input and the linear correlations were found therebetween, by finding a linear solution between the number of new cases in a given state versus the number of new cases in all of the states in the previous week, including itself. This provided a good baseline of the "ripple in a pond" effect to map out the traffic between the various (potentially nearby) states determining how the effect of one state affects the other states over time.

The immune resistance to the pandemic caused by immunity and vaccination can then be modeled as a second order differential equation, creating a sinusoidal wave pattern. In this way, each state's immunity over time is a function of the historical population of infected in that state. For COVID-19 in the US, the solutions for all the states were very similar, providing confidence in the model and cross-validation for the methodology.

A number of states not only didn't fit the numbers, but couldn't fit any numbers, having no wave behavior at all, causing the algorithm to route around such data. The algorithm under consideration has certain assumptions which were made based on the idea of contagion, which imposes certain conditions on the data. Other types of data may have similar rules that cannot logically be violated. Data that implicitly violates those conditions can be dropped as noise. This could be caused by the population being too low for any signal to overcome the random noise of the process, or by an adversary inputting arbitrary data into the input parameters for that state. However, the algorithm was able to route around both forms of noise similarly, as it detects when these conditions of the data are no longer being met, and so the data is no longer relied upon as much as other data that does meet these conditions.

Sudden, drastic changes in the amount of noise actually provides insight of a potential hidden signal, such as a mutation. The algorithm can then introduce this newly found pattern to fine-tune its assumptions and parameters. The final estimation for the contagion was therefore much more accurate and precise than the generally accepted methodology, which has a great deal of inertia and is slow to

change, versus an algorithm that notices drastic changes in data right away. As a result, the new algorithm focused more closely on valid data and away from noise, allowing for a better prediction.

This algorithm of data mining real data in potentially false data, is useful in other types of problems as well. Among those are difficult physics simulations and types of economic modeling.

5.3 DIFFICULT PHYSICS SIMULATIONS

There are many physics simulations that cannot be feasibly performed because the conditions change at different speeds at different places in the simulation. For example, near black holes, the 'speed of time' increases, slowing the relative progression of events. A possible model to this is a time counterforce to the progression of events, as in the above differential equations. As a result, a physics simulation can be remapped onto the surface of a wave, and a calculation in proper time can be mapped to the similar place in the wave. This can be aided by a rainbow table of flagpoints that can be placed along the wave to act as an aid to navigation on the wave, so it can be easier for a computer to determine where, and when, objects are located on the progression of time. This creates a "reverse" differential equation, where time is the dependent variable rather than the independent variable. After this, everything can be dependent upon the new flow of time. For example, by mapping a function onto the surface of an arctangent curve.

The reverse chaos method especially adds an incredible amount of insights to such problems that are numerically unstable, in that a small change on the border results in drastic changes elsewhere, for example supersonic fluids. For example, in the equation $y=1/x$, if 0 is approached from the negative direction, the result decreases without bound, but if it increases in the positive direction, the function increases without bound. Values very near to zero have difficulty being mapped to a single solution, since the result may be a very large, or very negative number. One can take an empirical value of a

number of nearby values to determine an approximate location along the function. For example, if my current values is one billion and one, I can recognize that my input value must be between 1/one billion and 1/two billion, and that it could not possibly have been negative 1/two billion. In this way, I can navigate between various flagpoints to determine the location on the wave along both the t and the $f(t)$ axis.

5.4 ECONOMIC MODELING

Other uses for this procedure are also envisioned. The success of the model on very highly numerical data, such as virus propagation, can also provide insights into the use of the model in less empirical circumstances, such as customer service.

There is an inertial effect of someone who regularly shops at one store being familiar with the layout, and would tend not to shop at a nearby store, even if the price were very slightly cheaper, or the customer service is somewhat better. In this case, the customer only switches to the other store if the expected difference in customer experience and prices at the new store are greater than that individual customer's inertial effects that are anchoring the customer to the old store. As a result, multiple nearby stores can drop customer service or raise prices in tandem; as long as the increase is slow and gradual enough, a condition state is never reached such that a given store's deviation from the surrounding stores' value is greater than the customer's inertial hesitancy to switch stores. The minimum customer service a store must provide is thus heavily dependent on the nearby stores that sell similar items. One store can raise prices or cut service by (amount less than inertia constant), causing other vendors to also cut service and raise prices by (amount less than inertia constant), bringing them back into par. This has important connotations in economic modeling, creating a natural monopolistic force even in absence of a single monopoly.

The inertial effect or monopolistic pressure can be calculated as the amount of price increase that is finally necessary to pull away a given amount of custom from nearby establishments. This is the customer's switching inertia. Measuring this switch inertia can be useful in antitrust policies to determine the amount of monopolistic pressure a given entity emits, empirically. This measurement of the amount of price or value difference required to get a customer to switch stores is proportional to the ability of the store's magnetism to keep customers at that store. In a True Monopoly, this value is infinite. In a perfectly level system, this inertia value is 0.

For example, there is a pressure force on gas prices that is applied to a station from the adjacent stations. People may go next door to save ten cents on gas who would be hesitant to drive all the way across town to save the same amount. As a result, the rate of change of gas prices is heavily "contagious" from adjacent gas stations; gas stations have a tendency to somewhat match nearby stations. If some gas stations are far away from any others, this pressure does not exist, causing "islands" of high gas prices to develop, independent of the wholesale price of fuel or locality taxes, as island gas stations can get away with charging more, without customers fleeing to an adjacent station. The gas station that is far distant from any other can raise prices quite significantly before it finally becomes worthwhile to drive all that distance. In addition, if there is a peninsula of gas stations, the price may change, but very slowly, as there is a large propagation delay across the peninsula, leading to a large price gradient across the peninsula, as a wave of prices gradually travels down the peninsula.

Alternatively, this differential equation can be used in price management routines to see how much a given price would influence not only the demand curve in a single step, but how much a price increase or decrease would affect other vendors of the product, and what the final state of such a price change would be, both in the number of customers and the profit so derived.

For example, a gas station raising prices by x cents per gallon may not reduce the demand curve, as other gas stations can respond similarly, allowing all such stations to increase profits.

Similarly, reducing prices can lead to a "race to the bottom", as other competitors match the lower price. Similarly, cutting costs by reducing product quality may trigger a similar race to the bottom, as other vendors cut quality by the same amount to match prices. As a result the quality/price curve is not as sharp as it may first appear, as not only customers, but other providers will change to match.

The price of gas can be modeled as a system of linear equations, where each gas station is one node and has a listed price for regular unleaded gas. The price of gas at that station the next week is then proportional to the price of gas at that station the previous week, as well as the price of adjacent gas stations in the previous week; if the price of other gas stations is higher, the station may raise their prices to compensate. If the price is lower, the price may similarly lower to compensate, to avoid driving off business. This causes a sudden change in gas prices to "spread" across the map over the course of several weeks. The addition of an "Outside" value of the price of gas to account for a global increase in raw materials can also be added, similar to the "Outside" state in this thesis. The price of gas in several gas stations can then be tracked and a vector of linear coefficients can be determined between the various gas stations' prices to determine the ability of each one to influence the other. If one station finds itself in an island or peninsula, that can be evidence that that station would be better off raising prices to take advantage of a captive audience (such as at an airport). Similarly, if a station realizes that a number of stations are dependent on its prices, that may provide an opportunity to either slowly raise prices in tandem, or undercut competitors with a deep, sudden price cut, depending on circumstances.

A similar methodology can be used to monitor monopolistic practices of a small number of vendors of a product. For example, both Coke and Pepsi have seen high profits as of late by both increasing prices. The ability to switch to the adjacent vendor on the price "island" is limited by the only other common vendor on the "island". If both vendors raise prices in tandem, there would be little switching from one to the other due to price.

Additionally, if changing prices by one gas station does not effect a second gas station in any way, it can be inferred that the stations are on separate islands, and are therefore not true competitors, as there is nothing a gas station on one island can do to draw customers away from the second island. This can be a sign by anti-trust regulators to determine local monopolies that have drastically different service than nearby alleged competitors, that no one is actually capable of switching to.

```
In [1]: import pandas as pd
import numpy as np
import matplotlib.pyplot as plt
import seaborn as sns
import scipy as sp

from datetime import datetime as dt
from numpy import nan as NaN
from sklearn.linear_model import LinearRegression

import os
import math

print("done")
```

done

```
In [2]: %pwd
#Where am I?
```

```
Out[2]: 'C:\\Users\\admin\\anaconda3\\aThesis'
```

```
In [3]: #Reading data and partitioning it to the relivant variables.
rawDataSet = pd.read_excel('c19.xls', sheet_name = '19')

# 50 states + DC = 51 "states"
state = rawDataSet["state"]
valuesOfDataSet = rawDataSet["new_cases"]
deaths = rawDataSet["new_deaths"]
endDate = rawDataSet["end_date"]

print("Reading data")
```

Reading data

```
In [4]: fig = plt.figure()
plt.show()
#test
```

<Figure size 432x288 with 0 Axes>

```
In [5]: maxTime = 173
# There are 173 weeks of data in the CDC data set of 2020-01-23 thru 2023-05-10

maxStates = 60
# 50 "real" states, 1 district (DC), 1 NY City, and 8 of territories, etc.
```

```
In [6]: #initialization for for loop vars
j = 0
t = 0
yValues = np.ones(99)
finalXvalues = np.ones(61)
thousand = np.ones(maxTime) * 1000
thousandRow = pd.DataFrame(thousand).transpose()

# reshape as a 60 X 173 array
states = valuesOfDataSet.values.reshape(maxStates, maxTime)
statesNames = state.values.reshape(maxStates, maxTime)
statesNames = statesNames[:, 0]
states = pd.DataFrame(states)

#add the names of the states as the column headers
states = states.transpose()
states.columns = statesNames
states = states.transpose()

# An extra 61 node for Outside the US
states = pd.concat([states, thousandRow])
# Note: the Outside row is the state of " 0 ", which looks like "0", which is a good

states
# 60 State object Rows, 173 weeks in columns.
# Week 0 is the first week of the pandemic; week 172 is the final week.
# This comes out to 0- 172 instead of 1- 173.
```

```
Out[6]:
```

	0	1	2	3	4	5	6	7	8	9	...	163	164
AK	0.0	0.0	0.0	0.0	0.0	0.0	0.0	0.0	11.0	52.0	...	582.0	448.0
AL	0.0	0.0	0.0	0.0	0.0	0.0	0.0	3.0	58.0	411.0	...	2471.0	1890.0
AR	0.0	0.0	1.0	3.0	1.0	3.0	0.0	8.0	70.0	279.0	...	1448.0	1240.0
AS	0.0	0.0	0.0	0.0	0.0	0.0	0.0	0.0	0.0	0.0	...	0.0	0.0
AZ	0.0	1.0	0.0	0.0	0.0	0.0	0.0	8.0	18.0	374.0	...	3220.0	4892.0
...
WA	1.0	0.0	0.0	0.0	0.0	0.0	44.0	329.0	848.0	1644.0	...	4042.0	4020.0
WI	0.0	0.0	0.0	0.0	0.0	0.0	0.0	3.0	108.0	510.0	...	4178.0	3856.0
WV	0.0	0.0	0.0	0.0	0.0	0.0	0.0	0.0	1.0	38.0	...	1414.0	1412.0
WY	0.0	0.0	0.0	0.0	0.0	0.0	0.0	2.0	18.0	34.0	...	281.0	257.0
0	1000.0	1000.0	1000.0	1000.0	1000.0	1000.0	1000.0	1000.0	1000.0	1000.0	...	1000.0	1000.0

61 rows × 173 columns

```

In [7]: oldSize = 53
interpolateDistance = 119

currentStates = states.loc[:, :oldSize]
yValues = (states.loc[:, 1:oldSize+1])
finalXvals = ()

#includes internal spread (state itself), however, Outside, the 61st outside "state",
for j in range(maxStates): # Loop in states, j= 1 to 60: each in states
    #starting at t=2, for each state, y= that state's value at t,
    #and is a linear combination of the values at all 60 nodes at t-1:
    #Y = X1*s1 + X2*s2, ... X52 * s60 for some X values 1- 60.
    #This is a basic linear line of best fit, and is actually only 1 line of code when
    regress = LinearRegression(fit_intercept = False, positive = True)
    tempHold = currentStates.transpose()
    tempHold.columns = tempHold.columns.astype(str)
    re = regress.fit(tempHold, yValues.iloc[j, :])
    XvaluesIteration = re.coef_

    # Not doing it this way any more
    #finalXvalues = math.linearBestFit(yValues, states)
    #finalXvalues = states.index[j], re.coef_, re.intercept_

    #The names of each state, values
    print(states.index[j], XvaluesIteration)
    finalXvals = np.append(finalXvals, XvaluesIteration)

    #tempHold = states.iloc[:, oldSize:oldSize + interpolateDistance]
    #tempHold = tempHold.transpose()
    #tempHold = re.predict(tempHold)
    #print(tempHold)
    #futureStates = pd.concat([tempHold, futureStates])

```

```

AK [4.33840852e-01 0.00000000e+00 0.00000000e+00 0.00000000e+00
0.00000000e+00 0.00000000e+00 0.00000000e+00 0.00000000e+00
0.00000000e+00 0.00000000e+00 0.00000000e+00 0.00000000e+00
0.00000000e+00 3.72566559e-01 0.00000000e+00 0.00000000e+00
0.00000000e+00 0.00000000e+00 0.00000000e+00 0.00000000e+00
0.00000000e+00 0.00000000e+00 0.00000000e+00 0.00000000e+00
0.00000000e+00 0.00000000e+00 0.00000000e+00 0.00000000e+00
4.16275469e+00 0.00000000e+00 0.00000000e+00 0.00000000e+00
1.79590545e-01 0.00000000e+00 0.00000000e+00 0.00000000e+00
5.81967986e-02 0.00000000e+00 0.00000000e+00 0.00000000e+00
0.00000000e+00 0.00000000e+00 0.00000000e+00 0.00000000e+00
0.00000000e+00 0.00000000e+00 0.00000000e+00 0.00000000e+00
0.00000000e+00 0.00000000e+00 0.00000000e+00 0.00000000e+00
0.00000000e+00 0.00000000e+00 0.00000000e+00 0.00000000e+00
0.00000000e+00 4.41529380e-05 0.00000000e+00 1.52180652e-02
0.00000000e+00]

```

```

AL [3.09769083e-01 0.00000000e+00 0.00000000e+00 0.00000000e+00
7.91040352e-02 0.00000000e+00 0.00000000e+00 0.00000000e+00
0.00000000e+00 1.37814333e-02 2.86551257e-02 0.00000000e+00
0.00000000e+00 9.34387804e-01 0.00000000e+00 0.00000000e+00
1.74841917e-01 0.00000000e+00 0.00000000e+00 0.00000000e+00
0.00000000e+00 0.00000000e+00 0.00000000e+00 0.00000000e+00
0.00000000e+00 0.00000000e+00 1.36689531e-02 0.00000000e+00
1.66340977e+02 2.61684336e-01 0.00000000e+00 0.00000000e+00
0.00000000e+00 0.00000000e+00 0.00000000e+00 0.00000000e+00
1.09071165e-01 0.00000000e+00 0.00000000e+00 0.00000000e+00
0.00000000e+00 0.00000000e+00 0.00000000e+00 0.00000000e+00

```

```

0.00000000e+00 0.00000000e+00 0.00000000e+00 0.00000000e+00
0.00000000e+00 0.00000000e+00 2.12927772e-01 0.00000000e+00
0.00000000e+00 0.00000000e+00 2.13658345e+00 0.00000000e+00
0.00000000e+00 0.00000000e+00 0.00000000e+00 0.00000000e+00
6.47464817e-01]
AR [0.00000000e+00 5.74572992e-02 5.55928964e-01 0.00000000e+00
0.00000000e+00 0.00000000e+00 0.00000000e+00 0.00000000e+00
0.00000000e+00 0.00000000e+00 0.00000000e+00 0.00000000e+00
9.65968076e-03 0.00000000e+00 0.00000000e+00 0.00000000e+00
0.00000000e+00 0.00000000e+00 0.00000000e+00 0.00000000e+00
0.00000000e+00 0.00000000e+00 0.00000000e+00 0.00000000e+00
0.00000000e+00 0.00000000e+00 0.00000000e+00 0.00000000e+00
3.38371502e+01 0.00000000e+00 0.00000000e+00 0.00000000e+00
1.96025058e-01 0.00000000e+00 0.00000000e+00 0.00000000e+00
0.00000000e+00 0.00000000e+00 0.00000000e+00 0.00000000e+00
0.00000000e+00 0.00000000e+00 0.00000000e+00 0.00000000e+00
4.29747034e-02 0.00000000e+00 0.00000000e+00 0.00000000e+00
0.00000000e+00 7.70983793e-02 4.89013421e-02 0.00000000e+00
0.00000000e+00 0.00000000e+00 0.00000000e+00 0.00000000e+00
0.00000000e+00 0.00000000e+00 1.77988320e-01 0.00000000e+00
2.52210742e-01]
AS [0. 0. 0. 0. 0. 0. 0. 0. 0. 0. 0. 0. 0. 0. 0. 0. 0. 0. 0. 0.
0. 0. 0. 0. 0. 0. 0. 0. 0. 0. 0. 0. 0. 0. 0. 0. 0. 0. 0. 0.
0. 0. 0. 0. 0. 0. 0. 0. 0. 0. 0. 0. 0. 0. 0. 0. 0. 0. 0. 0.]
AZ [0.00000000e+00 0.00000000e+00 0.00000000e+00 0.00000000e+00
6.76681294e-01 2.57057104e-02 0.00000000e+00 0.00000000e+00
0.00000000e+00 0.00000000e+00 0.00000000e+00 0.00000000e+00
0.00000000e+00 0.00000000e+00 0.00000000e+00 0.00000000e+00
0.00000000e+00 0.00000000e+00 0.00000000e+00 0.00000000e+00
0.00000000e+00 0.00000000e+00 6.85015368e-02 0.00000000e+00
0.00000000e+00 0.00000000e+00 0.00000000e+00 0.00000000e+00
0.00000000e+00 0.00000000e+00 0.00000000e+00 0.00000000e+00
1.72266641e-01 0.00000000e+00 0.00000000e+00 0.00000000e+00
0.00000000e+00 0.00000000e+00 0.00000000e+00 0.00000000e+00
0.00000000e+00 0.00000000e+00 7.59569859e-01 8.50017033e+02
0.00000000e+00 0.00000000e+00 1.84653016e-02 0.00000000e+00
0.00000000e+00 0.00000000e+00 0.00000000e+00 0.00000000e+00
0.00000000e+00 0.00000000e+00 0.00000000e+00 0.00000000e+00
4.19946659e-01]
CA [0. 0. 0. 0. 0.33796258 0.43902781
0. 0. 0. 0.09782357 0. 0.
0. 0. 0. 0. 0. 0.
0. 0. 0. 0. 0. 0.
0. 0. 0. 0. 0. 0.
0. 0. 0. 0. 0. 0.
0. 0.97688814 0. 0. 0. 0.
0. 0. 1.4591806 0. 0. 0.
0. 0. 0. 0. 0. 0.
0. ]
CO [0. 0. 0. 0. 0. 0.
0.33576748 0. 0. 0. 0. 0.
0. 0. 0. 0.13530653 0. 0.
0. 0. 0. 0. 0. 0.
0. 0. 0. 0. 0. 0.
0. 0. 0.08496784 0. 0. 0.
0. 0. 0. 0.01574976 0. 0.
0. 0. 0. 0. 0. 0.
0. 1.08451019 0. 0. 0. 0.
0. 0. 0. 0. 0. 1.97079352
0. ]

```

CT [0. 0. 0. 0. 0. 0.
0. 0. 0. 0. 0. 0.
0. 0. 0. 0. 0. 0.
0. 0.09932846 0. 0. 0. 0.
0. 0. 0. 0. 0. 0.
0. 0. 0.13419056 0. 0. 0.
0. 0. 0. 0. 0.72265285 0.
0. 0.15030951 0. 0. 0. 0.
0. 0. 0. 0. 0. 0.
0.]

DC [0.00000000e+00 0.00000000e+00 0.00000000e+00 0.00000000e+00
0.00000000e+00 0.00000000e+00 0.00000000e+00 0.00000000e+00
5.16381211e-01 0.00000000e+00 5.33220397e-05 0.00000000e+00
0.00000000e+00 0.00000000e+00 0.00000000e+00 0.00000000e+00
0.00000000e+00 0.00000000e+00 0.00000000e+00 0.00000000e+00
0.00000000e+00 0.00000000e+00 0.00000000e+00 0.00000000e+00
0.00000000e+00 4.27326283e-03 0.00000000e+00 0.00000000e+00
0.00000000e+00 0.00000000e+00 0.00000000e+00 0.00000000e+00
0.00000000e+00 0.00000000e+00 0.00000000e+00 0.00000000e+00
0.00000000e+00 0.00000000e+00 0.00000000e+00 8.24144783e-03
0.00000000e+00 0.00000000e+00 0.00000000e+00 0.00000000e+00
0.00000000e+00 0.00000000e+00 5.66567898e-02 0.00000000e+00
0.00000000e+00 0.00000000e+00 0.00000000e+00 0.00000000e+00
0.00000000e+00 0.00000000e+00 0.00000000e+00 0.00000000e+00
0.00000000e+00 0.00000000e+00 0.00000000e+00 0.00000000e+00
9.28862477e-02]

DE [0. 0. 0. 0. 0. 0.00325545
0. 0. 0. 0.04492638 0. 0.
0. 0. 0. 0. 0. 0.
0. 0. 0. 0.00593024 0. 0.
0. 0. 0. 0. 0. 0.
0. 0. 0. 0. 0. 0.
0. 0. 0.0033142 0. 0. 0.
0.0295854 0. 0. 0. 0.48047137 0.
0. 0. 0. 0. 0. 0.
0. 0. 0. 0. 0. 0.
0.07589609]

FL [0.00000000e+00 0.00000000e+00 0.00000000e+00 0.00000000e+00
4.37308089e-01 0.00000000e+00 0.00000000e+00 0.00000000e+00
0.00000000e+00 0.00000000e+00 6.66413033e-01 0.00000000e+00
0.00000000e+00 1.64303356e-01 0.00000000e+00 0.00000000e+00
5.25694292e-01 0.00000000e+00 0.00000000e+00 0.00000000e+00
0.00000000e+00 2.03352053e-01 0.00000000e+00 0.00000000e+00
0.00000000e+00 0.00000000e+00 0.00000000e+00 0.00000000e+00
0.00000000e+00 0.00000000e+00 0.00000000e+00 0.00000000e+00
0.00000000e+00 0.00000000e+00 0.00000000e+00 0.00000000e+00
0.00000000e+00 0.00000000e+00 0.00000000e+00 0.00000000e+00
0.00000000e+00 0.00000000e+00 0.00000000e+00 0.00000000e+00
0.00000000e+00 0.00000000e+00 0.00000000e+00 0.00000000e+00
0.00000000e+00 0.00000000e+00 0.00000000e+00 3.11467389e+03
0.00000000e+00 0.00000000e+00 0.00000000e+00 0.00000000e+00
0.00000000e+00 0.00000000e+00 0.00000000e+00 0.00000000e+00
0.00000000e+00 0.00000000e+00 0.00000000e+00 0.00000000e+00
1.86861224e+00]

FSM [0.00000000e+00 0.00000000e+00 0.00000000e+00 0.00000000e+00
8.96519695e-08 0.00000000e+00 0.00000000e+00 0.00000000e+00
0.00000000e+00 0.00000000e+00 0.00000000e+00 0.00000000e+00
0.00000000e+00 0.00000000e+00 0.00000000e+00 0.00000000e+00
0.00000000e+00 0.00000000e+00 0.00000000e+00 0.00000000e+00
4.85899265e-06 0.00000000e+00 0.00000000e+00 0.00000000e+00
0.00000000e+00 0.00000000e+00 0.00000000e+00 0.00000000e+00
0.00000000e+00 0.00000000e+00 0.00000000e+00 0.00000000e+00


```

0.00000000e+00 0.00000000e+00 0.00000000e+00 0.00000000e+00
0.00000000e+00 0.00000000e+00 1.26132665e-07 0.00000000e+00
0.00000000e+00 0.00000000e+00 0.00000000e+00 0.00000000e+00
0.00000000e+00 0.00000000e+00 0.00000000e+00 0.00000000e+00
0.00000000e+00 0.00000000e+00 0.00000000e+00 0.00000000e+00
0.00000000e+00 0.00000000e+00 0.00000000e+00 0.00000000e+00
0.00000000e+00 0.00000000e+00 0.00000000e+00 0.00000000e+00
0.00000000e+00 0.00000000e+00 0.00000000e+00 0.00000000e+00
0.00000000e+00]
GA [0.00000000e+00 8.20484758e-01 0.00000000e+00 0.00000000e+00
1.11773142e-01 2.03572851e-02 0.00000000e+00 0.00000000e+00
0.00000000e+00 0.00000000e+00 1.15174545e-01 0.00000000e+00
8.63021666e-03 0.00000000e+00 0.00000000e+00 0.00000000e+00
0.00000000e+00 0.00000000e+00 0.00000000e+00 0.00000000e+00
0.00000000e+00 0.00000000e+00 0.00000000e+00 0.00000000e+00
0.00000000e+00 0.00000000e+00 0.00000000e+00 0.00000000e+00
0.00000000e+00 0.00000000e+00 0.00000000e+00 6.29878395e-02
0.00000000e+00 0.00000000e+00 0.00000000e+00 0.00000000e+00
0.00000000e+00 0.00000000e+00 5.28781882e-02 0.00000000e+00
0.00000000e+00 0.00000000e+00 0.00000000e+00 0.00000000e+00
0.00000000e+00 0.00000000e+00 0.00000000e+00 1.71690294e+03
3.24294683e-02 0.00000000e+00 5.44822530e-02 7.07531138e-03
0.00000000e+00 0.00000000e+00 0.00000000e+00 0.00000000e+00
0.00000000e+00 0.00000000e+00 0.00000000e+00 0.00000000e+00
9.03481647e-01]
GU [0.      0.      0.      0.      0.      0.
0.      0.      0.      0.      0.      0.
0.      0.73686895 0.04153216 0.      0.      0.
0.      0.      0.      0.      0.      0.
0.      0.      0.      0.      4.26294809 0.
0.      0.      0.00476813 0.      0.      0.
0.      0.      0.      0.      0.      0.
0.      0.      0.      0.      0.      0.
0.      0.      0.      0.      0.      0.
0.      0.      0.      0.      0.      0.
0.      0.      0.      0.      0.      0.
0.      ]
HI [0.00000000e+00 0.00000000e+00 0.00000000e+00 0.00000000e+00
0.00000000e+00 0.00000000e+00 0.00000000e+00 0.00000000e+00
0.00000000e+00 0.00000000e+00 6.71377579e-04 0.00000000e+00
0.00000000e+00 1.62908279e-02 6.75553788e-01 0.00000000e+00
0.00000000e+00 0.00000000e+00 0.00000000e+00 0.00000000e+00
0.00000000e+00 0.00000000e+00 0.00000000e+00 0.00000000e+00
0.00000000e+00 0.00000000e+00 0.00000000e+00 0.00000000e+00
1.00485116e+01 0.00000000e+00 0.00000000e+00 0.00000000e+00
4.76945214e-03 0.00000000e+00 0.00000000e+00 0.00000000e+00
0.00000000e+00 0.00000000e+00 0.00000000e+00 0.00000000e+00
0.00000000e+00 0.00000000e+00 0.00000000e+00 0.00000000e+00
0.00000000e+00 0.00000000e+00 0.00000000e+00 3.87262119e+01
0.00000000e+00 0.00000000e+00 0.00000000e+00 0.00000000e+00
0.00000000e+00 0.00000000e+00 2.34005096e+00 0.00000000e+00
0.00000000e+00 0.00000000e+00 0.00000000e+00 0.00000000e+00
4.86093515e-03]
IA [0.      0.      0.      0.      0.      0.
0.      0.      0.      0.      0.      0.
0.07437522 4.89885033 0.      0.11564757 0.      0.
0.      0.      0.      0.      0.      0.
0.      0.      0.      0.      0.      0.
0.      0.      1.06835334 0.      0.      0.
0.      0.      0.      0.      0.      0.
0.      0.      0.      0.      0.      0.
0.      0.66032224 0.      0.      0.      0.
0.      0.      0.      0.      0.      0.
0.14746971]

```

ID [8.67135329e-01 0.00000000e+00 0.00000000e+00 0.00000000e+00
0.00000000e+00 0.00000000e+00 0.00000000e+00 0.00000000e+00
0.00000000e+00 0.00000000e+00 1.62457553e-02 0.00000000e+00
0.00000000e+00 1.04841094e+00 0.00000000e+00 0.00000000e+00
1.73981144e-01 0.00000000e+00 0.00000000e+00 0.00000000e+00
0.00000000e+00 0.00000000e+00 0.00000000e+00 0.00000000e+00
0.00000000e+00 0.00000000e+00 0.00000000e+00 0.00000000e+00
2.45767295e+01 0.00000000e+00 0.00000000e+00 0.00000000e+00
1.19129758e-01 0.00000000e+00 0.00000000e+00 0.00000000e+00
0.00000000e+00 0.00000000e+00 0.00000000e+00 0.00000000e+00
0.00000000e+00 0.00000000e+00 0.00000000e+00 0.00000000e+00
0.00000000e+00 0.00000000e+00 0.00000000e+00 0.00000000e+00
0.00000000e+00 2.23380371e-01 1.50644685e-02 0.00000000e+00
0.00000000e+00 0.00000000e+00 0.00000000e+00 0.00000000e+00
0.00000000e+00 0.00000000e+00 0.00000000e+00 0.00000000e+00
1.35325268e-01]

IL [0. 0. 0. 0. 0. 0.
0. 0. 2.73045171 0. 0. 0.
0.1054787 0. 0. 0. 0. 0.25329707
0. 0. 0. 0. 0. 0.
0. 0. 0. 0. 0. 0.
0. 0. 1.45878765 0. 0. 0.
0. 0. 0. 0.05105017 0. 0.
0. 0. 0. 0. 0.32846927 0.
0. 4.05689125 0. 0. 0. 0.
0. 0. 0. 0. 0. 0.
0.31914274]

IN [1.83866889e+00 0.00000000e+00 0.00000000e+00 0.00000000e+00
0.00000000e+00 0.00000000e+00 3.37762888e-01 0.00000000e+00
0.00000000e+00 0.00000000e+00 0.00000000e+00 0.00000000e+00
0.00000000e+00 1.74515217e+00 0.00000000e+00 8.28176239e-02
0.00000000e+00 0.00000000e+00 0.00000000e+00 0.00000000e+00
0.00000000e+00 0.00000000e+00 0.00000000e+00 0.00000000e+00
0.00000000e+00 9.67826177e-03 0.00000000e+00 0.00000000e+00
1.41327593e+01 0.00000000e+00 0.00000000e+00 0.00000000e+00
0.00000000e+00 0.00000000e+00 0.00000000e+00 0.00000000e+00
0.00000000e+00 0.00000000e+00 0.00000000e+00 0.00000000e+00
0.00000000e+00 0.00000000e+00 0.00000000e+00 0.00000000e+00
0.00000000e+00 0.00000000e+00 1.17471579e+00 0.00000000e+00
0.00000000e+00 9.77808457e-01 1.33350624e-01 0.00000000e+00
0.00000000e+00 0.00000000e+00 0.00000000e+00 0.00000000e+00
0.00000000e+00 0.00000000e+00 2.38681797e-01 0.00000000e+00
0.00000000e+00]

KS [0.08858036 0. 0. 0. 0.
0.1222471 0. 0. 0. 0. 0.
0.05027515 0.82264582 0. 0.09496475 0. 0.
0. 0. 0. 0. 0. 0.
0. 0. 0. 0. 0. 0.
0. 0. 0. 0. 0. 0.
0. 0. 0. 0. 0. 0.
0. 0.79290342 0.06818557 0. 0. 0.
0. 0. 0. 0. 0.14478736 0.
0.]

KY [0.00000000e+00 0.00000000e+00 3.85801830e-01 0.00000000e+00
0.00000000e+00 0.00000000e+00 0.00000000e+00 0.00000000e+00
0.00000000e+00 0.00000000e+00 5.53916098e-03 0.00000000e+00
0.00000000e+00 1.85842928e+00 0.00000000e+00 0.00000000e+00
0.00000000e+00 0.00000000e+00 0.00000000e+00 0.00000000e+00
0.00000000e+00 0.00000000e+00 0.00000000e+00 0.00000000e+00
0.00000000e+00 0.00000000e+00 0.00000000e+00 0.00000000e+00
0.00000000e+00 0.00000000e+00 0.00000000e+00 0.00000000e+00

```

4.58066528e-01 0.00000000e+00 0.00000000e+00 0.00000000e+00
0.00000000e+00 0.00000000e+00 0.00000000e+00 0.00000000e+00
0.00000000e+00 0.00000000e+00 0.00000000e+00 0.00000000e+00
9.77430232e-02 0.00000000e+00 5.45444423e-01 2.21662183e+02
0.00000000e+00 0.00000000e+00 0.00000000e+00 0.00000000e+00
0.00000000e+00 0.00000000e+00 0.00000000e+00 0.00000000e+00
0.00000000e+00 0.00000000e+00 1.14243235e+00 0.00000000e+00
0.00000000e+00]
LA [0.      0.      0.      0.      0.07996661 0.
0.      0.      0.      0.      0.02963014 0.
0.      0.      0.      0.15898998 0.      0.
0.      0.      0.      0.44496871 0.      0.
0.      0.00534616 0.      0.      0.      0.
0.      0.      0.      0.      0.      0.
0.      0.      0.      0.01175926 0.      0.
0.      0.      0.      0.      0.      0.
0.      0.      0.03121161 0.      0.      0.
0.      0.      0.      0.      0.      0.
0.79208377]
MA [ 0.      0.      0.      0.      0.      0.
0.      0.      0.      0.      0.      0.
0.      0.      0.      0.      0.      0.
0.      0.      0.      0.      27.35892033 0.
0.      0.      0.      0.      0.      0.
0.      0.      0.28041119 0.03141124 0.      0.
0.      0.      0.      0.      2.25645764 0.
0.      0.      0.06276643 0.      0.      0.
0.      0.      0.      0.      0.      0.
0.      ]
MD [0.00000000e+00 0.00000000e+00 0.00000000e+00 0.00000000e+00
0.00000000e+00 0.00000000e+00 0.00000000e+00 0.00000000e+00
2.63721064e+00 0.00000000e+00 0.00000000e+00 0.00000000e+00
0.00000000e+00 0.00000000e+00 0.00000000e+00 1.33143817e-01
0.00000000e+00 0.00000000e+00 0.00000000e+00 0.00000000e+00
0.00000000e+00 1.30838661e-01 0.00000000e+00 7.79377714e-02
0.00000000e+00 0.00000000e+00 0.00000000e+00 0.00000000e+00
2.01509568e+00 0.00000000e+00 0.00000000e+00 0.00000000e+00
0.00000000e+00 0.00000000e+00 0.00000000e+00 0.00000000e+00
0.00000000e+00 0.00000000e+00 0.00000000e+00 0.00000000e+00
0.00000000e+00 0.00000000e+00 0.00000000e+00 0.00000000e+00
0.00000000e+00 0.00000000e+00 9.06680415e-01 0.00000000e+00
0.00000000e+00 0.00000000e+00 3.06500844e-02 0.00000000e+00
0.00000000e+00 0.00000000e+00 0.00000000e+00 0.00000000e+00
0.00000000e+00 0.00000000e+00 2.25673332e-03 0.00000000e+00
3.93755853e-01]
ME [0.00000000e+00 0.00000000e+00 0.00000000e+00 0.00000000e+00
0.00000000e+00 1.22720279e-03 0.00000000e+00 0.00000000e+00
0.00000000e+00 0.00000000e+00 0.00000000e+00 1.24311507e+02
0.00000000e+00 0.00000000e+00 0.00000000e+00 0.00000000e+00
0.00000000e+00 0.00000000e+00 0.00000000e+00 0.00000000e+00
0.00000000e+00 0.00000000e+00 0.00000000e+00 0.00000000e+00
5.15789417e-02 0.00000000e+00 0.00000000e+00 0.00000000e+00
0.00000000e+00 0.00000000e+00 0.00000000e+00 0.00000000e+00
0.00000000e+00 0.00000000e+00 2.49201844e-01 0.00000000e+00
0.00000000e+00 0.00000000e+00 4.47794185e-03 0.00000000e+00
0.00000000e+00 0.00000000e+00 0.00000000e+00 0.00000000e+00
0.00000000e+00 0.00000000e+00 0.00000000e+00 0.00000000e+00
0.00000000e+00 0.00000000e+00 0.00000000e+00 0.00000000e+00
0.00000000e+00 0.00000000e+00 0.00000000e+00 0.00000000e+00
0.00000000e+00 0.00000000e+00 1.37275669e-01 0.00000000e+00
0.00000000e+00]

```

MI	0.	0.	0.	0.	0.	0.
0.	0.	0.	0.	0.	0.	0.
0.	0.	0.	0.10410175	0.	0.	0.
0.	0.	0.	0.	0.	0.	0.
0.	0.43825002	0.	0.	0.	0.	0.
0.	0.	1.45065234	0.	0.	0.	0.
0.	0.	0.	0.063103	0.	0.	0.
0.	0.	0.	0.	0.	0.	0.
0.	0.28466062	0.	0.	0.	0.	0.
0.	0.	0.	0.	0.	0.	1.9347288

0.20833302]

MN [0.00000000e+00 0.00000000e+00 0.00000000e+00 0.00000000e+00
0.00000000e+00 0.00000000e+00 2.63041863e-01 0.00000000e+00
0.00000000e+00 0.00000000e+00 0.00000000e+00 0.00000000e+00
0.00000000e+00 0.00000000e+00 0.00000000e+00 5.32172326e-01
0.00000000e+00 0.00000000e+00 0.00000000e+00 0.00000000e+00
0.00000000e+00 0.00000000e+00 0.00000000e+00 0.00000000e+00
0.00000000e+00 0.00000000e+00 8.46773963e-02 0.00000000e+00
0.00000000e+00 0.00000000e+00 0.00000000e+00 0.00000000e+00
1.65043501e+00 0.00000000e+00 0.00000000e+00 0.00000000e+00
0.00000000e+00 0.00000000e+00 0.00000000e+00 0.00000000e+00
0.00000000e+00 0.00000000e+00 0.00000000e+00 0.00000000e+00
0.00000000e+00 0.00000000e+00 0.00000000e+00 6.86083314e+02
0.00000000e+00 0.00000000e+00 0.00000000e+00 0.00000000e+00
0.00000000e+00 0.00000000e+00 0.00000000e+00 0.00000000e+00
0.00000000e+00 0.00000000e+00 0.00000000e+00 0.00000000e+00
0.00000000e+00]

MO [1.12197893e+00 0.00000000e+00 0.00000000e+00 0.00000000e+00
0.00000000e+00 0.00000000e+00 0.00000000e+00 0.00000000e+00
0.00000000e+00 0.00000000e+00 0.00000000e+00 0.00000000e+00
1.14447163e-01 5.29819220e+00 0.00000000e+00 1.74392916e-02
0.00000000e+00 0.00000000e+00 0.00000000e+00 0.00000000e+00
0.00000000e+00 0.00000000e+00 0.00000000e+00 0.00000000e+00
0.00000000e+00 0.00000000e+00 0.00000000e+00 0.00000000e+00
5.86448186e+01 0.00000000e+00 0.00000000e+00 0.00000000e+00
1.63269462e+00 0.00000000e+00 0.00000000e+00 0.00000000e+00
0.00000000e+00 0.00000000e+00 0.00000000e+00 0.00000000e+00
0.00000000e+00 0.00000000e+00 0.00000000e+00 0.00000000e+00
0.00000000e+00 0.00000000e+00 0.00000000e+00 0.00000000e+00
0.00000000e+00 9.69110113e-02 2.00279782e-01 0.00000000e+00
0.00000000e+00 0.00000000e+00 0.00000000e+00 0.00000000e+00
0.00000000e+00 0.00000000e+00 0.00000000e+00 0.00000000e+00
0.00000000e+00]

MP [0.00000000e+00 0.00000000e+00 0.00000000e+00 0.00000000e+00
0.00000000e+00 0.00000000e+00 0.00000000e+00 0.00000000e+00
0.00000000e+00 0.00000000e+00 4.04304932e-06 0.00000000e+00
0.00000000e+00 3.61475829e-03 0.00000000e+00 0.00000000e+00
0.00000000e+00 0.00000000e+00 0.00000000e+00 0.00000000e+00
0.00000000e+00 1.14112943e-05 0.00000000e+00 0.00000000e+00
0.00000000e+00 0.00000000e+00 0.00000000e+00 0.00000000e+00
0.00000000e+00 0.00000000e+00 0.00000000e+00 0.00000000e+00
0.00000000e+00 0.00000000e+00 0.00000000e+00 0.00000000e+00
0.00000000e+00 0.00000000e+00 0.00000000e+00 8.69850322e-06
0.00000000e+00 0.00000000e+00 0.00000000e+00 0.00000000e+00
0.00000000e+00 0.00000000e+00 0.00000000e+00 0.00000000e+00
0.00000000e+00 0.00000000e+00 1.79191666e-05 0.00000000e+00
0.00000000e+00 0.00000000e+00 0.00000000e+00 0.00000000e+00
0.00000000e+00 0.00000000e+00 0.00000000e+00 0.00000000e+00
1.42423894e-03]

MS [0.00000000e+00 4.28720909e-03 2.28530908e-02 0.00000000e+00
9.47862400e-04 0.00000000e+00 0.00000000e+00 0.00000000e+00
0.00000000e+00 2.70598155e-01 4.19116600e-02 0.00000000e+00

```

0.00000000e+00 0.00000000e+00 0.00000000e+00 0.00000000e+00
1.17863439e-01 0.00000000e+00 0.00000000e+00 0.00000000e+00
0.00000000e+00 0.00000000e+00 0.00000000e+00 0.00000000e+00
0.00000000e+00 0.00000000e+00 4.81095940e-03 0.00000000e+00
4.95576530e+01 1.31617635e-01 0.00000000e+00 0.00000000e+00
0.00000000e+00 0.00000000e+00 0.00000000e+00 0.00000000e+00
4.66920728e-02 1.46597096e-01 0.00000000e+00 0.00000000e+00
0.00000000e+00 0.00000000e+00 8.04725926e-02 0.00000000e+00
0.00000000e+00 0.00000000e+00 0.00000000e+00 0.00000000e+00
0.00000000e+00 0.00000000e+00 4.24200585e-02 0.00000000e+00
0.00000000e+00 0.00000000e+00 0.00000000e+00 0.00000000e+00
0.00000000e+00 0.00000000e+00 0.00000000e+00 0.00000000e+00
5.14181930e-01]
MT [0.      0.      0.      0.      0.      0.
0.      0.      0.      0.      0.      0.
0.      1.69034837 0.      0.      0.      0.
0.      0.      0.01118974 0.      0.      0.
0.      0.      0.      0.      0.      0.
0.13338696 0.      0.      0.      0.      0.
0.      0.      0.      0.      0.      0.
0.      0.      0.      0.      0.      0.
0.      0.28174607 0.      0.      0.      0.
0.      0.      0.      0.06572043 0.      0.
0.      ]
NC [0.00000000e+00 0.00000000e+00 1.16086143e+00 0.00000000e+00
7.24221721e-02 7.51834633e-03 0.00000000e+00 0.00000000e+00
0.00000000e+00 7.69653993e-01 0.00000000e+00 0.00000000e+00
0.00000000e+00 0.00000000e+00 0.00000000e+00 0.00000000e+00
0.00000000e+00 0.00000000e+00 0.00000000e+00 0.00000000e+00
0.00000000e+00 0.00000000e+00 0.00000000e+00 0.00000000e+00
0.00000000e+00 0.00000000e+00 0.00000000e+00 0.00000000e+00
4.31417773e+01 7.30080745e-02 0.00000000e+00 2.02093700e-01
0.00000000e+00 0.00000000e+00 5.82685500e-02 0.00000000e+00
0.00000000e+00 0.00000000e+00 0.00000000e+00 0.00000000e+00
0.00000000e+00 0.00000000e+00 0.00000000e+00 0.00000000e+00
5.24700367e-02 0.00000000e+00 4.93167048e-01 0.00000000e+00
0.00000000e+00 0.00000000e+00 6.17889854e-02 0.00000000e+00
0.00000000e+00 0.00000000e+00 0.00000000e+00 0.00000000e+00
0.00000000e+00 0.00000000e+00 6.10261893e-02 0.00000000e+00
4.13484180e-01]
ND [0.      0.      0.      0.      0.      0.
0.      0.      0.      0.      0.      0.
0.      4.69025155 0.      0.      0.      0.
0.      0.      0.      0.      0.      0.
0.      0.      0.      0.      2.74284778 0.
0.      0.      0.25927085 0.      0.      0.
0.      0.      0.      0.      0.      0.
0.      0.      0.      0.      0.      0.
0.      0.36085167 0.      0.      0.      0.
0.      0.      0.      0.      0.      0.
0.      ]
NE [0.      0.      0.      0.      0.      0.
0.      0.      0.16591866 0.      0.      0.
0.02127342 0.      0.      0.01932181 0.      0.02065921
0.      0.      0.      0.      0.      0.
0.      0.      0.      0.      0.      0.
0.      0.      0.06764903 0.04593345 0.      0.
0.      0.      0.      0.      0.      0.
0.      0.      0.      0.      0.      0.
0.      1.0833431 0.      0.      0.      0.
0.      0.      0.      0.      0.      0.
0.0893231 ]

```

NH [0.00000000e+00 0.00000000e+00 0.00000000e+00 0.00000000e+00
0.00000000e+00 0.00000000e+00 3.34727588e-03 0.00000000e+00
0.00000000e+00 0.00000000e+00 0.00000000e+00 1.78573083e+02
0.00000000e+00 0.00000000e+00 0.00000000e+00 0.00000000e+00
0.00000000e+00 0.00000000e+00 0.00000000e+00 0.00000000e+00
0.00000000e+00 0.00000000e+00 0.00000000e+00 0.00000000e+00
0.00000000e+00 0.00000000e+00 0.00000000e+00 0.00000000e+00
0.00000000e+00 0.00000000e+00 0.00000000e+00 0.00000000e+00
0.00000000e+00 0.00000000e+00 4.21115103e-01 0.00000000e+00
0.00000000e+00 0.00000000e+00 0.00000000e+00 0.00000000e+00
0.00000000e+00 0.00000000e+00 0.00000000e+00 2.17190874e-03
0.00000000e+00 0.00000000e+00 2.19457127e-01 0.00000000e+00
0.00000000e+00 0.00000000e+00 0.00000000e+00 0.00000000e+00
0.00000000e+00 0.00000000e+00 0.00000000e+00 0.00000000e+00
0.00000000e+00 0.00000000e+00 1.35389757e-01 0.00000000e+00
0.00000000e+00]

NJ [0. 0. 0. 0. 0. 0.
0.16226932 0. 0. 0. 0. 0.
0. 0. 0. 0. 0. 0.
0. 0. 0. 0. 0. 0.
0. 0.15488539 0. 0. 0. 0.
0. 0. 0. 0. 0. 0.
0. 0. 0.08038639 0.52737166 0. 0.
0. 0. 0. 0. 0.90812213 0.
0. 0.72866887 0. 0. 0. 0.
0. 0. 0. 0. 0. 0.
0.]

NM [0.00000000e+00 0.00000000e+00 0.00000000e+00 0.00000000e+00
7.12750102e-03 8.97631318e-06 1.62091469e-01 0.00000000e+00
0.00000000e+00 0.00000000e+00 0.00000000e+00 0.00000000e+00
0.00000000e+00 0.00000000e+00 0.00000000e+00 0.00000000e+00
0.00000000e+00 0.00000000e+00 0.00000000e+00 0.00000000e+00
0.00000000e+00 0.00000000e+00 0.00000000e+00 0.00000000e+00
0.00000000e+00 0.00000000e+00 0.00000000e+00 0.00000000e+00
0.00000000e+00 0.00000000e+00 0.00000000e+00 0.00000000e+00
3.54898847e-02 1.42866991e-01 0.00000000e+00 0.00000000e+00
7.94713690e-02 0.00000000e+00 0.00000000e+00 0.00000000e+00
0.00000000e+00 0.00000000e+00 0.00000000e+00 0.00000000e+00
0.00000000e+00 0.00000000e+00 3.23509406e-02 1.27150207e+03
0.00000000e+00 1.37614774e-01 4.46217725e-03 0.00000000e+00
8.20758196e-02 0.00000000e+00 0.00000000e+00 0.00000000e+00
0.00000000e+00 0.00000000e+00 7.41908080e-02 0.00000000e+00
0.00000000e+00]

NV [1.19689027 0. 0. 0.02659907 0.
0. 0. 0. 0. 0.0222601 0.
0. 0. 0. 0. 0. 0.
0. 0. 0. 0.1182556 0. 0.
0. 0. 0.1201737 0. 0. 0.
0. 0. 0. 0. 0. 0.
0. 0. 0. 0. 0. 0.
0. 0. 0. 0. 0. 0.
0. 0. 0.08246552 0. 0. 0.
0. 0. 0. 0. 0. 0.
0.0564439]

NY [0. 0. 0. 0. 0. 0.
0. 0. 0. 0. 0. 0.
0. 0. 0. 0. 0. 0.
0. 0.06236821 0. 0. 0. 0.
0. 0. 0. 0. 0. 0.
0. 0. 0.45061854 0.3029183 0. 0.
0. 0. 0. 0. 0. 0.]

0.	0.	0.00299471	0.	0.	0.
0.	0.	0.	0.	2.13383046	0.
0.02458514]					
NYC	[0.	0.	0.	0.	0.
0.	0.	0.	0.	0.	0.
0.	0.	0.	0.	0.	0.
0.	0.	0.	0.	0.	0.
0.	0.	0.	0.	0.	0.
0.	0.	0.	0.	0.	0.
0.	0.	0.	0.87341923	0.	0.
0.	0.	0.	0.	0.	0.
0.	0.	0.	0.	0.	0.
0.	0.	0.	0.	0.62621572	0.
0.68045929]					
OH	[2.70795275	0.	0.	0.	0.03295101
0.67700651	0.	0.	0.	0.	0.
0.	0.	0.	0.	0.	0.
0.	0.	0.	0.	0.	0.
0.	0.15107002	0.	0.	0.	0.
0.	0.	0.	0.	0.	0.
0.	0.	0.	0.	0.	0.
0.	0.	0.	0.	0.7834657	0.
0.	0.	0.19170376	0.	0.	0.
0.	0.	0.	0.	1.46761989	0.
0.]					
OK	[0.00000000e+00	0.00000000e+00	3.97232615e-01	0.00000000e+00	0.00000000e+00
0.00000000e+00	0.00000000e+00	0.00000000e+00	0.00000000e+00	0.00000000e+00	0.00000000e+00
0.00000000e+00	0.00000000e+00	1.81170587e-05	0.00000000e+00	0.00000000e+00	0.00000000e+00
3.98872085e-03	8.71514018e-01	0.00000000e+00	6.31417131e-02	0.00000000e+00	0.00000000e+00
0.00000000e+00	0.00000000e+00	0.00000000e+00	0.00000000e+00	0.00000000e+00	0.00000000e+00
8.44550128e-02	0.00000000e+00	0.00000000e+00	0.00000000e+00	0.00000000e+00	0.00000000e+00
0.00000000e+00	0.00000000e+00	0.00000000e+00	5.18122673e-02	0.00000000e+00	0.00000000e+00
0.00000000e+00	0.00000000e+00	0.00000000e+00	0.00000000e+00	0.00000000e+00	0.00000000e+00
3.25675452e-01	0.00000000e+00	0.00000000e+00	0.00000000e+00	0.00000000e+00	0.00000000e+00
0.00000000e+00	0.00000000e+00	0.00000000e+00	0.00000000e+00	0.00000000e+00	0.00000000e+00
0.00000000e+00	0.00000000e+00	0.00000000e+00	0.00000000e+00	0.00000000e+00	0.00000000e+00
0.00000000e+00	0.00000000e+00	0.00000000e+00	3.52073896e+02	0.00000000e+00	0.00000000e+00
2.93674651e-02	0.00000000e+00	9.31112729e-02	0.00000000e+00	0.00000000e+00	0.00000000e+00
0.00000000e+00	0.00000000e+00	0.00000000e+00	0.00000000e+00	0.00000000e+00	0.00000000e+00
0.00000000e+00	0.00000000e+00	7.11487908e-01	0.00000000e+00	0.00000000e+00	0.00000000e+00
0.00000000e+00]					
OR	[0.48206416	0.	0.11273074	0.	0.00791134
0.05597792	0.	0.	0.	0.	0.
0.	0.	0.	0.	0.	0.
0.	0.	0.	0.0279397	0.	0.
0.	0.	0.02522256	0.	0.	0.
0.	0.	0.	0.	0.	0.
0.10193906	0.	0.	0.	0.	0.
0.	0.	0.	0.	0.	0.
0.	0.	0.01861357	0.00182314	0.	0.
0.	0.	0.	0.	0.	0.
0.02264588]					
PA	[1.22382397	0.	0.	0.	0.
0.	0.	0.	0.	0.	0.
0.	0.	0.	0.	0.	0.
0.	0.	0.	0.	0.	0.
0.	0.3455752	0.	0.	0.	0.
0.	0.	0.	0.	2.51702382	0.
0.	0.	0.00284436	0.	0.	0.
0.05874878	0.12090951	0.	0.	2.39963416	0.
0.	0.	0.09720822	0.	0.	0.
0.	0.	0.	0.	0.	0.

```
0. ]  
PR [1.44450921e-01 0.00000000e+00 0.00000000e+00 0.00000000e+00  
0.00000000e+00 0.00000000e+00 0.00000000e+00 0.00000000e+00  
0.00000000e+00 0.00000000e+00 0.00000000e+00 0.00000000e+00  
0.00000000e+00 3.24898491e-01 0.00000000e+00 0.00000000e+00  
0.00000000e+00 0.00000000e+00 0.00000000e+00 0.00000000e+00  
0.00000000e+00 0.00000000e+00 0.00000000e+00 0.00000000e+00  
0.00000000e+00 0.00000000e+00 0.00000000e+00 3.63790698e-02  
1.11990999e+01 0.00000000e+00 0.00000000e+00 0.00000000e+00  
0.00000000e+00 0.00000000e+00 0.00000000e+00 0.00000000e+00  
0.00000000e+00 0.00000000e+00 0.00000000e+00 0.00000000e+00  
0.00000000e+00 2.90797957e-03 0.00000000e+00 0.00000000e+00  
0.00000000e+00 0.00000000e+00 0.00000000e+00 0.00000000e+00  
0.00000000e+00 0.00000000e+00 5.61696096e-02 0.00000000e+00  
0.00000000e+00 0.00000000e+00 3.85408429e+00 0.00000000e+00  
0.00000000e+00 2.85458222e-02 0.00000000e+00 0.00000000e+00  
0.00000000e+00]  
PW [0. 0. 0. 0. 0. 0. 0. 0. 0. 0. 0. 0. 0. 0. 0. 0. 0. 0. 0. 0. 0. 0.  
0. 0. 0. 0. 0. 0. 0. 0. 0. 0. 0. 0. 0. 0. 0. 0. 0. 0. 0. 0. 0. 0.  
0. 0. 0. 0. 0. 0. 0. 0. 0. 0. 0. 0. 0. 0. 0. 0.]  
RI [ 0.      0.      0.      0.      0.      0.  
0.      0.      0.      0.      0.      0.  
0.      0.      0.      0.      0.      0.  
0.      0.05688679 0.      0.      11.28600904 0.  
0.      0.      0.      0.      0.      0.  
0.01973239 0.      0.02334211 0.      0.      0.  
0.      0.      0.02135015 0.      0.3672282 0.  
0.      0.12428071 0.      0.      0.      0.  
0.      0.      0.      0.      0.      0.  
0.      ]  
RMI [0.00000000e+00 0.00000000e+00 0.00000000e+00 0.00000000e+00  
0.00000000e+00 0.00000000e+00 0.00000000e+00 0.00000000e+00  
0.00000000e+00 0.00000000e+00 0.00000000e+00 0.00000000e+00  
0.00000000e+00 9.08331850e-04 0.00000000e+00 2.75767036e-06  
0.00000000e+00 0.00000000e+00 0.00000000e+00 0.00000000e+00  
0.00000000e+00 0.00000000e+00 0.00000000e+00 0.00000000e+00  
0.00000000e+00 0.00000000e+00 0.00000000e+00 0.00000000e+00  
0.00000000e+00 0.00000000e+00 0.00000000e+00 0.00000000e+00  
0.00000000e+00 0.00000000e+00 0.00000000e+00 0.00000000e+00  
0.00000000e+00 0.00000000e+00 0.00000000e+00 0.00000000e+00  
0.00000000e+00 0.00000000e+00 0.00000000e+00 0.00000000e+00  
0.00000000e+00 0.00000000e+00 0.00000000e+00 0.00000000e+00  
0.00000000e+00 0.00000000e+00 0.00000000e+00 0.00000000e+00  
0.00000000e+00 0.00000000e+00 0.00000000e+00 0.00000000e+00  
0.00000000e+00]  
SC [0.00000000e+00 0.00000000e+00 2.73071315e-01 0.00000000e+00  
2.05616382e-01 8.56979307e-03 0.00000000e+00 0.00000000e+00  
0.00000000e+00 0.00000000e+00 3.68283912e-03 7.16783215e+02  
0.00000000e+00 1.05823811e+00 1.16194157e-01 0.00000000e+00  
0.00000000e+00 0.00000000e+00 0.00000000e+00 0.00000000e+00  
0.00000000e+00 0.00000000e+00 0.00000000e+00 0.00000000e+00  
0.00000000e+00 0.00000000e+00 0.00000000e+00 0.00000000e+00  
2.63985481e+01 0.00000000e+00 0.00000000e+00 0.00000000e+00  
0.00000000e+00 0.00000000e+00 0.00000000e+00 0.00000000e+00  
0.00000000e+00 0.00000000e+00 0.00000000e+00 0.00000000e+00  
0.00000000e+00 0.00000000e+00 0.00000000e+00 0.00000000e+00  
0.00000000e+00 0.00000000e+00 0.00000000e+00 0.00000000e+00  
3.36820279e-01 0.00000000e+00 0.00000000e+00 0.00000000e+00  
0.00000000e+00 0.00000000e+00 0.00000000e+00 0.00000000e+00  
0.00000000e+00 0.00000000e+00 0.00000000e+00 0.00000000e+00
```


5.00396850e-01]

SD [0.00000000e+00 0.00000000e+00 0.00000000e+00 0.00000000e+00
0.00000000e+00 0.00000000e+00 0.00000000e+00 0.00000000e+00
0.00000000e+00 0.00000000e+00 0.00000000e+00 0.00000000e+00
0.00000000e+00 3.55679007e+00 0.00000000e+00 0.00000000e+00
0.00000000e+00 0.00000000e+00 0.00000000e+00 0.00000000e+00
0.00000000e+00 0.00000000e+00 0.00000000e+00 0.00000000e+00
0.00000000e+00 0.00000000e+00 0.00000000e+00 0.00000000e+00
4.77398618e+01 0.00000000e+00 0.00000000e+00 0.00000000e+00
6.94786826e-02 0.00000000e+00 0.00000000e+00 0.00000000e+00
0.00000000e+00 0.00000000e+00 0.00000000e+00 0.00000000e+00
0.00000000e+00 0.00000000e+00 0.00000000e+00 0.00000000e+00
0.00000000e+00 0.00000000e+00 0.00000000e+00 0.00000000e+00
0.00000000e+00 6.17611066e-01 0.00000000e+00 0.00000000e+00
0.00000000e+00 0.00000000e+00 0.00000000e+00 0.00000000e+00
0.00000000e+00 5.51658417e-03 0.00000000e+00 0.00000000e+00
0.00000000e+00]

TN [0.00000000e+00 0.00000000e+00 0.00000000e+00 0.00000000e+00
0.00000000e+00 0.00000000e+00 0.00000000e+00 0.00000000e+00
0.00000000e+00 7.18809198e-01 0.00000000e+00 0.00000000e+00
0.00000000e+00 0.00000000e+00 0.00000000e+00 0.00000000e+00
1.59361617e+00 0.00000000e+00 0.00000000e+00 0.00000000e+00
0.00000000e+00 0.00000000e+00 0.00000000e+00 0.00000000e+00
0.00000000e+00 0.00000000e+00 0.00000000e+00 0.00000000e+00
1.77262367e+02 0.00000000e+00 0.00000000e+00 0.00000000e+00
0.00000000e+00 0.00000000e+00 0.00000000e+00 0.00000000e+00
0.00000000e+00 4.33340299e-01 0.00000000e+00 0.00000000e+00
5.05012555e-02 0.00000000e+00 0.00000000e+00 6.78637906e-02
0.00000000e+00 0.00000000e+00 0.00000000e+00 0.00000000e+00
0.00000000e+00 0.00000000e+00 2.41031785e-01 0.00000000e+00
0.00000000e+00 0.00000000e+00 0.00000000e+00 0.00000000e+00
0.00000000e+00 0.00000000e+00 0.00000000e+00 0.00000000e+00
3.27562710e-02]

TX [0.00000000e+00 0.00000000e+00 2.38400317e+00 0.00000000e+00
4.88781858e-01 0.00000000e+00 0.00000000e+00 0.00000000e+00
0.00000000e+00 0.00000000e+00 3.08269121e-01 0.00000000e+00
5.50421215e-02 0.00000000e+00 0.00000000e+00 0.00000000e+00
0.00000000e+00 0.00000000e+00 0.00000000e+00 0.00000000e+00
0.00000000e+00 3.63256804e-01 0.00000000e+00 0.00000000e+00
0.00000000e+00 0.00000000e+00 9.46913629e-02 0.00000000e+00
3.08370923e+01 0.00000000e+00 0.00000000e+00 0.00000000e+00
2.10774875e-01 0.00000000e+00 0.00000000e+00 0.00000000e+00
0.00000000e+00 2.60402572e-01 0.00000000e+00 0.00000000e+00
0.00000000e+00 0.00000000e+00 0.00000000e+00 0.00000000e+00
0.00000000e+00 0.00000000e+00 0.00000000e+00 4.17513894e+03
0.00000000e+00 0.00000000e+00 4.76272474e-01 4.59288089e-02
0.00000000e+00 0.00000000e+00 0.00000000e+00 0.00000000e+00
0.00000000e+00 0.00000000e+00 0.00000000e+00 0.00000000e+00
1.04822641e+00]

UT [0. 0. 0.28094675 0. 0.0048118 0.
0. 0. 0. 0. 0. 0.
0. 0. 0. 0. 0. 0.
0. 0. 0. 0. 0. 0.
0. 0. 0.14623845 0. 0. 0.
0. 0. 0. 0. 0. 0.
0. 0. 0. 0. 0.0428161 0.
0. 1.09080658 0.02579313 0. 0.22771938 0.
0. 0. 0. 0. 0.23994446 0.
0.09385827]

VA [0.00000000e+00 0.00000000e+00 1.83746504e-01 0.00000000e+00
0.00000000e+00 1.20029272e-02 0.00000000e+00 0.00000000e+00

1.43108667e+00 6.31300343e-01 8.03597337e-03 7.42739259e+03
 2.68443364e-02 8.22713568e-01 1.06963929e-01 0.00000000e+00
 0.00000000e+00 0.00000000e+00 0.00000000e+00 0.00000000e+00
 0.00000000e+00 0.00000000e+00 0.00000000e+00 7.05170079e-02
 0.00000000e+00 0.00000000e+00 0.00000000e+00 0.00000000e+00
 0.00000000e+00 0.00000000e+00 0.00000000e+00 6.35009419e-02
 0.00000000e+00 0.00000000e+00 0.00000000e+00 0.00000000e+00
 0.00000000e+00 0.00000000e+00 2.46452289e-02 0.00000000e+00
 0.00000000e+00 0.00000000e+00 0.00000000e+00 0.00000000e+00
 0.00000000e+00 0.00000000e+00 1.47921529e-01 4.62293811e+02
 0.00000000e+00 0.00000000e+00 0.00000000e+00 0.00000000e+00
 0.00000000e+00 2.50369293e-01 0.00000000e+00 0.00000000e+00
 0.00000000e+00 0.00000000e+00 2.42022320e-01 0.00000000e+00
 1.46613370e-01]
 VI [2.93690556e-03 0.00000000e+00 0.00000000e+00 0.00000000e+00
 0.00000000e+00 0.00000000e+00 0.00000000e+00 0.00000000e+00
 0.00000000e+00 0.00000000e+00 3.36126037e-04 5.63842192e+01
 0.00000000e+00 0.00000000e+00 0.00000000e+00 0.00000000e+00
 0.00000000e+00 0.00000000e+00 0.00000000e+00 0.00000000e+00
 0.00000000e+00 0.00000000e+00 0.00000000e+00 0.00000000e+00
 0.00000000e+00 0.00000000e+00 3.48592554e-05 0.00000000e+00
 1.17845812e-01 0.00000000e+00 0.00000000e+00 0.00000000e+00
 0.00000000e+00 0.00000000e+00 0.00000000e+00 0.00000000e+00
 0.00000000e+00 0.00000000e+00 0.00000000e+00 0.00000000e+00
 0.00000000e+00 0.00000000e+00 0.00000000e+00 0.00000000e+00
 0.00000000e+00 0.00000000e+00 0.00000000e+00 0.00000000e+00
 0.00000000e+00 0.00000000e+00 0.00000000e+00 0.00000000e+00
 0.00000000e+00 0.00000000e+00 6.66384329e-01 0.00000000e+00
 0.00000000e+00 0.00000000e+00 0.00000000e+00 0.00000000e+00
 1.49572637e-03]
 VT [0.00000000e+00 0.00000000e+00 0.00000000e+00 0.00000000e+00
 1.72725640e-04 0.00000000e+00 2.51078796e-03 0.00000000e+00
 0.00000000e+00 0.00000000e+00 0.00000000e+00 3.26700447e+01
 0.00000000e+00 0.00000000e+00 0.00000000e+00 0.00000000e+00
 0.00000000e+00 0.00000000e+00 0.00000000e+00 0.00000000e+00
 7.89052826e-03 0.00000000e+00 0.00000000e+00 0.00000000e+00
 7.86304991e-02 0.00000000e+00 0.00000000e+00 0.00000000e+00
 0.00000000e+00 0.00000000e+00 0.00000000e+00 0.00000000e+00
 0.00000000e+00 0.00000000e+00 0.00000000e+00 0.00000000e+00
 0.00000000e+00 0.00000000e+00 5.23747256e-03 0.00000000e+00
 0.00000000e+00 0.00000000e+00 0.00000000e+00 0.00000000e+00
 0.00000000e+00 0.00000000e+00 0.00000000e+00 6.52980858e+01
 0.00000000e+00 0.00000000e+00 0.00000000e+00 0.00000000e+00
 0.00000000e+00 0.00000000e+00 0.00000000e+00 1.20243637e-01
 0.00000000e+00 0.00000000e+00 0.00000000e+00 0.00000000e+00
 0.00000000e+00]
 WA [0.00000000e+00 0.00000000e+00 1.85553506e-01 0.00000000e+00
 3.49100841e-02 0.00000000e+00 3.21678621e-01 0.00000000e+00
 0.00000000e+00 0.00000000e+00 0.00000000e+00 0.00000000e+00
 0.00000000e+00 0.00000000e+00 0.00000000e+00 0.00000000e+00
 0.00000000e+00 0.00000000e+00 0.00000000e+00 0.00000000e+00
 0.00000000e+00 1.05724678e-01 0.00000000e+00 0.00000000e+00
 0.00000000e+00 0.00000000e+00 0.00000000e+00 0.00000000e+00
 0.00000000e+00 0.00000000e+00 0.00000000e+00 0.00000000e+00
 0.00000000e+00 0.00000000e+00 0.00000000e+00 0.00000000e+00
 0.00000000e+00 0.00000000e+00 0.00000000e+00 0.00000000e+00
 0.00000000e+00 0.00000000e+00 0.00000000e+00 1.86334857e+02
 0.00000000e+00 0.00000000e+00 5.27148593e-02 0.00000000e+00
 0.00000000e+00 0.00000000e+00 0.00000000e+00 0.00000000e+00
 0.00000000e+00 0.00000000e+00 1.53895910e-02 0.00000000e+00
 4.93828161e-01]

WI [0.00000000e+00 0.00000000e+00 0.00000000e+00 0.00000000e+00
0.00000000e+00 0.00000000e+00 0.00000000e+00 0.00000000e+00
0.00000000e+00 0.00000000e+00 0.00000000e+00 0.00000000e+00
6.82420380e-02 1.09370789e+01 0.00000000e+00 0.00000000e+00
0.00000000e+00 0.00000000e+00 0.00000000e+00 0.00000000e+00
0.00000000e+00 0.00000000e+00 0.00000000e+00 0.00000000e+00
0.00000000e+00 0.00000000e+00 0.00000000e+00 0.00000000e+00
1.13806272e+02 0.00000000e+00 0.00000000e+00 0.00000000e+00
0.00000000e+00 0.00000000e+00 0.00000000e+00 0.00000000e+00
0.00000000e+00 0.00000000e+00 0.00000000e+00 0.00000000e+00
0.00000000e+00 0.00000000e+00 0.00000000e+00 0.00000000e+00
0.00000000e+00 0.00000000e+00 0.00000000e+00 0.00000000e+00
1.17453479e-02 3.38599002e+00 0.00000000e+00 0.00000000e+00
0.00000000e+00 0.00000000e+00 0.00000000e+00 0.00000000e+00
0.00000000e+00 1.18906901e-01 0.00000000e+00 0.00000000e+00
0.00000000e+00]

WV [0.191932 0. 0. 0. 0. 0.
0.01273428 0. 0. 0. 0. 0.
0. 0. 0. 0. 0. 0.
0. 0. 0. 0. 0. 0.
0. 0.00373553 0. 0. 0. 0.
0. 0. 0. 0. 0. 0.
0. 0. 0. 0. 0. 0.
0. 0. 0. 0. 0.04076951 0.
0. 0.04965205 0.0269017 0. 0. 0.
0. 0. 0. 0. 0.67623847 0.
0.]

WY [0.00000000e+00 0.00000000e+00 0.00000000e+00 0.00000000e+00
0.00000000e+00 0.00000000e+00 0.00000000e+00 0.00000000e+00
0.00000000e+00 0.00000000e+00 0.00000000e+00 0.00000000e+00
1.05712190e-03 6.62034908e-02 0.00000000e+00 2.12079707e-03
0.00000000e+00 0.00000000e+00 0.00000000e+00 0.00000000e+00
0.00000000e+00 0.00000000e+00 0.00000000e+00 0.00000000e+00
0.00000000e+00 0.00000000e+00 0.00000000e+00 0.00000000e+00
0.00000000e+00 0.00000000e+00 0.00000000e+00 0.00000000e+00
1.42883030e-02 0.00000000e+00 0.00000000e+00 0.00000000e+00
0.00000000e+00 0.00000000e+00 0.00000000e+00 0.00000000e+00
0.00000000e+00 0.00000000e+00 0.00000000e+00 0.00000000e+00
0.00000000e+00 0.00000000e+00 0.00000000e+00 1.05569605e+02
0.00000000e+00 3.10306663e-01 0.00000000e+00 0.00000000e+00
0.00000000e+00 0.00000000e+00 0.00000000e+00 0.00000000e+00
0.00000000e+00 3.19591640e-03 0.00000000e+00 3.01662937e-01
0.00000000e+00]

```

In [8]: finalXvals = finalXvals.reshape(60, 61)# 60 STATES HAVE 61 ENTRIES EACH (61's 'Outside'
# to each of themselves, all other states, and the Outside state, for each of the 60
# this is correct, x[1] has 61 entries. They are the same as state 1.
finalXvals = np.array(finalXvals)

futureStates = pd.DataFrame(currentStates).copy()
newLine = range(61)
thousand = [1000]
thousand = pd.DataFrame(thousand)

# Prediction loop, for future distance of (interpolatDistance)
for t in range(oldSize, interpolateDistance + oldSize):
    tempVector = futureStates.iloc[:, t] # All of the values of all 61 states at the

    # dot product vector with matrix finalXvals to make the prediction.
    newLine = np.dot( np.array(tempVector), finalXvals.transpose() )
    newLine = pd.DataFrame(newLine)
    newLine = pd.concat([newLine, thousand]) # add the thousand outside vector element

    #print(futureStates.shape)

    futureStates = np.concatenate((futureStates, newLine), axis = 1)
    futureStates = pd.DataFrame(futureStates)

futureStates.head

```

```

Out[8]: <bound method NDFrame.head of
0      1      2      3      4      5
6      7      8      \
0      0.0      0.0      0.0      0.0      0.0      0.0      0.0      0.0      11.0
1      0.0      0.0      0.0      0.0      0.0      0.0      0.0      3.0      58.0
2      0.0      0.0      1.0      3.0      1.0      3.0      0.0      8.0      70.0
3      0.0      0.0      0.0      0.0      0.0      0.0      0.0      0.0      0.0
4      0.0      1.0      0.0      0.0      0.0      0.0      0.0      8.0      18.0
..      ...      ...      ...      ...      ...      ...      ...      ...      ...
56      1.0      0.0      0.0      0.0      0.0      0.0      44.0      329.0      848.0
57      0.0      0.0      0.0      0.0      0.0      0.0      0.0      3.0      108.0
58      0.0      0.0      0.0      0.0      0.0      0.0      0.0      0.0      1.0
59      0.0      0.0      0.0      0.0      0.0      0.0      0.0      2.0      18.0
60      1000.0      1000.0      1000.0      1000.0      1000.0      1000.0      1000.0      1000.0      1000.0

      9      ...      163      164      165      166      \
0      52.0      ...      4390.482430      4414.549648      4438.565733      4462.530793
1      411.0      ...      36217.297658      36411.162160      36604.614797      36797.656443
2      279.0      ...      23860.313714      23988.857075      24117.127346      24245.125105
3      0.0      ...      0.000000      0.000000      0.000000      0.000000
4      374.0      ...      70574.955499      70967.668398      71359.546990      71750.593040
..      ...      ...      ...      ...      ...      ...
56      1644.0      ...      24493.358588      24624.646651      24755.655788      24886.386592
57      510.0      ...      44801.079935      45042.158516      45282.724905      45522.780189
58      38.0      ...      11699.195045      11764.633607      11829.933145      11895.093952
59      34.0      ...      4207.021603      4229.788727      4252.507480      4275.177965
60      1000.0      ...      1000.000000      1000.000000      1000.000000      1000.000000

      167      168      169      170      171      \
0      4486.444937      4510.308274      4534.120911      4557.882957      4581.594518
1      36990.287967      37182.510240      37374.324130      37565.730504      37756.730226
2      24372.850930      24500.305398      24627.489083      24754.402561      24881.046406
3      0.000000      0.000000      0.000000      0.000000      0.000000
4      72140.808310      72530.194561      72918.753551      73306.487033      73693.396760
..      ...      ...      ...      ...      ...

```

56	25016.839652	25147.015557	25276.914897	25406.538258	25535.886228
57	45762.325457	46001.361795	46239.890283	46477.912004	46715.428034
58	11960.116322	12025.000550	12089.746927	12154.355747	12218.827302
59	4297.800284	4320.374540	4342.900836	4365.379272	4387.809952
60	1000.000000	1000.000000	1000.000000	1000.000000	1000.000000

	172
0	4605.255703
1	37947.324161
2	25007.421189
3	0.000000
4	74079.484480
..	...
56	25664.959391
57	46952.439450
58	12283.161883
59	4410.192976
60	1000.000000

[61 rows x 173 columns]>

```
In [9]: predict = futureStates.copy()
predict = predict.loc[:, oldSize: (oldSize + interpolateDistance) ]
actual = states.loc[:, oldSize: (oldSize + interpolateDistance) ]
difference = predict.values - actual
print(difference)
```

	53	54	55	56	57	58	\
AK	0.0	86.699611	-4.457053	171.075491	110.042695	159.313441	
AL	0.0	697.249744	5198.265478	8665.068476	8364.005567	7897.941692	
AR	0.0	-5.046033	1231.996000	5593.755156	6314.955709	1851.176476	
AS	0.0	0.000000	0.000000	0.000000	0.000000	0.000000	
AZ	0.0	13449.257309	16067.166989	22855.806708	21135.607426	22144.834657	
..	
WA	0.0	-186.983570	2032.259982	3727.152758	3081.250508	3117.223618	
WI	0.0	1166.127387	3110.693431	4787.567652	6259.296421	7285.480320	
WV	0.0	656.276888	1357.647467	1995.384076	2162.359572	1976.191352	
WY	0.0	39.621452	122.784276	209.736505	170.724305	478.858457	
0	0.0	0.000000	0.000000	0.000000	0.000000	0.000000	

	59	60	61	62	...	163	\
AK	186.515580	259.138255	314.927161	162.471057	...	3808.482430	
AL	10218.852879	6114.728876	10798.920200	11256.401316	...	33746.297658	
AR	6758.128106	6837.932641	7406.997641	7665.310531	...	22412.313714	
AS	0.000000	0.000000	0.000000	0.000000	...	0.000000	
AZ	19752.887515	21842.476925	22464.615306	21982.372677	...	67354.955499	
..	
WA	3833.921592	3179.349151	3213.804612	1672.773288	...	20451.358588	
WI	8901.895362	9925.526886	10452.124487	10784.870184	...	40623.079935	
WV	2019.696816	1576.767069	1238.316784	839.742130	...	10285.195045	
WY	604.627897	730.616860	783.807104	898.449425	...	3926.021603	
0	0.000000	0.000000	0.000000	0.000000	...	0.000000	

	164	165	166	167	168	\
AK	3966.549648	3942.565733	3948.530793	4085.444937	4152.308274	
AL	34521.162160	34642.614797	34733.656443	34970.287967	35550.510240	
AR	22748.857075	23127.127346	23464.125105	23454.850930	23786.305398	
AS	0.000000	-1.000000	-3.000000	-2.000000	0.000000	
AZ	66075.668398	68708.546990	68487.593040	69209.808310	68855.194561	
..	
WA	20604.646651	21181.655788	21662.386592	21746.839652	22718.015557	
WI	41186.158516	41539.724905	41391.780189	42279.325457	43307.361795	

WV	10352.633607	10801.933145	10741.093952	10943.116322	11057.000550
WY	3972.788727	4039.507480	4073.177965	4166.800284	4162.374540
0	0.000000	0.000000	0.000000	0.000000	0.000000
	169	170	171	172	
AK	4173.120911	4277.882957	4393.594518	4406.255703	
AL	35814.324130	36051.730504	36292.730226	36650.324161	
AR	23576.489083	24041.402561	23983.046406	24350.421189	
AS	-3.000000	0.000000	0.000000	-2.000000	
AZ	69510.753551	69300.487033	70487.396760	71471.484480	
..	
WA	22885.914897	23141.538258	23726.886228	24095.959391	
WI	43905.890283	44945.912004	45169.428034	45428.439450	
WV	11410.746927	11583.355747	11955.827302	12089.161883	
WY	4227.900836	4225.379272	4258.809952	4044.192976	
0	0.000000	0.000000	0.000000	0.000000	

[61 rows x 120 columns]

In []:

In [10]: *#Similar Waves phase*

In [11]: *# find internal contageon = each state from end of training Xn * X*

```

autoCorrelate = list()

for j in range(maxStates): # for each state, grab its correlation with itself in the
    autoCorrelate.append(finalXvals[j, j] )

autoCorrelate.append(0) # for the outside state

autoCorrelate

```

Out[11]: [0.4338408517134921,
0.0,
0.5559289639052066,
0.0,
0.6766812941736081,
0.439027806633437,
0.3357674789919865,
0.0,
0.516381210512584,
0.04492637588811812,
0.6664130333739763,
0.0,
0.008630216656186242,
0.7368689523066959,
0.6755537884749124,
0.11564756933637281,
0.17398114397538755,
0.2532970719053044,
0.0,
0.0,
0.0,
0.44496870703847313,
0.0,
0.07793777143841489,
0.0515789417451891,
0.43825001991080337,

```

0.08467739634533024,
0.0,
0.0,
0.13161763460178547,
0.13338695548649157,
0.20209369971255745,
0.2592708539806615,
0.04593345149281187,
0.4211151034566458,
0.0,
0.07947136904516236,
0.0,
0.4506185447127101,
0.8734192290484437,
0.0,
0.0,
0.0,
0.12090951203043761,
0.0,
0.0,
0.3672281951985964,
0.0,
0.33682027853552216,
0.6176110659653083,
0.24103178540784148,
0.04592880885971314,
0.2277193782746182,
0.25036929298173327,
0.6663843288595278,
0.12024363729798618,
0.0,
0.11890690127342535,
0.676238471657536,
0.30166293731430227,
0]

```

In [12]: `print(oldSize)`

53

```

In [13]: tot = list()
         for j in range(oldSize + 1):
             newLine = np.multiply(autoCorrelate, states.iloc[:, j] )
             tot.append(newLine)

         tot = pd.DataFrame(tot)#reshape(118,61)
         tot.head()

# not being used:
# tempVector = futureStates.iloc[:, t] # All of the values of all 61 states at the c
# dot product vector with matrix finalXvals to make the prediction.

```

Out[13]:

	AK	AL	AR	AS	AZ	CA	CO	CT	DC	DE	...	TX	UT	VA	VI	VT	WA
0	0.0	0.0	0.000000	0.0	0.000000	0.000000	0.0	0.0	0.0	0.224632	...	0.0	0.0	0.0	0.0	0.0	0.0
1	0.0	0.0	0.000000	0.0	0.676681	0.878056	0.0	0.0	0.0	0.000000	...	0.0	0.0	0.0	0.0	0.0	0.0
2	0.0	0.0	0.555929	0.0	0.000000	2.634167	0.0	0.0	0.0	0.179706	...	0.0	0.0	0.0	0.0	0.0	0.0
3	0.0	0.0	1.667787	0.0	0.000000	3.512222	0.0	0.0	0.0	0.044926	...	0.0	0.0	0.0	0.0	0.0	0.0

	AK	AL	AR	AS	AZ	CA	CO	CT	DC	DE	...	TX	UT	VA	VI	VT	WA
4	0.0	0.0	0.555929	0.0	0.000000	6.146389	0.0	0.0	0.0	0.044926	...	0.0	0.0	0.0	0.0	0.0	0.0

5 rows × 61 columns

```
In [14]: s_it = currentStates.copy()
s_it = s_it.transpose()
# Python's for loops use per-column, not per-row, so states are on top and time is on
# instead of visa-versa, as it is in the other sections.
s = 0

print(s_it)
```

	AK	AL	AR	AS	AZ	CA	CO	CT	\
0	0.0	0.0	0.0	0.0	0.0	0.0	0.0	0.0	
1	0.0	0.0	0.0	0.0	1.0	2.0	0.0	0.0	
2	0.0	0.0	1.0	0.0	0.0	6.0	0.0	0.0	
3	0.0	0.0	3.0	0.0	0.0	8.0	0.0	0.0	
4	0.0	0.0	1.0	0.0	0.0	14.0	0.0	0.0	
5	0.0	0.0	3.0	0.0	0.0	22.0	0.0	0.0	
6	0.0	0.0	0.0	0.0	0.0	28.0	1.0	0.0	
7	0.0	3.0	8.0	0.0	8.0	140.0	41.0	5.0	
8	11.0	58.0	70.0	0.0	18.0	468.0	238.0	119.0	
9	52.0	411.0	279.0	0.0	374.0	2312.0	1137.0	1081.0	
10	86.0	703.0	374.0	0.0	1012.0	5169.0	2327.0	3217.0	
11	86.0	1439.0	490.0	0.0	1313.0	8972.0	2542.0	5316.0	
12	65.0	1693.0	668.0	0.0	1243.0	7368.0	2671.0	6806.0	
13	37.0	1385.0	901.0	0.0	1504.0	10980.0	2531.0	5981.0	
14	18.0	1287.0	699.0	0.0	1736.0	11112.0	4394.0	5282.0	
15	19.0	1790.0	649.0	0.0	2498.0	12343.0	2805.0	4431.0	
16	15.0	2053.0	723.0	0.0	2509.0	12265.0	2616.0	3840.0	
17	15.0	2364.0	925.0	0.0	2690.0	13039.0	2352.0	3360.0	
18	23.0	3077.0	1042.0	0.0	2413.0	14969.0	2060.0	2759.0	
19	91.0	2691.0	1876.0	0.0	5035.0	18736.0	2057.0	1657.0	
20	98.0	3705.0	2724.0	0.0	7498.0	18533.0	1251.0	843.0	
21	97.0	5282.0	2682.0	0.0	11085.0	20884.0	1371.0	662.0	
22	108.0	4937.0	4294.0	0.0	19253.0	33293.0	1587.0	554.0	
23	199.0	6769.0	3365.0	0.0	23925.0	42569.0	1978.0	660.0	
24	253.0	8502.0	3449.0	0.0	24499.0	57083.0	2238.0	536.0	
25	421.0	12045.0	4108.0	0.0	22740.0	58522.0	3267.0	527.0	
26	508.0	12400.0	4649.0	0.0	19264.0	66518.0	3704.0	575.0	
27	684.0	12058.0	5594.0	0.0	17657.0	62193.0	4152.0	1329.0	
28	601.0	10671.0	5415.0	0.0	13935.0	49959.0	3319.0	685.0	
29	491.0	8896.0	4779.0	0.0	7233.0	61840.0	2499.0	482.0	
30	558.0	7477.0	4230.0	0.0	6117.0	53386.0	2176.0	607.0	
31	465.0	8208.0	3913.0	0.0	3909.0	41022.0	2102.0	906.0	
32	474.0	8336.0	4444.0	0.0	3392.0	33604.0	2071.0	888.0	
33	547.0	5821.0	4874.0	0.0	3680.0	28054.0	2013.0	763.0	
34	529.0	6362.0	4935.0	0.0	3366.0	23947.0	3075.0	1295.0	
35	642.0	6474.0	5589.0	0.0	5381.0	25106.0	4262.0	1149.0	
36	833.0	7875.0	5539.0	0.0	3220.0	23721.0	4229.0	1235.0	
37	1020.0	6313.0	5183.0	0.0	4033.0	21364.0	4890.0	1814.0	
38	1341.0	7535.0	6206.0	0.0	5096.0	24635.0	6715.0	2497.0	
39	1538.0	7985.0	6427.0	0.0	6275.0	23575.0	8616.0	3010.0	
40	2614.0	12170.0	7040.0	0.0	7253.0	32061.0	12285.0	4256.0	
41	2727.0	10152.0	7168.0	0.0	9468.0	33103.0	20509.0	6246.0	
42	3598.0	9710.0	10652.0	0.0	14530.0	46951.0	29132.0	9368.0	
43	4316.0	14851.0	11340.0	0.0	17939.0	66610.0	37337.0	12287.0	
44	4112.0	15830.0	12594.0	0.0	27748.0	101588.0	35899.0	12124.0	

45	4524.0	17510.0	11911.0	0.0	30129.0	108911.0	34116.0	12274.0
46	4622.0	23359.0	15149.0	0.0	41622.0	184852.0	31348.0	19122.0
47	3417.0	25453.0	15451.0	0.0	46684.0	263456.0	22623.0	17233.0
48	2223.0	28929.0	14873.0	0.0	43988.0	305346.0	17252.0	12924.0
49	1724.0	22251.0	15229.0	0.0	39216.0	271394.0	13697.0	12958.0
50	2026.0	27365.0	19429.0	0.0	62191.0	280190.0	16083.0	15791.0
51	1973.0	26811.0	19328.0	0.0	67049.0	311715.0	16469.0	21122.0
52	1377.0	18659.0	14198.0	0.0	48815.0	247717.0	11987.0	13558.0
53	1181.0	19432.0	12587.0	0.0	48017.0	158085.0	10395.0	13205.0

	DC	DE	...	TX	UT	VA	VI	VT	WA \
0	0.0	5.0	...	0.0	0.0	0.0	0.0	0.0	1.0
1	0.0	0.0	...	0.0	0.0	0.0	0.0	0.0	0.0
2	0.0	4.0	...	0.0	0.0	0.0	0.0	0.0	0.0
3	0.0	1.0	...	0.0	0.0	0.0	0.0	0.0	0.0
4	0.0	1.0	...	0.0	0.0	0.0	0.0	0.0	0.0
5	0.0	2.0	...	0.0	0.0	0.0	0.0	0.0	0.0
6	0.0	0.0	...	0.0	0.0	0.0	0.0	0.0	44.0
7	2.0	4.0	...	21.0	2.0	7.0	0.0	1.0	329.0
8	37.0	20.0	...	156.0	50.0	71.0	2.0	7.0	848.0
9	192.0	130.0	...	925.0	272.0	317.0	15.0	44.0	1644.0
10	355.0	300.0	...	2421.0	660.0	1088.0	13.0	182.0	3259.0
11	854.0	764.0	...	4003.0	830.0	2164.0	15.0	278.0	2689.0
12	757.0	900.0	...	4321.0	723.0	2848.0	6.0	221.0	2061.0
13	1009.0	1308.0	...	4237.0	909.0	3769.0	3.0	80.0	1804.0
14	900.0	1418.0	...	6041.0	1032.0	4697.0	3.0	39.0	1670.0
15	1355.0	1338.0	...	6611.0	1092.0	6026.0	9.0	44.0	1960.0
16	1123.0	1180.0	...	7609.0	1030.0	5757.0	3.0	30.0	1482.0
17	967.0	1142.0	...	7590.0	1102.0	6166.0	0.0	14.0	1351.0
18	855.0	752.0	...	5366.0	988.0	7336.0	0.0	17.0	1609.0
19	610.0	608.0	...	7845.0	1809.0	6655.0	1.0	24.0	1906.0
20	521.0	426.0	...	21117.0	2375.0	5267.0	2.0	80.0	2115.0
21	310.0	411.0	...	18944.0	2493.0	3598.0	1.0	64.0	2308.0
22	281.0	423.0	...	29179.0	3461.0	3738.0	3.0	34.0	3185.0
23	237.0	784.0	...	46674.0	3970.0	3708.0	14.0	46.0	3732.0
24	277.0	791.0	...	50227.0	4154.0	4162.0	32.0	47.0	4448.0
25	384.0	837.0	...	63779.0	4302.0	6153.0	121.0	44.0	5636.0
26	503.0	752.0	...	59348.0	4415.0	6862.0	77.0	54.0	5755.0
27	470.0	701.0	...	55386.0	3605.0	7601.0	65.0	52.0	5769.0
28	444.0	593.0	...	58536.0	3099.0	7061.0	96.0	24.0	5111.0
29	516.0	484.0	...	78709.0	2741.0	7471.0	158.0	33.0	4447.0
30	395.0	464.0	...	59198.0	2453.0	6503.0	189.0	57.0	4201.0
31	368.0	504.0	...	32903.0	2678.0	6434.0	202.0	41.0	3660.0
32	355.0	720.0	...	31176.0	2682.0	7058.0	114.0	56.0	3326.0
33	310.0	653.0	...	23266.0	2847.0	6777.0	53.0	34.0	2744.0
34	356.0	710.0	...	36350.0	4198.0	7070.0	35.0	38.0	2919.0
35	307.0	711.0	...	35316.0	6224.0	6229.0	58.0	34.0	3238.0
36	276.0	821.0	...	27697.0	7254.0	5677.0	28.0	28.0	3998.0
37	371.0	912.0	...	24971.0	7446.0	5423.0	4.0	42.0	4021.0
38	435.0	893.0	...	24682.0	8574.0	7914.0	6.0	84.0	4448.0
39	366.0	963.0	...	34157.0	9034.0	7167.0	9.0	72.0	4713.0
40	475.0	1014.0	...	44225.0	11036.0	7983.0	16.0	144.0	5157.0
41	628.0	1182.0	...	41803.0	12884.0	9079.0	35.0	125.0	7363.0
42	778.0	1769.0	...	57949.0	18358.0	10674.0	25.0	224.0	10833.0
43	1086.0	2610.0	...	62126.0	22409.0	12330.0	50.0	534.0	14514.0
44	1051.0	3383.0	...	97579.0	22011.0	17447.0	58.0	757.0	19245.0
45	1326.0	3941.0	...	92464.0	18517.0	16175.0	68.0	498.0	17005.0
46	2012.0	5562.0	...	96907.0	20363.0	24651.0	109.0	797.0	20885.0
47	1748.0	5939.0	...	121612.0	18370.0	25128.0	130.0	740.0	17673.0
48	1624.0	4344.0	...	133398.0	17084.0	26893.0	139.0	706.0	16528.0
49	1532.0	4508.0	...	114742.0	14372.0	25210.0	64.0	604.0	13170.0
50	1724.0	5635.0	...	150087.0	21015.0	32965.0	75.0	782.0	17350.0

51	2118.0	5247.0	...	153453.0	19967.0	35266.0	60.0	1162.0	19270.0
52	1803.0	4538.0	...	136650.0	13453.0	43025.0	139.0	1142.0	13123.0
53	1462.0	3958.0	...	112996.0	12287.0	32937.0	68.0	962.0	11156.0
	WI	WV		WY					0
0	0.0	0.0		0.0					1000.0
1	0.0	0.0		0.0					1000.0
2	0.0	0.0		0.0					1000.0
3	0.0	0.0		0.0					1000.0
4	0.0	0.0		0.0					1000.0
5	0.0	0.0		0.0					1000.0
6	0.0	0.0		0.0					1000.0
7	3.0	0.0		2.0					1000.0
8	108.0	1.0		18.0					1000.0
9	510.0	38.0		34.0					1000.0
10	935.0	152.0		120.0					1000.0
11	1154.0	292.0		129.0					1000.0
12	1011.0	220.0		86.0					1000.0
13	1124.0	239.0		50.0					1000.0
14	1675.0	168.0		101.0					1000.0
15	2380.0	130.0		76.0					1000.0
16	2003.0	157.0		66.0					1000.0
17	2508.0	168.0		93.0					1000.0
18	3053.0	323.0		73.0					1000.0
19	2935.0	188.0		41.0					1000.0
20	2194.0	119.0		80.0					1000.0
21	1861.0	179.0		134.0					1000.0
22	2309.0	257.0		161.0					1000.0
23	3438.0	347.0		215.0					1000.0
24	3952.0	729.0		233.0					1000.0
25	5574.0	851.0		232.0					1000.0
26	6122.0	653.0		306.0					1000.0
27	6202.0	1067.0		360.0					1000.0
28	5890.0	877.0		259.0					1000.0
29	5329.0	862.0		186.0					1000.0
30	5224.0	783.0		304.0					1000.0
31	4768.0	738.0		293.0					1000.0
32	4871.0	1119.0		227.0					1000.0
33	6208.0	1157.0		268.0					1000.0
34	9374.0	1388.0		437.0					1000.0
35	13217.0	1313.0		624.0					1000.0
36	16343.0	1335.0		782.0					1000.0
37	16425.0	1300.0		967.0					1000.0
38	19880.0	1673.0		1247.0					1000.0
39	33637.0	1911.0		1727.0					1000.0
40	29343.0	2333.0		2339.0					1000.0
41	35727.0	2921.0		3366.0					1000.0
42	44062.0	4215.0		4500.0					1000.0
43	49316.0	6064.0		5367.0					1000.0
44	41777.0	6785.0		5400.0					1000.0
45	28488.0	6853.0		3604.0					1000.0
46	31250.0	8557.0		3222.0					1000.0
47	25982.0	8388.0		2517.0					1000.0
48	22282.0	9086.0		2170.0					1000.0
49	15782.0	8289.0		1473.0					1000.0
50	19773.0	10456.0		1807.0					1000.0
51	22021.0	9569.0		2296.0					1000.0
52	15101.0	7427.0		1635.0					1000.0
53	12482.0	6094.0		1254.0					1000.0

[54 rows x 61 columns]

```
In [15]: s_it = s_it - tot
s_it
```

```
Out[15]:
```

	AK	AL	AR	AS	AZ	CA	CO	CT	
0	0.000000	0.0	0.000000	0.0	0.000000	0.000000	0.000000	0.0	0
1	0.000000	0.0	0.000000	0.0	0.323319	1.121944	0.000000	0.0	0
2	0.000000	0.0	0.444071	0.0	0.000000	3.365833	0.000000	0.0	0
3	0.000000	0.0	1.332213	0.0	0.000000	4.487778	0.000000	0.0	0
4	0.000000	0.0	0.444071	0.0	0.000000	7.853611	0.000000	0.0	0
5	0.000000	0.0	1.332213	0.0	0.000000	12.341388	0.000000	0.0	0
6	0.000000	0.0	0.000000	0.0	0.000000	15.707221	0.664233	0.0	0
7	0.000000	3.0	3.552568	0.0	2.586550	78.536107	27.233533	5.0	0
8	6.227751	58.0	31.084973	0.0	5.819737	262.534986	158.087340	119.0	17
9	29.440276	411.0	123.895819	0.0	120.921196	1296.967711	755.232376	1081.0	92
10	48.689687	703.0	166.082567	0.0	327.198530	2899.665268	1545.669076	3217.0	171
11	48.689687	1439.0	217.594808	0.0	424.517461	5033.042519	1688.479068	5316.0	413
12	36.800345	1693.0	296.639452	0.0	401.885151	4133.243121	1774.165064	6806.0	366
13	20.947888	1385.0	400.108004	0.0	486.271334	6159.474683	1681.172511	5981.0	487
14	10.190865	1287.0	310.405654	0.0	561.281273	6233.523013	2918.637697	5282.0	435
15	10.757024	1790.0	288.202102	0.0	807.650127	6924.079783	1863.172221	4431.0	655
16	8.492387	2053.0	321.063359	0.0	811.206633	6880.323952	1737.632275	3840.0	543
17	8.492387	2364.0	410.765708	0.0	869.727319	7314.516429	1562.274889	3360.0	467
18	13.021660	3077.0	462.722020	0.0	780.168037	8397.192763	1368.318993	2759.0	413
19	51.520482	2691.0	833.077264	0.0	1627.909684	10510.375015	1366.326296	1657.0	295
20	55.483597	3705.0	1209.649502	0.0	2424.243656	10396.497660	830.954884	843.0	251
21	54.917437	5282.0	1190.998519	0.0	3583.987854	11715.343286	910.662786	662.0	149
22	61.145188	4937.0	1906.841029	0.0	6224.855043	18676.447234	1054.137011	554.0	135
23	112.665671	6769.0	1494.299036	0.0	7735.400037	23880.025299	1313.851927	660.0	114
24	143.238265	8502.0	1531.601003	0.0	7920.984974	32021.975714	1486.552382	536.0	133
25	238.353001	12045.0	1824.243816	0.0	7352.267370	32829.214700	2170.047646	527.0	185
26	287.608847	12400.0	2064.486247	0.0	6228.411549	37314.748358	2460.317258	575.0	243
27	387.252857	12058.0	2484.133376	0.0	5708.838389	34888.543622	2757.893427	1329.0	227
28	340.261648	10671.0	2404.644660	0.0	4505.446166	28025.609808	2204.587737	685.0	214
29	277.984142	8896.0	2122.215481	0.0	2338.564199	34690.520438	1659.917070	482.0	249
30	315.916805	7477.0	1878.420483	0.0	1977.740524	29948.061515	1445.369966	607.0	191

	AK	AL	AR	AS	AZ	CA	CO	CT	
31	263.264004	8208.0	1737.649964	0.0	1263.852821	23012.201316	1396.216759	906.0	177
32	268.359436	8336.0	1973.451684	0.0	1096.697050	18850.909586	1375.625551	888.0	171
33	309.689054	5821.0	2164.402230	0.0	1189.812837	15737.513913	1337.100065	763.0	149
34	299.498189	6362.0	2191.490563	0.0	1088.290764	13433.601115	2042.515002	1295.0	172
35	363.474173	6474.0	2481.913021	0.0	1739.777956	14083.767887	2830.959005	1149.0	148
36	471.610571	7875.0	2459.709469	0.0	1041.086233	13306.821399	2809.039331	1235.0	133
37	577.482331	6313.0	2301.620180	0.0	1303.944341	11984.609939	3248.097028	1814.0	179
38	759.219418	7535.0	2755.904850	0.0	1647.632125	13819.549984	4460.321379	2497.0	210
39	870.752770	7985.0	2854.044549	0.0	2028.824879	13224.919459	5723.027401	3010.0	177
40	1479.940014	12170.0	3126.260094	0.0	2345.030573	17985.329492	8160.096521	4256.0	229
41	1543.915997	10152.0	3183.101187	0.0	3061.181507	18569.862517	13622.744773	6246.0	303
42	2037.040616	9710.0	4730.244676	0.0	4697.820796	26338.205451	19350.421802	9368.0	376
43	2443.542884	14851.0	5035.765549	0.0	5800.014264	37366.357800	24800.449637	12287.0	525
44	2328.046418	15830.0	5592.630629	0.0	8971.447449	56988.043180	23845.283272	12124.0	508
45	2561.303987	17510.0	5289.330111	0.0	9741.269288	61096.042552	22660.956687	12274.0	641
46	2616.787583	23359.0	6727.232126	0.0	13457.171174	103696.831888	20822.361069	19122.0	973
47	1934.565810	25453.0	6861.341579	0.0	15093.810463	147791.490176	15026.932323	17233.0	845
48	1258.571787	28929.0	6604.668520	0.0	14222.143232	171290.615356	11459.339452	12924.0	785
49	976.058372	22251.0	6762.757809	0.0	12679.266368	152244.487447	9097.992840	12958.0	740
50	1147.038434	27365.0	8627.856160	0.0	20107.513634	157178.798859	10682.851635	15791.0	833
51	1117.032000	26811.0	8583.004986	0.0	21678.195907	174863.447255	10939.245388	21122.0	1024
52	779.601147	18659.0	6304.920570	0.0	15782.802625	138962.348824	7962.155229	13558.0	871
53	668.633954	19432.0	5589.522131	0.0	15524.794298	88681.289188	6904.697056	13205.0	707

54 rows × 61 columns

```
In [16]: for s in s_it: # loop in states. Note s is the postal abbreviation here.
    print(s)
    s_i = s_it.loc[:, s]
    sizeOf = s_i.size #in case we change interpolate distance later
    s_i = s_i.to_numpy()

    frequencies = sp.fft.fftfreq(sizeOf, d = 1.0)
    fourierAmps = sp.fft.fft(s_i)
    amplitudes = (2/(sizeOf)) * np.abs(fourierAmps)

    # getting all frequencies, not only top ones, because why not?
    #top_indices = np.argmax(np.abs(fourierAmps), -2)[-2:]

    # Exclude zero-freqencires
    amplitudes = amplitudes[frequencies != 0]
    frequencies = frequencies[frequencies != 0]

    #dominantFreqs = [frequencies[j] for j in top_indices]
    #dominantAmps = [np.abs(fourierAm[j] ) for j in top_indices]

    # Wavelength = 1 / frequency
    print("Wavelengths:")
    print(1 / frequencies)
    # print("Amps1:", dominantAmps)
    print("Amps:")
    print(amplitudes)

    #tempHold = sp.integrate.solve_ivp(func(t, s_i), (53,91), [0])
    #errors_it = fourier.error
```

AK

Wavelengths:

```
[ 54.          27.          18.          13.5          10.8
   9.          7.71428571  6.75          6.          5.4
  4.90909091  4.5          4.15384615  3.85714286  3.6
  3.375       3.17647059  3.          2.84210526  2.7
  2.57142857  2.45454545  2.34782609  2.25       2.16
  2.07692308 -2.          -2.07692308 -2.16       -2.25
 -2.34782609 -2.45454545 -2.57142857 -2.7        -2.84210526
 -3.          -3.17647059 -3.375       -3.6        -3.85714286
 -4.15384615 -4.5        -4.90909091 -5.4        -6.
 -6.75        -7.71428571 -9.          -10.8       -13.5
 -18.         -27.         -54.          ]
```

Amps:

```
[819.07507582 515.74491509 342.78975059 132.20330949 70.34771811
 88.24584004 79.13183276 70.80088881 68.35317785 55.41500457
 49.69329091 33.13659861 17.69861029 22.35345957 24.79815266
 38.77939323 37.67978607 19.16559297 5.36827941 22.52441404
 40.15059787 29.01681982 7.16215508 11.25544674 25.22919031
 17.22038727 3.62761232 17.22038727 25.22919031 11.25544674
 7.16215508 29.01681982 40.15059787 22.52441404 5.36827941
 19.16559297 37.67978607 38.77939323 24.79815266 22.35345957
 17.69861029 33.13659861 49.69329091 55.41500457 68.35317785
 70.80088881 79.13183276 88.24584004 70.34771811 132.20330949
 342.78975059 515.74491509 819.07507582]
```

AL

Wavelengths:

```
[ 54.          27.          18.          13.5          10.8
   9.          7.71428571  6.75          6.          5.4
  4.90909091  4.5          4.15384615  3.85714286  3.6
```

[illegible]

AZ

Wavelengths:

```
[ 54.          27.          18.          13.5          10.8
   9.          7.71428571   6.75          6.          5.4
  4.90909091   4.5          4.15384615   3.85714286   3.6
  3.375        3.17647059   3.          2.84210526   2.7
  2.57142857   2.45454545   2.34782609   2.25          2.16
  2.07692308   -2.          -2.07692308   -2.16          -2.25
 -2.34782609   -2.45454545   -2.57142857   -2.7          -2.84210526
 -3.          -3.17647059   -3.375        -3.6          -3.85714286
 -4.15384615   -4.5          -4.90909091   -5.4          -6.
 -6.75         -7.71428571   -9.          -10.8         -13.5
 -18.          -27.          -54.          ]
```

Amps:

```
[3729.43419515 5466.88415282 2307.37770094 2415.87453985 693.2168274
1281.74752634 852.88314425 952.09297073 918.96745968 651.18547513
595.5847208 370.02868481 301.9562907 121.30696113 134.33862043
286.39235827 400.04249158 458.24032065 520.5358166 375.94035269
471.73637485 347.69999293 424.76174063 485.88990494 353.92933936
269.13163818 205.06788286 269.13163818 353.92933936 485.88990494
424.76174063 347.69999293 471.73637485 375.94035269 520.5358166
458.24032065 400.04249158 286.39235827 134.33862043 121.30696113
301.9562907 370.02868481 595.5847208 651.18547513 918.96745968
952.09297073 852.88314425 1281.74752634 693.2168274 2415.87453985
2307.37770094 5466.88415282 3729.43419515]
```

CA

Wavelengths:

```
[ 54.          27.          18.          13.5          10.8
   9.          7.71428571   6.75          6.          5.4
  4.90909091   4.5          4.15384615   3.85714286   3.6
  3.375        3.17647059   3.          2.84210526   2.7
  2.57142857   2.45454545   2.34782609   2.25          2.16
  2.07692308   -2.          -2.07692308   -2.16          -2.25
 -2.34782609   -2.45454545   -2.57142857   -2.7          -2.84210526
 -3.          -3.17647059   -3.375        -3.6          -3.85714286
 -4.15384615   -4.5          -4.90909091   -5.4          -6.
 -6.75         -7.71428571   -9.          -10.8         -13.5
 -18.          -27.          -54.          ]
```

Amps:

```
[37005.93920734 40317.65626101 29671.28677629 18941.71287956
13437.72134301 7410.40012042 4020.09151589 3828.00073514
3449.08097242 5143.28286105 4625.40413925 5159.31320224
4470.83081721 2865.55956978 2076.88225282 176.47039198
185.12390821 1338.07921601 1210.65532574 950.44057516
1226.94716976 1531.70044698 1825.50863201 1970.63188048
1907.44002746 1218.9891465 626.91759121 1218.9891465
1907.44002746 1970.63188048 1825.50863201 1531.70044698
1226.94716976 950.44057516 1210.65532574 1338.07921601
185.12390821 176.47039198 2076.88225282 2865.55956978
4470.83081721 5159.31320224 4625.40413925 5143.28286105
3449.08097242 3828.00073514 4020.09151589 7410.40012042
13437.72134301 18941.71287956 29671.28677629 40317.65626101
37005.93920734]
```

CO

Wavelengths:

```
[ 54.          27.          18.          13.5          10.8
   9.          7.71428571   6.75          6.          5.4
  4.90909091   4.5          4.15384615   3.85714286   3.6
  3.375        3.17647059   3.          2.84210526   2.7
  2.57142857   2.45454545   2.34782609   2.25          2.16
  2.07692308   -2.          -2.07692308   -2.16          -2.25
 -2.34782609   -2.45454545   -2.57142857   -2.7          -2.84210526
```

-3.	-3.17647059	-3.375	-3.6	-3.85714286
-4.15384615	-4.5	-4.90909091	-5.4	-6.
-6.75	-7.71428571	-9.	-10.8	-13.5
-18.	-27.	-54.]	

Amps:

[6505.13956845	5252.29222303	3137.15396436	1430.48955554	1139.57227178
1430.718206	1238.46383823	709.86995848	340.41672489	250.18743644
276.89016939	246.10181028	256.08348261	154.85618599	234.2877643
140.97064259	149.81595307	151.25751435	59.75874862	95.06574089
262.5006444	289.90184475	197.66141557	192.1635595	142.31261959
112.33839319	125.53994647	112.33839319	142.31261959	192.1635595
197.66141557	289.90184475	262.5006444	95.06574089	59.75874862
151.25751435	149.81595307	140.97064259	234.2877643	154.85618599
256.08348261	246.10181028	276.89016939	250.18743644	340.41672489
709.86995848	1238.46383823	1430.718206	1139.57227178	1430.48955554
3137.15396436	5252.29222303	6505.13956845]		

CT

Wavelengths:

[54.	27.	18.	13.5	10.8
9.	7.71428571	6.75	6.	5.4
4.90909091	4.5	4.15384615	3.85714286	3.6
3.375	3.17647059	3.	2.84210526	2.7
2.57142857	2.45454545	2.34782609	2.25	2.16
2.07692308	-2.	-2.07692308	-2.16	-2.25
-2.34782609	-2.45454545	-2.57142857	-2.7	-2.84210526
-3.	-3.17647059	-3.375	-3.6	-3.85714286
-4.15384615	-4.5	-4.90909091	-5.4	-6.
-6.75	-7.71428571	-9.	-10.8	-13.5
-18.	-27.	-54.]	

Amps:

[5007.78588554	4562.36465941	3341.17194659	791.55938424	268.63736964
786.50537911	1100.08554365	1051.86863216	755.24323701	639.94520864
888.42155282	619.48324868	408.06361029	316.47214508	283.78564136
327.73070085	411.36420705	220.456656	96.46763467	184.16995136
337.65291396	432.04293363	490.39071951	453.60500554	505.15445185
371.96859874	354.7037037	371.96859874	505.15445185	453.60500554
490.39071951	432.04293363	337.65291396	184.16995136	96.46763467
220.456656	411.36420705	327.73070085	283.78564136	316.47214508
408.06361029	619.48324868	888.42155282	639.94520864	755.24323701
1051.86863216	1100.08554365	786.50537911	268.63736964	791.55938424
3341.17194659	4562.36465941	5007.78588554]		

DC

Wavelengths:

[54.	27.	18.	13.5	10.8
9.	7.71428571	6.75	6.	5.4
4.90909091	4.5	4.15384615	3.85714286	3.6
3.375	3.17647059	3.	2.84210526	2.7
2.57142857	2.45454545	2.34782609	2.25	2.16
2.07692308	-2.	-2.07692308	-2.16	-2.25
-2.34782609	-2.45454545	-2.57142857	-2.7	-2.84210526
-3.	-3.17647059	-3.375	-3.6	-3.85714286
-4.15384615	-4.5	-4.90909091	-5.4	-6.
-6.75	-7.71428571	-9.	-10.8	-13.5
-18.	-27.	-54.]	

Amps:

[145.27346047	256.65185446	215.71571338	27.74199852	48.87262423
41.1766427	44.14918274	52.29628494	50.82102078	37.97830251
34.6484084	39.9421977	10.75021695	10.8295779	3.2454682
20.34263142	18.02669806	14.67924768	8.4274244	13.01826837
12.9622446	17.32587825	32.01814428	17.36111237	6.85216493
19.04739595	21.33296216	19.04739595	6.85216493	17.36111237
32.01814428	17.32587825	12.9622446	13.01826837	8.4274244

14.67924768	18.02669806	20.34263142	3.2454682	10.8295779
10.75021695	39.9421977	34.6484084	37.97830251	50.82102078
52.29628494	44.14918274	41.1766427	48.87262423	27.74199852
215.71571338	256.65185446	145.27346047]		

DE

Wavelengths:

[54.	27.	18.	13.5	10.8
9.	7.71428571	6.75	6.	5.4
4.90909091	4.5	4.15384615	3.85714286	3.6
3.375	3.17647059	3.	2.84210526	2.7
2.57142857	2.45454545	2.34782609	2.25	2.16
2.07692308	-2.	-2.07692308	-2.16	-2.25
-2.34782609	-2.45454545	-2.57142857	-2.7	-2.84210526
-3.	-3.17647059	-3.375	-3.6	-3.85714286
-4.15384615	-4.5	-4.90909091	-5.4	-6.
-6.75	-7.71428571	-9.	-10.8	-13.5
-18.	-27.	-54.]	

Amps:

[1344.51777054	1326.69290559	972.83529044	365.76119496	218.91345821
207.94630538	216.61366692	267.57131474	207.76050996	187.0207299
172.28486267	109.34556415	47.18919294	27.43931779	95.91079347
125.31843813	138.69590777	152.79249948	102.18693197	84.10549564
67.40742711	53.13445097	68.85470986	64.90708323	59.00929516
62.51580284	78.66976815	62.51580284	59.00929516	64.90708323
68.85470986	53.13445097	67.40742711	84.10549564	102.18693197
152.79249948	138.69590777	125.31843813	95.91079347	27.43931779
47.18919294	109.34556415	172.28486267	187.0207299	207.76050996
267.57131474	216.61366692	207.94630538	218.91345821	365.76119496
972.83529044	1326.69290559	1344.51777054]		

FL

Wavelengths:

[54.	27.	18.	13.5	10.8
9.	7.71428571	6.75	6.	5.4
4.90909091	4.5	4.15384615	3.85714286	3.6
3.375	3.17647059	3.	2.84210526	2.7
2.57142857	2.45454545	2.34782609	2.25	2.16
2.07692308	-2.	-2.07692308	-2.16	-2.25
-2.34782609	-2.45454545	-2.57142857	-2.7	-2.84210526
-3.	-3.17647059	-3.375	-3.6	-3.85714286
-4.15384615	-4.5	-4.90909091	-5.4	-6.
-6.75	-7.71428571	-9.	-10.8	-13.5
-18.	-27.	-54.]	

Amps:

[6666.69173163	8800.87087822	5797.99046613	3836.96038624	2397.9429135
2423.02292248	1810.00866943	1808.03280923	1146.84134175	1150.30598703
896.75657154	903.51766943	891.29944265	644.78761719	633.3092023
206.50139003	459.15840599	348.71705357	509.45112485	369.79082471
329.71907266	572.62970711	315.13968479	756.40213767	284.17652079
630.19762716	167.90543987	630.19762716	284.17652079	756.40213767
315.13968479	572.62970711	329.71907266	369.79082471	509.45112485
348.71705357	459.15840599	206.50139003	633.3092023	644.78761719
891.29944265	903.51766943	896.75657154	1150.30598703	1146.84134175
1808.03280923	1810.00866943	2423.02292248	2397.9429135	3836.96038624
5797.99046613	8800.87087822	6666.69173163]		

FSM

Wavelengths:

[54.	27.	18.	13.5	10.8
9.	7.71428571	6.75	6.	5.4
4.90909091	4.5	4.15384615	3.85714286	3.6
3.375	3.17647059	3.	2.84210526	2.7
2.57142857	2.45454545	2.34782609	2.25	2.16
2.07692308	-2.	-2.07692308	-2.16	-2.25

-2.34782609	-2.45454545	-2.57142857	-2.7	-2.84210526
-3.	-3.17647059	-3.375	-3.6	-3.85714286
-4.15384615	-4.5	-4.90909091	-5.4	-6.
-6.75	-7.71428571	-9.	-10.8	-13.5
-18.	-27.	-54.]	

Amps:

[0.03703704 0.03703704 0.03703704 0.03703704 0.03703704 0.03703704
0.03703704 0.03703704 0.03703704 0.03703704 0.03703704 0.03703704
0.03703704 0.03703704 0.03703704 0.03703704 0.03703704 0.03703704
0.03703704 0.03703704 0.03703704 0.03703704 0.03703704 0.03703704
0.03703704 0.03703704 0.03703704 0.03703704 0.03703704 0.03703704
0.03703704 0.03703704 0.03703704 0.03703704 0.03703704 0.03703704
0.03703704 0.03703704 0.03703704 0.03703704 0.03703704 0.03703704
0.03703704 0.03703704 0.03703704 0.03703704 0.03703704 0.03703704
0.03703704 0.03703704 0.03703704 0.03703704 0.03703704 0.03703704]

GA

Wavelengths:

[54.	27.	18.	13.5	10.8
9.	7.71428571	6.75	6.	5.4
4.90909091	4.5	4.15384615	3.85714286	3.6
3.375	3.17647059	3.	2.84210526	2.7
2.57142857	2.45454545	2.34782609	2.25	2.16
2.07692308	-2.	-2.07692308	-2.16	-2.25
-2.34782609	-2.45454545	-2.57142857	-2.7	-2.84210526
-3.	-3.17647059	-3.375	-3.6	-3.85714286
-4.15384615	-4.5	-4.90909091	-5.4	-6.
-6.75	-7.71428571	-9.	-10.8	-13.5
-18.	-27.	-54.]	

Amps:

[12692.48173685 13435.54292665 9505.61757824 5955.29753213
4923.95171731 4538.04866663 2844.15466165 1650.50294262
2669.21317066 3035.94788645 2142.28858675 1065.26569332
722.50647037 1365.58007346 1033.58178992 487.04816016
1372.37646225 2056.86136141 1576.53295817 318.77771156
855.59851005 1867.63391032 2281.81806898 1078.22056614
354.28661597 1052.56319948 2035.3556 1052.56319948
354.28661597 1078.22056614 2281.81806898 1867.63391032
855.59851005 318.77771156 1576.53295817 2056.86136141
1372.37646225 487.04816016 1033.58178992 1365.58007346
722.50647037 1065.26569332 2142.28858675 3035.94788645
2669.21317066 1650.50294262 2844.15466165 4538.04866663
4923.95171731 5955.29753213 9505.61757824 13435.54292665
12692.48173685]

GU

Wavelengths:

[54.	27.	18.	13.5	10.8
9.	7.71428571	6.75	6.	5.4
4.90909091	4.5	4.15384615	3.85714286	3.6
3.375	3.17647059	3.	2.84210526	2.7
2.57142857	2.45454545	2.34782609	2.25	2.16
2.07692308	-2.	-2.07692308	-2.16	-2.25
-2.34782609	-2.45454545	-2.57142857	-2.7	-2.84210526
-3.	-3.17647059	-3.375	-3.6	-3.85714286
-4.15384615	-4.5	-4.90909091	-5.4	-6.
-6.75	-7.71428571	-9.	-10.8	-13.5
-18.	-27.	-54.]	

Amps:

[56.16992553 31.84735513 12.02542543 11.27464894 17.85732084 12.65836898
4.44897877 6.69398888 7.29233594 9.25391469 6.32340294 2.73807839
7.01802278 7.91860132 6.9659055 4.33297552 1.01926233 3.55525907
5.97753908 6.79569899 4.92167487 1.43297726 2.05314308 3.48592315
3.3919765 1.65307676 0.1754207 1.65307676 3.3919765 3.48592315]

2.05314308 1.43297726 4.92167487 6.79569899 5.97753908 3.55525907
 1.01926233 4.33297552 6.9659055 7.91860132 7.01802278 2.73807839
 6.32340294 9.25391469 7.29233594 6.69398888 4.44897877 12.65836898
 17.85732084 11.27464894 12.02542543 31.84735513 56.16992553]

HI

Wavelengths:

[54. 27. 18. 13.5 10.8
 9. 7.71428571 6.75 6. 5.4
 4.90909091 4.5 4.15384615 3.85714286 3.6
 3.375 3.17647059 3. 2.84210526 2.7
 2.57142857 2.45454545 2.34782609 2.25 2.16
 2.07692308 -2. -2.07692308 -2.16 -2.25
 -2.34782609 -2.45454545 -2.57142857 -2.7 -2.84210526
 -3. -3.17647059 -3.375 -3.6 -3.85714286
 -4.15384615 -4.5 -4.90909091 -5.4 -6.
 -6.75 -7.71428571 -9. -10.8 -13.5
 -18. -27. -54.]

Amps:

[165.61718143 49.12255265 112.86870997 23.27966338 62.4397216
 40.52744698 17.72591107 35.51422867 2.72346027 16.1378401
 14.73441501 11.59121088 5.55738173 11.88883996 9.85795315
 3.53132093 5.76300569 8.37165614 11.17646746 7.16652708
 7.64643936 4.64308446 11.93292024 9.77659089 7.91303077
 11.53881213 4.66241222 11.53881213 7.91303077 9.77659089
 11.93292024 4.64308446 7.64643936 7.16652708 11.17646746
 8.37165614 5.76300569 3.53132093 9.85795315 11.88883996
 5.55738173 11.59121088 14.73441501 16.1378401 2.72346027
 35.51422867 17.72591107 40.52744698 62.4397216 23.27966338
 112.86870997 49.12255265 165.61718143]

IA

Wavelengths:

[54. 27. 18. 13.5 10.8
 9. 7.71428571 6.75 6. 5.4
 4.90909091 4.5 4.15384615 3.85714286 3.6
 3.375 3.17647059 3. 2.84210526 2.7
 2.57142857 2.45454545 2.34782609 2.25 2.16
 2.07692308 -2. -2.07692308 -2.16 -2.25
 -2.34782609 -2.45454545 -2.57142857 -2.7 -2.84210526
 -3. -3.17647059 -3.375 -3.6 -3.85714286
 -4.15384615 -4.5 -4.90909091 -5.4 -6.
 -6.75 -7.71428571 -9. -10.8 -13.5
 -18. -27. -54.]

Amps:

[6022.21380013 4069.47089319 1907.64622492 1610.83309703 1565.85658363
 2143.41023874 1336.0116614 916.02661772 699.33292841 891.58146742
 785.35846879 569.01865799 388.22518346 341.77424468 441.67312254
 337.15818825 86.12732016 204.67800362 143.90844779 291.13822943
 258.34096796 88.96263079 291.00020337 292.25305949 428.12429549
 403.00095805 404.50935254 403.00095805 428.12429549 292.25305949
 291.00020337 88.96263079 258.34096796 291.13822943 143.90844779
 204.67800362 86.12732016 337.15818825 441.67312254 341.77424468
 388.22518346 569.01865799 785.35846879 891.58146742 699.33292841
 916.02661772 1336.0116614 2143.41023874 1565.85658363 1610.83309703
 1907.64622492 4069.47089319 6022.21380013]

ID

Wavelengths:

[54. 27. 18. 13.5 10.8
 9. 7.71428571 6.75 6. 5.4
 4.90909091 4.5 4.15384615 3.85714286 3.6
 3.375 3.17647059 3. 2.84210526 2.7
 2.57142857 2.45454545 2.34782609 2.25 2.16
 2.07692308 -2. -2.07692308 -2.16 -2.25

-2.34782609	-2.45454545	-2.57142857	-2.7	-2.84210526
-3.	-3.17647059	-3.375	-3.6	-3.85714286
-4.15384615	-4.5	-4.90909091	-5.4	-6.
-6.75	-7.71428571	-9.	-10.8	-13.5
-18.	-27.	-54.]	

Amps:

[2983.66958758	1678.741041	1273.75713689	109.40526467	183.67899191
194.42133213	158.97376376	247.38949994	150.71547183	245.5144589
158.27159672	228.24077336	167.23949079	81.60580412	109.74971052
142.01401824	87.42167185	78.31005868	20.45401503	44.10944447
23.32682565	94.5623639	170.76737235	180.25130533	177.1667854
153.93172729	86.82375976	153.93172729	177.1667854	180.25130533
170.76737235	94.5623639	23.32682565	44.10944447	20.45401503
78.31005868	87.42167185	142.01401824	109.74971052	81.60580412
167.23949079	228.24077336	158.27159672	245.5144589	150.71547183
247.38949994	158.97376376	194.42133213	183.67899191	109.40526467
1273.75713689	1678.741041	2983.66958758]		

IL

Wavelengths:

[54.	27.	18.	13.5	10.8
9.	7.71428571	6.75	6.	5.4
4.90909091	4.5	4.15384615	3.85714286	3.6
3.375	3.17647059	3.	2.84210526	2.7
2.57142857	2.45454545	2.34782609	2.25	2.16
2.07692308	-2.	-2.07692308	-2.16	-2.25
-2.34782609	-2.45454545	-2.57142857	-2.7	-2.84210526
-3.	-3.17647059	-3.375	-3.6	-3.85714286
-4.15384615	-4.5	-4.90909091	-5.4	-6.
-6.75	-7.71428571	-9.	-10.8	-13.5
-18.	-27.	-54.]	

Amps:

[16427.89082726	13646.8322085	6298.61605222	3803.66389622
2339.52685591	3906.18858519	2511.24092887	1622.72078104
371.12995987	1103.08350674	1583.03570347	1601.21427737
1058.14010541	483.56458219	634.02755574	550.00504205
427.67610651	477.94205519	717.53184998	687.80421945
381.1218245	367.50737812	507.90316761	879.76334873
824.81870588	428.19993129	24.77947495	428.19993129
824.81870588	879.76334873	507.90316761	367.50737812
381.1218245	687.80421945	717.53184998	477.94205519
427.67610651	550.00504205	634.02755574	483.56458219
1058.14010541	1601.21427737	1583.03570347	1103.08350674
371.12995987	1622.72078104	2511.24092887	3906.18858519
2339.52685591	3803.66389622	6298.61605222	13646.8322085
16427.89082726]			

IN

Wavelengths:

[54.	27.	18.	13.5	10.8
9.	7.71428571	6.75	6.	5.4
4.90909091	4.5	4.15384615	3.85714286	3.6
3.375	3.17647059	3.	2.84210526	2.7
2.57142857	2.45454545	2.34782609	2.25	2.16
2.07692308	-2.	-2.07692308	-2.16	-2.25
-2.34782609	-2.45454545	-2.57142857	-2.7	-2.84210526
-3.	-3.17647059	-3.375	-3.6	-3.85714286
-4.15384615	-4.5	-4.90909091	-5.4	-6.
-6.75	-7.71428571	-9.	-10.8	-13.5
-18.	-27.	-54.]	

Amps:

[14609.89674777	10788.91813661	6470.21261316	1580.08248881
543.73460385	1687.84997528	1913.88029594	1485.93147199
830.9088344	803.07540462	1052.15046133	1240.15815021

986.32244165	546.89072988	647.69501143	571.24243379
668.57096734	611.38840959	137.26022574	239.64306929
370.33093194	717.69050786	701.75479893	600.52272256
508.72577986	315.36627995	126.07407407	315.36627995
508.72577986	600.52272256	701.75479893	717.69050786
370.33093194	239.64306929	137.26022574	611.38840959
668.57096734	571.24243379	647.69501143	546.89072988
986.32244165	1240.15815021	1052.15046133	803.07540462
830.9088344	1485.93147199	1913.88029594	1687.84997528
543.73460385	1580.08248881	6470.21261316	10788.91813661

14609.89674777]

KS

Wavelengths:

[54.	27.	18.	13.5	10.8
9.	7.71428571	6.75	6.	5.4
4.90909091	4.5	4.15384615	3.85714286	3.6
3.375	3.17647059	3.	2.84210526	2.7
2.57142857	2.45454545	2.34782609	2.25	2.16
2.07692308	-2.	-2.07692308	-2.16	-2.25
-2.34782609	-2.45454545	-2.57142857	-2.7	-2.84210526
-3.	-3.17647059	-3.375	-3.6	-3.85714286
-4.15384615	-4.5	-4.90909091	-5.4	-6.
-6.75	-7.71428571	-9.	-10.8	-13.5
-18.	-27.	-54.		

Amps:

[6409.13482864	4063.21942997	2383.92774426	368.65730869	444.48514123
1385.8860294	980.73842952	704.48351142	71.05554349	537.5800089
440.64557012	502.45664449	480.3770715	265.56872059	254.95759597
199.40784837	146.61034876	196.94595152	132.5589957	117.53743111
249.83572928	265.2036481	285.17025186	447.68698574	408.26222491
196.60209157	31.96296296	196.60209157	408.26222491	447.68698574
285.17025186	265.2036481	249.83572928	117.53743111	132.5589957
196.94595152	146.61034876	199.40784837	254.95759597	265.56872059
480.3770715	502.45664449	440.64557012	537.5800089	71.05554349
704.48351142	980.73842952	1385.8860294	444.48514123	368.65730869
2383.92774426	4063.21942997	6409.13482864]		

KY

Wavelengths:

[54.	27.	18.	13.5	10.8
9.	7.71428571	6.75	6.	5.4
4.90909091	4.5	4.15384615	3.85714286	3.6
3.375	3.17647059	3.	2.84210526	2.7
2.57142857	2.45454545	2.34782609	2.25	2.16
2.07692308	-2.	-2.07692308	-2.16	-2.25
-2.34782609	-2.45454545	-2.57142857	-2.7	-2.84210526
-3.	-3.17647059	-3.375	-3.6	-3.85714286
-4.15384615	-4.5	-4.90909091	-5.4	-6.
-6.75	-7.71428571	-9.	-10.8	-13.5
-18.	-27.	-54.		

Amps:

[8681.43720934	5488.76360051	3387.38038598	1332.16054471	1345.12501876
1523.49444333	1708.24608851	1445.77279113	1144.99936624	831.27969601
675.79238836	352.8643535	150.53129087	121.87262974	319.75086794
662.11724903	793.00937469	792.96898038	678.30027851	887.12457091
838.61962877	524.85214812	631.93006838	614.22807216	458.54299425
318.11908258	206.18518519	318.11908258	458.54299425	614.22807216
631.93006838	524.85214812	838.61962877	887.12457091	678.30027851
792.96898038	793.00937469	662.11724903	319.75086794	121.87262974
150.53129087	352.8643535	675.79238836	831.27969601	1144.99936624
1445.77279113	1708.24608851	1523.49444333	1345.12501876	1332.16054471
3387.38038598	5488.76360051	8681.43720934]		

LA

Wavelengths:

```
[ 54.      27.      18.      13.5      10.8
   9.      7.71428571  6.75      6.      5.4
  4.90909091  4.5      4.15384615  3.85714286  3.6
  3.375      3.17647059  3.      2.84210526  2.7
  2.57142857  2.45454545  2.34782609  2.25      2.16
  2.07692308 -2.      -2.07692308 -2.16      -2.25
 -2.34782609 -2.45454545 -2.57142857 -2.7      -2.84210526
 -3.      -3.17647059 -3.375      -3.6      -3.85714286
 -4.15384615 -4.5      -4.90909091 -5.4      -6.
 -6.75      -7.71428571 -9.      -10.8     -13.5
 -18.      -27.      -54.      ]
```

Amps:

```
[2270.15749946 3054.9789841 2502.18926227 1341.95140885 336.82722317
 661.97243033 853.18792474 1010.75255427 460.52272309 130.94861347
 118.29412317 398.52399156 437.47968845 102.05487355 248.35557949
 112.21393781 418.95193226 350.90134777 120.27500167 173.36566382
 195.43376366 496.33957543 327.17257693 217.2598769 87.82663982
 130.30239905 387.16516191 130.30239905 87.82663982 217.2598769
 327.17257693 496.33957543 195.43376366 173.36566382 120.27500167
 350.90134777 418.95193226 112.21393781 248.35557949 102.05487355
 437.47968845 398.52399156 118.29412317 130.94861347 460.52272309
 1010.75255427 853.18792474 661.97243033 336.82722317 1341.95140885
 2502.18926227 3054.9789841 2270.15749946]
```

MA

Wavelengths:

```
[ 54.      27.      18.      13.5      10.8
   9.      7.71428571  6.75      6.      5.4
  4.90909091  4.5      4.15384615  3.85714286  3.6
  3.375      3.17647059  3.      2.84210526  2.7
  2.57142857  2.45454545  2.34782609  2.25      2.16
  2.07692308 -2.      -2.07692308 -2.16      -2.25
 -2.34782609 -2.45454545 -2.57142857 -2.7      -2.84210526
 -3.      -3.17647059 -3.375      -3.6      -3.85714286
 -4.15384615 -4.5      -4.90909091 -5.4      -6.
 -6.75      -7.71428571 -9.      -10.8     -13.5
 -18.      -27.      -54.      ]
```

Amps:

```
[9817.70392174 8877.71656874 8054.81115987 3038.9403646 1270.25888169
 1852.63562373 2066.93959402 1629.78895871 1348.97382327 1603.67793055
 1608.51794324 1088.74391919 714.90945935 255.64173877 462.3750498
 686.08819289 703.9056465 560.05715954 148.77542294 367.31121207
 588.13493177 690.56187684 937.47356046 934.27248508 810.3638727
 683.2288845 510.48148148 683.2288845 810.3638727 934.27248508
 937.47356046 690.56187684 588.13493177 367.31121207 148.77542294
 560.05715954 703.9056465 686.08819289 462.3750498 255.64173877
 714.90945935 1088.74391919 1608.51794324 1603.67793055 1348.97382327
 1629.78895871 2066.93959402 1852.63562373 1270.25888169 3038.9403646
 8054.81115987 8877.71656874 9817.70392174]
```

MD

Wavelengths:

```
[ 54.      27.      18.      13.5      10.8
   9.      7.71428571  6.75      6.      5.4
  4.90909091  4.5      4.15384615  3.85714286  3.6
  3.375      3.17647059  3.      2.84210526  2.7
  2.57142857  2.45454545  2.34782609  2.25      2.16
  2.07692308 -2.      -2.07692308 -2.16      -2.25
 -2.34782609 -2.45454545 -2.57142857 -2.7      -2.84210526
 -3.      -3.17647059 -3.375      -3.6      -3.85714286
 -4.15384615 -4.5      -4.90909091 -5.4      -6.
 -6.75      -7.71428571 -9.      -10.8     -13.5
 -18.      -27.      -54.      ]
```

Amps:

```
[4101.69603686 4975.42342486 3393.1569845 398.44232314 877.18186838
1009.23273244 1208.53788751 974.27971923 784.81924848 467.05340567
576.34449804 603.95624457 331.31232502 64.96752107 75.66755843
213.29851365 401.21162359 327.02409692 198.05247365 169.15575652
208.82957554 250.97589868 257.01853652 422.77480439 302.25499357
243.12105274 261.69492065 243.12105274 302.25499357 422.77480439
257.01853652 250.97589868 208.82957554 169.15575652 198.05247365
327.02409692 401.21162359 213.29851365 75.66755843 64.96752107
331.31232502 603.95624457 576.34449804 467.05340567 784.81924848
974.27971923 1208.53788751 1009.23273244 877.18186838 398.44232314
3393.1569845 4975.42342486 4101.69603686]
```

ME

Wavelengths:

```
[ 54.          27.          18.          13.5          10.8
   9.          7.71428571  6.75          6.          5.4
  4.90909091  4.5          4.15384615  3.85714286  3.6
  3.375        3.17647059  3.          2.84210526  2.7
  2.57142857  2.45454545  2.34782609  2.25          2.16
  2.07692308 -2.          -2.07692308 -2.16          -2.25
 -2.34782609 -2.45454545 -2.57142857 -2.7          -2.84210526
 -3.          -3.17647059 -3.375        -3.6          -3.85714286
 -4.15384615 -4.5          -4.90909091 -5.4          -6.
 -6.75        -7.71428571 -9.          -10.8         -13.5
 -18.         -27.         -54.          ]
```

Amps:

```
[946.15867303 822.53948854 570.42758983 357.55565519 240.05272958
201.54829261 164.47230678 134.93519362 129.32815926 142.22503094
157.95673595 127.74611621 100.73478601 44.60960672 35.98448928
12.72234662 26.13030058 37.41617498 34.93044779 44.16324876
43.60636323 49.08933358 57.90852144 59.71660296 56.2460779
47.72978123 35.54822633 47.72978123 56.2460779 59.71660296
57.90852144 49.08933358 43.60636323 44.16324876 34.93044779
37.41617498 26.13030058 12.72234662 35.98448928 44.60960672
100.73478601 127.74611621 157.95673595 142.22503094 129.32815926
134.93519362 164.47230678 201.54829261 240.05272958 357.55565519
570.42758983 822.53948854 946.15867303]
```

MI

Wavelengths:

```
[ 54.          27.          18.          13.5          10.8
   9.          7.71428571  6.75          6.          5.4
  4.90909091  4.5          4.15384615  3.85714286  3.6
  3.375        3.17647059  3.          2.84210526  2.7
  2.57142857  2.45454545  2.34782609  2.25          2.16
  2.07692308 -2.          -2.07692308 -2.16          -2.25
 -2.34782609 -2.45454545 -2.57142857 -2.7          -2.84210526
 -3.          -3.17647059 -3.375        -3.6          -3.85714286
 -4.15384615 -4.5          -4.90909091 -5.4          -6.
 -6.75        -7.71428571 -9.          -10.8         -13.5
 -18.         -27.         -54.          ]
```

Amps:

```
[7444.97863716 6184.16943414 4071.22986552 1607.74190751 1606.24912838
1258.59939611 1257.42667091 1135.0746161 358.91135027 82.19021928
253.18189033 398.47273876 249.68304237 243.88010504 341.07454374
188.21346187 334.43218752 129.53690143 229.31276017 138.78519076
319.53016193 293.11317488 229.12409376 117.04554058 80.80246578
139.02444584 219.64424221 139.02444584 80.80246578 117.04554058
229.12409376 293.11317488 319.53016193 138.78519076 229.31276017
129.53690143 334.43218752 188.21346187 341.07454374 243.88010504
249.68304237 398.47273876 253.18189033 82.19021928 358.91135027
1135.0746161 1257.42667091 1258.59939611 1606.24912838 1607.74190751
4071.22986552 6184.16943414 7444.97863716]
```

MN

Wavelengths:

[54.	27.	18.	13.5	10.8
9.	7.71428571	6.75	6.	5.4
4.90909091	4.5	4.15384615	3.85714286	3.6
3.375	3.17647059	3.	2.84210526	2.7
2.57142857	2.45454545	2.34782609	2.25	2.16
2.07692308	-2.	-2.07692308	-2.16	-2.25
-2.34782609	-2.45454545	-2.57142857	-2.7	-2.84210526
-3.	-3.17647059	-3.375	-3.6	-3.85714286
-4.15384615	-4.5	-4.90909091	-5.4	-6.
-6.75	-7.71428571	-9.	-10.8	-13.5
-18.	-27.	-54.]	

Amps:

[10007.18195855	8030.59596298	4810.577719	3711.48686786
2215.89838224	2775.05617132	2004.53564326	1657.13526238
734.07022365	268.71107977	413.15043678	421.93431125
396.93639116	433.24646088	524.29977664	438.19145899
330.07750976	281.39061677	217.97705685	89.35382402
379.86552168	338.94438463	505.10640808	390.72229793
282.54093675	177.90011827	70.9544522	177.90011827
282.54093675	390.72229793	505.10640808	338.94438463
379.86552168	89.35382402	217.97705685	281.39061677
330.07750976	438.19145899	524.29977664	433.24646088
396.93639116	421.93431125	413.15043678	268.71107977
734.07022365	1657.13526238	2004.53564326	2775.05617132
2215.89838224	3711.48686786	4810.577719	8030.59596298
10007.18195855]			

MO

Wavelengths:

[54.	27.	18.	13.5	10.8
9.	7.71428571	6.75	6.	5.4
4.90909091	4.5	4.15384615	3.85714286	3.6
3.375	3.17647059	3.	2.84210526	2.7
2.57142857	2.45454545	2.34782609	2.25	2.16
2.07692308	-2.	-2.07692308	-2.16	-2.25
-2.34782609	-2.45454545	-2.57142857	-2.7	-2.84210526
-3.	-3.17647059	-3.375	-3.6	-3.85714286
-4.15384615	-4.5	-4.90909091	-5.4	-6.
-6.75	-7.71428571	-9.	-10.8	-13.5
-18.	-27.	-54.]	

Amps:

[11822.2230374	5937.29755001	4008.03490862	347.23959751
797.88684812	1848.09123377	2063.9909597	639.93585557
346.26809352	587.82069994	997.73690006	699.82245328
839.88221641	539.28652098	265.57308036	567.08909451
626.15483654	343.51588698	523.76256547	139.63054539
324.62454921	363.64927633	691.53654272	269.53437299
605.52242634	508.56797081	209.	508.56797081
605.52242634	269.53437299	691.53654272	363.64927633
324.62454921	139.63054539	523.76256547	343.51588698
626.15483654	567.08909451	265.57308036	539.28652098
839.88221641	699.82245328	997.73690006	587.82069994
346.26809352	639.93585557	2063.9909597	1848.09123377
797.88684812	347.23959751	4008.03490862	5937.29755001
11822.2230374]			

MP

Wavelengths:

[54.	27.	18.	13.5	10.8
9.	7.71428571	6.75	6.	5.4
4.90909091	4.5	4.15384615	3.85714286	3.6
3.375	3.17647059	3.	2.84210526	2.7

2.57142857	2.45454545	2.34782609	2.25	2.16
2.07692308	-2.	-2.07692308	-2.16	-2.25
-2.34782609	-2.45454545	-2.57142857	-2.7	-2.84210526
-3.	-3.17647059	-3.375	-3.6	-3.85714286
-4.15384615	-4.5	-4.90909091	-5.4	-6.
-6.75	-7.71428571	-9.	-10.8	-13.5
-18.	-27.	-54.		

Amps:

[1.48040859 0.83577182 0.49020488 0.71918681 0.59437648 0.71137726
0.59609842 0.45924716 0.51851852 0.22271021 0.77586116 0.8961527
0.5783696 0.62975736 0.64853247 0.60945008 0.51369629 0.12830006
0.51187554 0.21947807 0.58232706 0.27417205 1.21845064 0.85797448
0.8117587 0.60064832 0.07407407 0.60064832 0.8117587 0.85797448
1.21845064 0.27417205 0.58232706 0.21947807 0.51187554 0.12830006
0.51369629 0.60945008 0.64853247 0.62975736 0.5783696 0.8961527
0.77586116 0.22271021 0.51851852 0.45924716 0.59609842 0.71137726
0.59437648 0.71918681 0.49020488 0.83577182 1.48040859]

MS

Wavelengths:

[54.	27.	18.	13.5	10.8
9.	7.71428571	6.75	6.	5.4
4.90909091	4.5	4.15384615	3.85714286	3.6
3.375	3.17647059	3.	2.84210526	2.7
2.57142857	2.45454545	2.34782609	2.25	2.16
2.07692308	-2.	-2.07692308	-2.16	-2.25
-2.34782609	-2.45454545	-2.57142857	-2.7	-2.84210526
-3.	-3.17647059	-3.375	-3.6	-3.85714286
-4.15384615	-4.5	-4.90909091	-5.4	-6.
-6.75	-7.71428571	-9.	-10.8	-13.5
-18.	-27.	-54.		

Amps:

[3451.27889915 3266.57369884 2336.23663017 973.74222372 993.4893166
358.94055049 465.27257808 610.80071144 520.60128311 417.87235474
506.58390632 194.34306974 341.99234745 118.22654208 197.27194852
224.42725157 183.73245602 151.99851481 167.16520138 387.13894699
254.01095353 286.47495943 162.82599863 237.0271702 189.9641238
188.03381641 138.81252922 188.03381641 189.9641238 237.0271702
162.82599863 286.47495943 254.01095353 387.13894699 167.16520138
151.99851481 183.73245602 224.42725157 197.27194852 118.22654208
341.99234745 194.34306974 506.58390632 417.87235474 520.60128311
610.80071144 465.27257808 358.94055049 993.4893166 973.74222372
2336.23663017 3266.57369884 3451.27889915]

MT

Wavelengths:

[54.	27.	18.	13.5	10.8
9.	7.71428571	6.75	6.	5.4
4.90909091	4.5	4.15384615	3.85714286	3.6
3.375	3.17647059	3.	2.84210526	2.7
2.57142857	2.45454545	2.34782609	2.25	2.16
2.07692308	-2.	-2.07692308	-2.16	-2.25
-2.34782609	-2.45454545	-2.57142857	-2.7	-2.84210526
-3.	-3.17647059	-3.375	-3.6	-3.85714286
-4.15384615	-4.5	-4.90909091	-5.4	-6.
-6.75	-7.71428571	-9.	-10.8	-13.5
-18.	-27.	-54.		

Amps:

[2288.05748586 1301.90385747 682.38253504 284.94995281 209.64322858
224.55012243 242.11900873 226.62075259 101.26049648 51.13763765
110.2222135 140.67494287 132.88208579 96.22238526 69.0414555
66.48115535 87.1870163 97.00626484 56.92218691 65.7114693
104.8454033 114.7383714 107.72394653 51.19015887 49.59948252
22.73282714 47.47113677 22.73282714 49.59948252 51.19015887]

107.72394653	114.7383714	104.8454033	65.7114693	56.92218691
97.00626484	87.1870163	66.48115535	69.0414555	96.22238526
132.88208579	140.67494287	110.2222135	51.13763765	101.26049648
226.62075259	242.11900873	224.55012243	209.64322858	284.94995281
682.38253504	1301.90385747	2288.05748586]		

NC

Wavelengths:

[54.	27.	18.	13.5	10.8
9.	7.71428571	6.75	6.	5.4
4.90909091	4.5	4.15384615	3.85714286	3.6
3.375	3.17647059	3.	2.84210526	2.7
2.57142857	2.45454545	2.34782609	2.25	2.16
2.07692308	-2.	-2.07692308	-2.16	-2.25
-2.34782609	-2.45454545	-2.57142857	-2.7	-2.84210526
-3.	-3.17647059	-3.375	-3.6	-3.85714286
-4.15384615	-4.5	-4.90909091	-5.4	-6.
-6.75	-7.71428571	-9.	-10.8	-13.5
-18.	-27.	-54.]	

Amps:

[10684.96487257	9540.01495977	5596.9770672	4196.92360799
2728.13136296	2006.24880818	1719.61804051	1971.97032156
1512.61504898	1425.60624566	1225.01112714	844.26518285
622.25393153	61.56251069	425.04414003	590.35166729
813.3928694	818.98639667	559.71543052	674.88086185
832.18751038	857.83481577	934.46625447	732.11356371
597.25507484	346.82250117	255.83240154	346.82250117
597.25507484	732.11356371	934.46625447	857.83481577
832.18751038	674.88086185	559.71543052	818.98639667
813.3928694	590.35166729	425.04414003	61.56251069
622.25393153	844.26518285	1225.01112714	1425.60624566
1512.61504898	1971.97032156	1719.61804051	2006.24880818
2728.13136296	4196.92360799	5596.9770672	9540.01495977
10684.96487257]			

ND

Wavelengths:

[54.	27.	18.	13.5	10.8
9.	7.71428571	6.75	6.	5.4
4.90909091	4.5	4.15384615	3.85714286	3.6
3.375	3.17647059	3.	2.84210526	2.7
2.57142857	2.45454545	2.34782609	2.25	2.16
2.07692308	-2.	-2.07692308	-2.16	-2.25
-2.34782609	-2.45454545	-2.57142857	-2.7	-2.84210526
-3.	-3.17647059	-3.375	-3.6	-3.85714286
-4.15384615	-4.5	-4.90909091	-5.4	-6.
-6.75	-7.71428571	-9.	-10.8	-13.5
-18.	-27.	-54.]	

Amps:

[1994.48948612	1280.41500892	727.28959944	553.34648729	386.01210109
344.33687722	217.78869134	83.27170265	51.99251185	79.3615671
82.08566771	55.24020286	73.46769497	68.14419332	102.50724907
71.90552731	61.40803328	89.9929409	99.27290602	105.69661929
125.61765423	138.07061289	134.64977827	100.33320252	74.09356055
49.95713191	33.71689335	49.95713191	74.09356055	100.33320252
134.64977827	138.07061289	125.61765423	105.69661929	99.27290602
89.9929409	61.40803328	71.90552731	102.50724907	68.14419332
73.46769497	55.24020286	82.08566771	79.3615671	51.99251185
83.27170265	217.78869134	344.33687722	386.01210109	553.34648729
727.28959944	1280.41500892	1994.48948612]		

NE

Wavelengths:

[54.	27.	18.	13.5	10.8
9.	7.71428571	6.75	6.	5.4

4.90909091	4.5	4.15384615	3.85714286	3.6
3.375	3.17647059	3.	2.84210526	2.7
2.57142857	2.45454545	2.34782609	2.25	2.16
2.07692308	-2.	-2.07692308	-2.16	-2.25
-2.34782609	-2.45454545	-2.57142857	-2.7	-2.84210526
-3.	-3.17647059	-3.375	-3.6	-3.85714286
-4.15384615	-4.5	-4.90909091	-5.4	-6.
-6.75	-7.71428571	-9.	-10.8	-13.5
-18.	-27.	-54.]	

Amps:

[3912.60062742	3019.58059808	1176.50347517	797.62429993	405.4637297
836.53683406	594.7759879	355.09707776	126.10692873	237.74023156
284.79851062	313.29201432	201.33287534	148.54443542	152.80111789
148.02467086	94.39117379	70.27110505	58.35279852	56.22143394
106.75208266	116.09108754	158.40616499	197.80060006	79.70018068
145.63116868	78.26879278	145.63116868	79.70018068	197.80060006
158.40616499	116.09108754	106.75208266	56.22143394	58.35279852
70.27110505	94.39117379	148.02467086	152.80111789	148.54443542
201.33287534	313.29201432	284.79851062	237.74023156	126.10692873
355.09707776	594.7759879	836.53683406	405.4637297	797.62429993
1176.50347517	3019.58059808	3912.60062742]		

NH

Wavelengths:

[54.	27.	18.	13.5	10.8
9.	7.71428571	6.75	6.	5.4
4.90909091	4.5	4.15384615	3.85714286	3.6
3.375	3.17647059	3.	2.84210526	2.7
2.57142857	2.45454545	2.34782609	2.25	2.16
2.07692308	-2.	-2.07692308	-2.16	-2.25
-2.34782609	-2.45454545	-2.57142857	-2.7	-2.84210526
-3.	-3.17647059	-3.375	-3.6	-3.85714286
-4.15384615	-4.5	-4.90909091	-5.4	-6.
-6.75	-7.71428571	-9.	-10.8	-13.5
-18.	-27.	-54.]	

Amps:

[965.88117934	836.4898093	563.40224721	277.80676276	146.94827034
92.86117054	129.43415022	139.58644872	129.96982231	116.66581881
114.44821477	108.83291799	58.56522991	5.34770347	30.79442482
62.78863786	79.34019732	78.80701113	56.78431267	45.76202503
41.8108793	38.43100411	42.57682907	39.47151914	24.50251341
24.56377547	21.33298045	24.56377547	24.50251341	39.47151914
42.57682907	38.43100411	41.8108793	45.76202503	56.78431267
78.80701113	79.34019732	62.78863786	30.79442482	5.34770347
58.56522991	108.83291799	114.44821477	116.66581881	129.96982231
139.58644872	129.43415022	92.86117054	146.94827034	277.80676276
563.40224721	836.4898093	965.88117934]		

NJ

Wavelengths:

[54.	27.	18.	13.5	10.8
9.	7.71428571	6.75	6.	5.4
4.90909091	4.5	4.15384615	3.85714286	3.6
3.375	3.17647059	3.	2.84210526	2.7
2.57142857	2.45454545	2.34782609	2.25	2.16
2.07692308	-2.	-2.07692308	-2.16	-2.25
-2.34782609	-2.45454545	-2.57142857	-2.7	-2.84210526
-3.	-3.17647059	-3.375	-3.6	-3.85714286
-4.15384615	-4.5	-4.90909091	-5.4	-6.
-6.75	-7.71428571	-9.	-10.8	-13.5
-18.	-27.	-54.]	

Amps:

[10926.72383008	10904.52690105	9239.16651427	3135.13325007
1302.48245607	1364.08408767	3313.52479808	2862.10944213

1746.92085136	1116.65949432	1287.83630977	1300.44839123
1209.67730658	600.61102159	672.85245898	493.00620194
806.04272509	944.51302874	748.90272888	473.06551964
615.02284976	656.84841191	954.60330337	887.12717965
687.34922556	581.9676491	719.66666667	581.9676491
687.34922556	887.12717965	954.60330337	656.84841191
615.02284976	473.06551964	748.90272888	944.51302874
806.04272509	493.00620194	672.85245898	600.61102159
1209.67730658	1300.44839123	1287.83630977	1116.65949432
1746.92085136	2862.10944213	3313.52479808	1364.08408767
1302.48245607	3135.13325007	9239.16651427	10904.52690105
10926.72383008]			

NM

Wavelengths:

[54.	27.	18.	13.5	10.8
9.	7.71428571	6.75	6.	5.4
4.90909091	4.5	4.15384615	3.85714286	3.6
3.375	3.17647059	3.	2.84210526	2.7
2.57142857	2.45454545	2.34782609	2.25	2.16
2.07692308	-2.	-2.07692308	-2.16	-2.25
-2.34782609	-2.45454545	-2.57142857	-2.7	-2.84210526
-3.	-3.17647059	-3.375	-3.6	-3.85714286
-4.15384615	-4.5	-4.90909091	-5.4	-6.
-6.75	-7.71428571	-9.	-10.8	-13.5
-18.	-27.	-54.]	

Amps:

[3791.61971949	3101.49539114	1699.05247703	403.12977468	195.83636988
626.40939504	651.92483514	612.0605313	438.82418363	127.17397148
71.04371525	218.53802583	301.17306982	205.05802978	138.22960904
176.00920791	201.68825677	272.69057873	258.95395619	183.91611101
104.11941879	153.18640374	220.84343586	217.06970122	237.01641581
110.24130605	33.17312437	110.24130605	237.01641581	217.06970122
220.84343586	153.18640374	104.11941879	183.91611101	258.95395619
272.69057873	201.68825677	176.00920791	138.22960904	205.05802978
301.17306982	218.53802583	71.04371525	127.17397148	438.82418363
612.0605313	651.92483514	626.40939504	195.83636988	403.12977468
1699.05247703 3101.49539114 3791.61971949]				

NV

Wavelengths:

[54.	27.	18.	13.5	10.8
9.	7.71428571	6.75	6.	5.4
4.90909091	4.5	4.15384615	3.85714286	3.6
3.375	3.17647059	3.	2.84210526	2.7
2.57142857	2.45454545	2.34782609	2.25	2.16
2.07692308	-2.	-2.07692308	-2.16	-2.25
-2.34782609	-2.45454545	-2.57142857	-2.7	-2.84210526
-3.	-3.17647059	-3.375	-3.6	-3.85714286
-4.15384615	-4.5	-4.90909091	-5.4	-6.
-6.75	-7.71428571	-9.	-10.8	-13.5
-18.	-27.	-54.]	

Amps:

[5142.63806554	4398.99995457	3283.10145568	628.54109102	592.35781142
550.84364889	698.93141971	805.43618002	563.91640631	416.5014994
454.45644974	322.81861229	400.49615164	200.17285774	148.59399532
241.20612596	121.28772934	294.61220239	135.30639242	141.9490577
183.09515932	258.77399542	362.04262017	479.45072132	269.24517987
243.7991069	117.37037037	243.7991069	269.24517987	479.45072132
362.04262017	258.77399542	183.09515932	141.9490577	135.30639242
294.61220239	121.28772934	241.20612596	148.59399532	200.17285774
400.49615164	322.81861229	454.45644974	416.5014994	563.91640631
805.43618002	698.93141971	550.84364889	592.35781142	628.54109102
3283.10145568 4398.99995457 5142.63806554]				

NY

Wavelengths:

[54.	27.	18.	13.5	10.8
9.	7.71428571	6.75	6.	5.4
4.90909091	4.5	4.15384615	3.85714286	3.6
3.375	3.17647059	3.	2.84210526	2.7
2.57142857	2.45454545	2.34782609	2.25	2.16
2.07692308	-2.	-2.07692308	-2.16	-2.25
-2.34782609	-2.45454545	-2.57142857	-2.7	-2.84210526
-3.	-3.17647059	-3.375	-3.6	-3.85714286
-4.15384615	-4.5	-4.90909091	-5.4	-6.
-6.75	-7.71428571	-9.	-10.8	-13.5
-18.	-27.	-54.]	

Amps:

[8565.41086551	6813.39512225	7581.02222694	4378.53158778	1287.97071068
1125.11264513	2238.30257814	2424.78917768	1571.64003605	883.94615432
825.6657491	941.74231126	606.16564422	466.21268423	470.58582099
367.60179641	627.20284929	602.64093552	440.88967708	461.51499613
756.01569747	725.83406047	540.95403311	527.06107252	613.12315353
462.72932475	352.96741129	462.72932475	613.12315353	527.06107252
540.95403311	725.83406047	756.01569747	461.51499613	440.88967708
602.64093552	627.20284929	367.60179641	470.58582099	466.21268423
606.16564422	941.74231126	825.6657491	883.94615432	1571.64003605
2424.78917768	2238.30257814	1125.11264513	1287.97071068	4378.53158778
7581.02222694	6813.39512225	8565.41086551]		

NYC

Wavelengths:

[54.	27.	18.	13.5	10.8
9.	7.71428571	6.75	6.	5.4
4.90909091	4.5	4.15384615	3.85714286	3.6
3.375	3.17647059	3.	2.84210526	2.7
2.57142857	2.45454545	2.34782609	2.25	2.16
2.07692308	-2.	-2.07692308	-2.16	-2.25
-2.34782609	-2.45454545	-2.57142857	-2.7	-2.84210526
-3.	-3.17647059	-3.375	-3.6	-3.85714286
-4.15384615	-4.5	-4.90909091	-5.4	-6.
-6.75	-7.71428571	-9.	-10.8	-13.5
-18.	-27.	-54.]	

Amps:

[1103.62559657	817.95626452	1296.9768627	915.66086997	362.61069031
58.10298687	412.16818486	513.32752878	355.04214735	178.20958173
106.21667235	180.02142391	175.98386137	127.12577066	89.76809392
82.59213111	79.87135934	66.03144971	87.253199	131.89846229
123.85766053	77.11909229	74.05378403	115.21836011	126.71053154
94.3643609	56.24405589	94.3643609	126.71053154	115.21836011
74.05378403	77.11909229	123.85766053	131.89846229	87.253199
66.03144971	79.87135934	82.59213111	89.76809392	127.12577066
175.98386137	180.02142391	106.21667235	178.20958173	355.04214735
513.32752878	412.16818486	58.10298687	362.61069031	915.66086997
1296.9768627	817.95626452	1103.62559657]		

OH

Wavelengths:

[54.	27.	18.	13.5	10.8
9.	7.71428571	6.75	6.	5.4
4.90909091	4.5	4.15384615	3.85714286	3.6
3.375	3.17647059	3.	2.84210526	2.7
2.57142857	2.45454545	2.34782609	2.25	2.16
2.07692308	-2.	-2.07692308	-2.16	-2.25
-2.34782609	-2.45454545	-2.57142857	-2.7	-2.84210526
-3.	-3.17647059	-3.375	-3.6	-3.85714286
-4.15384615	-4.5	-4.90909091	-5.4	-6.
-6.75	-7.71428571	-9.	-10.8	-13.5

-18. -27. -54.]

Amps:

```
[21430.00845029 16861.14724897 10775.39975877 3194.92911098
 568.03205212 2424.37091894 2633.46788434 2854.49301882
2017.5784515 1742.79032985 1971.59324845 1592.06280592
1090.43113429 492.96448241 597.26462994 1063.39143645
 894.4873444 964.71018342 508.07755391 355.78174557
 837.82518316 1375.32981707 2095.21469837 1744.58265868
1377.54653093 1085.7731998 375.03703704 1085.7731998
1377.54653093 1744.58265868 2095.21469837 1375.32981707
 837.82518316 355.78174557 508.07755391 964.71018342
 894.4873444 1063.39143645 597.26462994 492.96448241
1090.43113429 1592.06280592 1971.59324845 1742.79032985
2017.5784515 2854.49301882 2633.46788434 2424.37091894
 568.03205212 3194.92911098 10775.39975877 16861.14724897
21430.00845029]
```

OK

Wavelengths:

```
[ 54.                27.                18.                13.5                10.8
 9.                7.71428571 6.75                6.                5.4
 4.90909091 4.5                4.15384615 3.85714286 3.6
 3.375                3.17647059 3.                2.84210526 2.7
 2.57142857 2.45454545 2.34782609 2.25                2.16
 2.07692308 -2.                -2.07692308 -2.16                -2.25
-2.34782609 -2.45454545 -2.57142857 -2.7                -2.84210526
-3.                -3.17647059 -3.375                -3.6                -3.85714286
-4.15384615 -4.5                -4.90909091 -5.4                -6.
-6.75                -7.71428571 -9.                -10.8                -13.5
-18.                -27.                -54.                ]
```

Amps:

```
[8642.65618425 5279.69612744 3601.99568786 1719.66822724 902.21507017
1556.60520217 1698.08203133 1161.13922937 816.78661838 346.5804335
 818.51201871 828.84697434 833.54142694 477.65756285 216.21952931
261.31628906 501.67156079 453.71271495 613.03372594 449.97646796
698.28500578 503.56678697 745.05942497 695.5756235 731.48301185
329.08709471 252.48148148 329.08709471 731.48301185 695.5756235
745.05942497 503.56678697 698.28500578 449.97646796 613.03372594
453.71271495 501.67156079 261.31628906 216.21952931 477.65756285
833.54142694 828.84697434 818.51201871 346.5804335 816.78661838
1161.13922937 1698.08203133 1556.60520217 902.21507017 1719.66822724
3601.99568786 5279.69612744 8642.65618425]
```

OR

Wavelengths:

```
[ 54.                27.                18.                13.5                10.8
 9.                7.71428571 6.75                6.                5.4
 4.90909091 4.5                4.15384615 3.85714286 3.6
 3.375                3.17647059 3.                2.84210526 2.7
 2.57142857 2.45454545 2.34782609 2.25                2.16
 2.07692308 -2.                -2.07692308 -2.16                -2.25
-2.34782609 -2.45454545 -2.57142857 -2.7                -2.84210526
-3.                -3.17647059 -3.375                -3.6                -3.85714286
-4.15384615 -4.5                -4.90909091 -5.4                -6.
-6.75                -7.71428571 -9.                -10.8                -13.5
-18.                -27.                -54.                ]
```

Amps:

```
[3025.32552462 2281.90628943 1532.43098191 432.3716243 93.67627795
339.93290208 496.79929576 449.76368983 339.54371667 250.05500433
244.70527372 201.24626112 89.34023471 56.86385379 9.46002901
 23.40828587 82.0735042 113.05474717 141.67637086 136.82297334
138.73638778 141.22269754 123.25576778 146.27293061 148.83497874
 88.54883759 35.51851852 88.54883759 148.83497874 146.27293061
123.25576778 141.22269754 138.73638778 136.82297334 141.67637086]
```

113.05474717	82.0735042	23.40828587	9.46002901	56.86385379
89.34023471	201.24626112	244.70527372	250.05500433	339.54371667
449.76368983	496.79929576	339.93290208	93.67627795	432.3716243
1532.43098191	2281.90628943	3025.32552462]		

PA

Wavelengths:

[54.	27.	18.	13.5	10.8
9.	7.71428571	6.75	6.	5.4
4.90909091	4.5	4.15384615	3.85714286	3.6
3.375	3.17647059	3.	2.84210526	2.7
2.57142857	2.45454545	2.34782609	2.25	2.16
2.07692308	-2.	-2.07692308	-2.16	-2.25
-2.34782609	-2.45454545	-2.57142857	-2.7	-2.84210526
-3.	-3.17647059	-3.375	-3.6	-3.85714286
-4.15384615	-4.5	-4.90909091	-5.4	-6.
-6.75	-7.71428571	-9.	-10.8	-13.5
-18.	-27.	-54.]	

Amps:

[16501.82232772	14186.59660525	10221.62767293	3591.3478182
1695.58822686	531.93229751	1608.25031421	2093.56781283
1789.54686428	1588.58304522	1846.43593574	1816.72152982
1171.70991701	570.54746198	674.22066705	726.22101675
955.0026778	815.78384957	451.24911946	254.06861784
549.03804545	800.07712992	929.59503191	849.80177403
897.86332395	730.83481915	539.6964418	730.83481915
897.86332395	849.80177403	929.59503191	800.07712992
549.03804545	254.06861784	451.24911946	815.78384957
955.0026778	726.22101675	674.22066705	570.54746198
1171.70991701	1816.72152982	1846.43593574	1588.58304522
1789.54686428	2093.56781283	1608.25031421	531.93229751
1695.58822686	3591.3478182	10221.62767293	14186.59660525
16501.82232772]			

PR

Wavelengths:

[54.	27.	18.	13.5	10.8
9.	7.71428571	6.75	6.	5.4
4.90909091	4.5	4.15384615	3.85714286	3.6
3.375	3.17647059	3.	2.84210526	2.7
2.57142857	2.45454545	2.34782609	2.25	2.16
2.07692308	-2.	-2.07692308	-2.16	-2.25
-2.34782609	-2.45454545	-2.57142857	-2.7	-2.84210526
-3.	-3.17647059	-3.375	-3.6	-3.85714286
-4.15384615	-4.5	-4.90909091	-5.4	-6.
-6.75	-7.71428571	-9.	-10.8	-13.5
-18.	-27.	-54.]	

Amps:

[2175.63393207	990.39953637	934.03641484	227.55414979	266.24365607
70.58075488	276.65931213	113.43277941	202.63045215	217.77525675
65.68100117	235.56985612	293.60576958	224.72976315	27.00904962
155.78803328	116.92391798	39.9013186	41.06855834	106.9338783
174.87475047	219.08387183	197.55702929	71.32172464	129.64603589
163.8950502	22.48148148	163.8950502	129.64603589	71.32172464
197.55702929	219.08387183	174.87475047	106.9338783	41.06855834
39.9013186	116.92391798	155.78803328	27.00904962	224.72976315
293.60576958	235.56985612	65.68100117	217.77525675	202.63045215
113.43277941	276.65931213	70.58075488	266.24365607	227.55414979
934.03641484	990.39953637	2175.63393207]		

PW

Wavelengths:

[54.	27.	18.	13.5	10.8
9.	7.71428571	6.75	6.	5.4
4.90909091	4.5	4.15384615	3.85714286	3.6

Wavelengths:

[54.	27.	18.	13.5	10.8
9.	7.71428571	6.75	6.	5.4
4.90909091	4.5	4.15384615	3.85714286	3.6
3.375	3.17647059	3.	2.84210526	2.7
2.57142857	2.45454545	2.34782609	2.25	2.16
2.07692308	-2.	-2.07692308	-2.16	-2.25
-2.34782609	-2.45454545	-2.57142857	-2.7	-2.84210526
-3.	-3.17647059	-3.375	-3.6	-3.85714286
-4.15384615	-4.5	-4.90909091	-5.4	-6.
-6.75	-7.71428571	-9.	-10.8	-13.5
-18.	-27.	-54.]	

Amps:

```
[4.22234909e+03 4.75237744e+03 2.55554356e+03 2.83158204e+03
1.14648544e+03 1.61584235e+03 9.88694168e+02 1.00288583e+03
1.01997038e+03 8.92938164e+02 7.94789386e+02 7.40526308e+02
5.33685955e+02 2.36795096e+02 2.48368516e+02 3.87551329e+02
4.24139679e+02 5.90278949e+02 2.92390926e+02 3.56479683e+02
2.75533303e+02 3.29891719e+02 4.34611121e+02 3.69555428e+02
2.95799936e+02 1.89149222e+02 1.89129032e+00 1.89149222e+02
2.95799936e+02 3.69555428e+02 4.34611121e+02 3.29891719e+02
2.75533303e+02 3.56479683e+02 2.92390926e+02 5.90278949e+02
4.24139679e+02 3.87551329e+02 2.48368516e+02 2.36795096e+02
5.33685955e+02 7.40526308e+02 7.94789386e+02 8.92938164e+02
1.01997038e+03 1.00288583e+03 9.88694168e+02 1.61584235e+03
1.14648544e+03 2.83158204e+03 2.55554356e+03 4.75237744e+03
4.22234909e+03]
```

SD

Wavelengths:

[54.	27.	18.	13.5	10.8
9.	7.71428571	6.75	6.	5.4
4.90909091	4.5	4.15384615	3.85714286	3.6
3.375	3.17647059	3.	2.84210526	2.7
2.57142857	2.45454545	2.34782609	2.25	2.16
2.07692308	-2.	-2.07692308	-2.16	-2.25
-2.34782609	-2.45454545	-2.57142857	-2.7	-2.84210526
-3.	-3.17647059	-3.375	-3.6	-3.85714286
-4.15384615	-4.5	-4.90909091	-5.4	-6.
-6.75	-7.71428571	-9.	-10.8	-13.5
-18.	-27.	-54.]	

Amps:

```
[1069.25183606 721.59157567 296.94723659 199.37187021 158.78272531
152.07834644 88.04435818 28.29462335 19.93790224 44.31442786
76.09325798 33.47753414 3.91232383 48.06851056 39.27955498
55.82517062 25.88683443 40.88427376 36.49895137 51.81510914
46.02061406 27.95989076 17.21023983 23.93651444 18.48587783
20.17822893 17.32080246 20.17822893 18.48587783 23.93651444
17.21023983 27.95989076 46.02061406 51.81510914 36.49895137
40.88427376 25.88683443 55.82517062 39.27955498 48.06851056
3.91232383 33.47753414 76.09325798 44.31442786 19.93790224
28.29462335 88.04435818 152.07834644 158.78272531 199.37187021
296.94723659 721.59157567 1069.25183606]
```

TN

Wavelengths:

[54.	27.	18.	13.5	10.8
9.	7.71428571	6.75	6.	5.4
4.90909091	4.5	4.15384615	3.85714286	3.6
3.375	3.17647059	3.	2.84210526	2.7
2.57142857	2.45454545	2.34782609	2.25	2.16
2.07692308	-2.	-2.07692308	-2.16	-2.25
-2.34782609	-2.45454545	-2.57142857	-2.7	-2.84210526
-3.	-3.17647059	-3.375	-3.6	-3.85714286
-4.15384615	-4.5	-4.90909091	-5.4	-6.

-6.75	-7.71428571	-9.	-10.8	-13.5
-18.	-27.	-54.]	

Amps:

[10830.65641603	8283.91099249	6231.48169566	2920.4024771	
2635.16936094	929.92577435	641.37525526	477.80130298	
673.48068	1153.24980196	1186.62237689	1242.44630643	
1090.39322539	665.3214453	545.22318045	563.44120998	
514.15809653	436.207397	642.01910589	1075.97604664	
1216.3189405	927.77986828	581.56115733	373.44546953	
520.7488093	558.09212729	543.84289066	558.09212729	
520.7488093	373.44546953	581.56115733	927.77986828	
1216.3189405	1075.97604664	642.01910589	436.207397	
514.15809653	563.44120998	545.22318045	665.3214453	
1090.39322539	1242.44630643	1186.62237689	1153.24980196	
673.48068	477.80130298	641.37525526	929.92577435	
2635.16936094	2920.4024771	6231.48169566	8283.91099249	
10830.65641603]				

TX

Wavelengths:

[54.	27.	18.	13.5	10.8
9.	7.71428571	6.75	6.	5.4
4.90909091	4.5	4.15384615	3.85714286	3.6
3.375	3.17647059	3.	2.84210526	2.7
2.57142857	2.45454545	2.34782609	2.25	2.16
2.07692308	-2.	-2.07692308	-2.16	-2.25
-2.34782609	-2.45454545	-2.57142857	-2.7	-2.84210526
-3.	-3.17647059	-3.375	-3.6	-3.85714286
-4.15384615	-4.5	-4.90909091	-5.4	-6.
-6.75	-7.71428571	-9.	-10.8	-13.5
-18.	-27.	-54.]	

Amps:

[35072.20962815	34831.99730416	22746.13381804	11777.15420811	
8754.46816208	7161.98351333	7725.99826277	5279.37922447	
5454.32902596	5634.93851115	1797.86181494	5574.91746521	
2529.24775094	3102.89340813	1078.32899398	1411.16703923	
809.08109895	4097.55545941	2098.84947667	3808.73051597	
3198.25612777	979.82785511	2945.57033403	1748.04459542	
2806.29202472	1505.45654314	152.43937476	1505.45654314	
2806.29202472	1748.04459542	2945.57033403	979.82785511	
3198.25612777	3808.73051597	2098.84947667	4097.55545941	
809.08109895	1411.16703923	1078.32899398	3102.89340813	
2529.24775094	5574.91746521	1797.86181494	5634.93851115	
5454.32902596	5279.37922447	7725.99826277	7161.98351333	
8754.46816208	11777.15420811	22746.13381804	34831.99730416	
35072.20962815]				

UT

Wavelengths:

[54.	27.	18.	13.5	10.8
9.	7.71428571	6.75	6.	5.4
4.90909091	4.5	4.15384615	3.85714286	3.6
3.375	3.17647059	3.	2.84210526	2.7
2.57142857	2.45454545	2.34782609	2.25	2.16
2.07692308	-2.	-2.07692308	-2.16	-2.25
-2.34782609	-2.45454545	-2.57142857	-2.7	-2.84210526
-3.	-3.17647059	-3.375	-3.6	-3.85714286
-4.15384615	-4.5	-4.90909091	-5.4	-6.
-6.75	-7.71428571	-9.	-10.8	-13.5
-18.	-27.	-54.]	

Amps:

[6008.44620261	4027.46767899	1646.33178649	672.51330742	374.10039851
1042.6652906	1092.0058392	751.36948706	296.8283095	312.96677214
310.65446881	333.05759477	307.87272542	238.6789876	257.41447114

313.83540647	253.21527143	306.8775577	215.50512328	252.36565971
319.96261411	319.89241936	294.21767166	295.0213713	258.43168276
177.96774042	8.75251371	177.96774042	258.43168276	295.0213713
294.21767166	319.89241936	319.96261411	252.36565971	215.50512328
306.8775577	253.21527143	313.83540647	257.41447114	238.6789876
307.87272542	333.05759477	310.65446881	312.96677214	296.8283095
751.36948706	1092.0058392	1042.6652906	374.10039851	672.51330742
1646.33178649	4027.46767899	6008.44620261		

VA

Wavelengths:

[54.	27.	18.	13.5	10.8
9.	7.71428571	6.75	6.	5.4
4.90909091	4.5	4.15384615	3.85714286	3.6
3.375	3.17647059	3.	2.84210526	2.7
2.57142857	2.45454545	2.34782609	2.25	2.16
2.07692308	-2.	-2.07692308	-2.16	-2.25
-2.34782609	-2.45454545	-2.57142857	-2.7	-2.84210526
-3.	-3.17647059	-3.375	-3.6	-3.85714286
-4.15384615	-4.5	-4.90909091	-5.4	-6.
-6.75	-7.71428571	-9.	-10.8	-13.5
-18.	-27.	-54.		

Amps:

[5982.25244066	5740.79515326	4384.03506739	2037.3523543	2066.62215338
1657.6725084	1486.44936902	1636.51636043	1377.77643415	1218.84857767
1125.10651517	977.6380868	793.39362296	586.80998368	466.11166141
582.65034811	548.02401788	692.27613721	621.73315158	437.33064335
344.15533377	366.25672589	544.7367658	403.74659294	468.81503691
330.51330412	137.62664499	330.51330412	468.81503691	403.74659294
544.7367658	366.25672589	344.15533377	437.33064335	621.73315158
692.27613721	548.02401788	582.65034811	466.11166141	586.80998368
793.39362296	977.6380868	1125.10651517	1218.84857767	1377.77643415
1636.51636043	1486.44936902	1657.6725084	2066.62215338	2037.3523543
4384.03506739	5740.79515326	5982.25244066		

VI

Wavelengths:

[54.	27.	18.	13.5	10.8
9.	7.71428571	6.75	6.	5.4
4.90909091	4.5	4.15384615	3.85714286	3.6
3.375	3.17647059	3.	2.84210526	2.7
2.57142857	2.45454545	2.34782609	2.25	2.16
2.07692308	-2.	-2.07692308	-2.16	-2.25
-2.34782609	-2.45454545	-2.57142857	-2.7	-2.84210526
-3.	-3.17647059	-3.375	-3.6	-3.85714286
-4.15384615	-4.5	-4.90909091	-5.4	-6.
-6.75	-7.71428571	-9.	-10.8	-13.5
-18.	-27.	-54.		

Amps:

[12.44596941	10.55538969	14.94574324	3.18528422	3.24774078	1.68353365
3.13227781	3.27242798	3.01904679	6.3524965	1.10327975	3.84776365
2.22334583	1.58138049	0.29710484	1.9595758	0.95055312	1.76895683
0.26165937	1.44829013	0.55896064	1.40260179	1.06858042	1.48049937
1.22156002	2.14973675	0.40775249	2.14973675	1.22156002	1.48049937
1.06858042	1.40260179	0.55896064	1.44829013	0.26165937	1.76895683
0.95055312	1.9595758	0.29710484	1.58138049	2.22334583	3.84776365
1.10327975	6.3524965	3.01904679	3.27242798	3.13227781	1.68353365
3.24774078	3.18528422	14.94574324	10.55538969	12.44596941	

VT

Wavelengths:

[54.	27.	18.	13.5	10.8
9.	7.71428571	6.75	6.	5.4
4.90909091	4.5	4.15384615	3.85714286	3.6
3.375	3.17647059	3.	2.84210526	2.7

2.57142857	2.45454545	2.34782609	2.25	2.16
2.07692308	-2.	-2.07692308	-2.16	-2.25
-2.34782609	-2.45454545	-2.57142857	-2.7	-2.84210526
-3.	-3.17647059	-3.375	-3.6	-3.85714286
-4.15384615	-4.5	-4.90909091	-5.4	-6.
-6.75	-7.71428571	-9.	-10.8	-13.5
-18.	-27.	-54.		

Amps:

[246.662728	191.73050915	142.86970213	76.52363125	53.83458057
47.56426266	73.81698887	79.47338169	50.95410767	30.45788978
31.38451807	51.69699437	39.63121985	16.38478375	5.71918647
10.03702328	23.93032043	23.31515452	14.56952475	2.92048179
12.77356861	17.7458808	25.23195661	24.88450701	23.36002621
14.29294278	0.71683852	14.29294278	23.36002621	24.88450701
25.23195661	17.7458808	12.77356861	2.92048179	14.56952475
23.31515452	23.93032043	10.03702328	5.71918647	16.38478375
39.63121985	51.69699437	31.38451807	30.45788978	50.95410767
79.47338169	73.81698887	47.56426266	53.83458057	76.52363125
142.86970213	191.73050915	246.662728		

WA

Wavelengths:

[54.	27.	18.	13.5	10.8
9.	7.71428571	6.75	6.	5.4
4.90909091	4.5	4.15384615	3.85714286	3.6
3.375	3.17647059	3.	2.84210526	2.7
2.57142857	2.45454545	2.34782609	2.25	2.16
2.07692308	-2.	-2.07692308	-2.16	-2.25
-2.34782609	-2.45454545	-2.57142857	-2.7	-2.84210526
-3.	-3.17647059	-3.375	-3.6	-3.85714286
-4.15384615	-4.5	-4.90909091	-5.4	-6.
-6.75	-7.71428571	-9.	-10.8	-13.5
-18.	-27.	-54.		

Amps:

[5547.80345695	4665.27068875	3332.68254612	907.66288361	130.31403317
857.21146668	1062.45791907	1103.24773293	713.1817721	486.14709495
376.85745861	399.77196648	371.48731659	99.90256126	152.67210804
187.45825252	237.19096169	252.42792232	279.76666843	167.8066631
272.01783429	326.56060279	514.48459234	482.96720028	386.61097959
226.65053759	55.51851852	226.65053759	386.61097959	482.96720028
514.48459234	326.56060279	272.01783429	167.8066631	279.76666843
252.42792232	237.19096169	187.45825252	152.67210804	99.90256126
371.48731659	399.77196648	376.85745861	486.14709495	713.1817721
1103.24773293	1062.45791907	857.21146668	130.31403317	907.66288361
3332.68254612	4665.27068875	5547.80345695]		

WI

Wavelengths:

[54.	27.	18.	13.5	10.8
9.	7.71428571	6.75	6.	5.4
4.90909091	4.5	4.15384615	3.85714286	3.6
3.375	3.17647059	3.	2.84210526	2.7
2.57142857	2.45454545	2.34782609	2.25	2.16
2.07692308	-2.	-2.07692308	-2.16	-2.25
-2.34782609	-2.45454545	-2.57142857	-2.7	-2.84210526
-3.	-3.17647059	-3.375	-3.6	-3.85714286
-4.15384615	-4.5	-4.90909091	-5.4	-6.
-6.75	-7.71428571	-9.	-10.8	-13.5
-18.	-27.	-54.		

Amps:

[13052.64553938	7819.7277068	3380.43384039	1700.781966
1443.1114676	1806.43364894	1536.03308357	730.81400907
162.49411273	432.4690934	634.20533698	1013.6525241
1184.87070471	863.28731715	751.90526722	602.8861846

261.6595915	152.84589175	365.54942479	284.74643374
189.5625737	554.18042102	808.98602508	662.04505385
253.67901997	63.79604934	278.65385074	63.79604934
253.67901997	662.04505385	808.98602508	554.18042102
189.5625737	284.74643374	365.54942479	152.84589175
261.6595915	602.8861846	751.90526722	863.28731715
1184.87070471	1013.6525241	634.20533698	432.4690934
162.49411273	730.81400907	1536.03308357	1806.43364894
1443.1114676	1700.781966	3380.43384039	7819.7277068

13052.64553938]

WV

Wavelengths:

[54.	27.	18.	13.5	10.8
9.	7.71428571	6.75	6.	5.4
4.90909091	4.5	4.15384615	3.85714286	3.6
3.375	3.17647059	3.	2.84210526	2.7
2.57142857	2.45454545	2.34782609	2.25	2.16
2.07692308	-2.	-2.07692308	-2.16	-2.25
-2.34782609	-2.45454545	-2.57142857	-2.7	-2.84210526
-3.	-3.17647059	-3.375	-3.6	-3.85714286
-4.15384615	-4.5	-4.90909091	-5.4	-6.
-6.75	-7.71428571	-9.	-10.8	-13.5
-18.	-27.	-54.]	

Amps:

[1030.59507396	723.62946687	488.34845378	243.12446839	128.89085059
146.97847756	145.7760981	117.41100124	80.69715908	53.92715132
59.6030044	58.14686883	35.44557108	7.15985733	30.74169014
36.54376582	53.12454258	39.8809942	44.28551825	36.82131843
55.78506888	55.3119531	68.67301053	44.48411931	41.48046655
25.37091993	1.73871932	25.37091993	41.48046655	44.48411931
68.67301053	55.3119531	55.78506888	36.82131843	44.28551825
39.8809942	53.12454258	36.54376582	30.74169014	7.15985733
35.44557108	58.14686883	59.6030044	53.92715132	80.69715908
117.41100124	145.7760981	146.97847756	128.89085059	243.12446839
488.34845378	723.62946687	1030.59507396]		

WY

Wavelengths:

[54.	27.	18.	13.5	10.8
9.	7.71428571	6.75	6.	5.4
4.90909091	4.5	4.15384615	3.85714286	3.6
3.375	3.17647059	3.	2.84210526	2.7
2.57142857	2.45454545	2.34782609	2.25	2.16
2.07692308	-2.	-2.07692308	-2.16	-2.25
-2.34782609	-2.45454545	-2.57142857	-2.7	-2.84210526
-3.	-3.17647059	-3.375	-3.6	-3.85714286
-4.15384615	-4.5	-4.90909091	-5.4	-6.
-6.75	-7.71428571	-9.	-10.8	-13.5
-18.	-27.	-54.]	

Amps:

[1018.12698049	692.93940512	394.90900941	200.96237806	204.24050892
222.57067153	187.7419337	116.82951046	27.93335079	32.303842
53.19795448	65.56281877	72.45900352	38.36869381	23.45187006
29.11253272	25.26202165	23.65599987	17.05165156	1.34614303
18.76395163	33.49864222	43.94563419	45.2848553	33.48691269
17.51430266	6.85404895	17.51430266	33.48691269	45.2848553
43.94563419	33.49864222	18.76395163	1.34614303	17.05165156
23.65599987	25.26202165	29.11253272	23.45187006	38.36869381
72.45900352	65.56281877	53.19795448	32.303842	27.93335079
116.82951046	187.7419337	222.57067153	204.24050892	200.96237806
394.90900941	692.93940512	1018.12698049]		

0

Wavelengths:

```
[ 54.          27.          18.          13.5          10.8
   9.          7.71428571   6.75          6.          5.4
  4.90909091   4.5          4.15384615   3.85714286   3.6
  3.375        3.17647059   3.          2.84210526   2.7
  2.57142857   2.45454545   2.34782609   2.25        2.16
  2.07692308  -2.          -2.07692308  -2.16        -2.25
 -2.34782609  -2.45454545  -2.57142857  -2.7        -2.84210526
 -3.          -3.17647059  -3.375        -3.6        -3.85714286
 -4.15384615  -4.5          -4.90909091  -5.4        -6.
 -6.75        -7.71428571  -9.          -10.8       -13.5
 -18.         -27.         -54.          ]
```

Amps:

```
[0. 0. 0. 0. 0. 0. 0. 0. 0. 0. 0. 0. 0. 0. 0. 0. 0. 0. 0. 0. 0. 0.
 0. 0. 0. 0. 0. 0. 0. 0. 0. 0. 0. 0. 0. 0. 0. 0. 0. 0. 0. 0. 0.
 0. 0. 0. 0. 0.]
```

```
In [17]: #Algorithm 2. SIMILAR WAVES
#Given: deltas_it, for i = 1, ..., 51, t = 1, ..., 100. // error from step 1
#1. Set s_it= deltas_it
#2. For i = 1 to 51 // loop over states
#3.     Determine y_i, for s = 1, ..., 52 = SolveIDP(ODEint(s_i)).y
#     Determine errors_it = y.error
# Set [z_1,38,...,z_51,38]=[s_1,38,...,s_51,38]
#5. For t = 1 to 53 // loop over weeks in 2021
#6.     Calculate [z_(1,38+t),...,z_(51,38+t)]=interpolate(y[0],y[1],[z_(1,37+t),...,z_
#7. Set Δ=z-s // Calculate prediction error
```

```
In [18]: # End Fourier Xform section
```

```
In [19]: # Reverse Chaos
```

```
In [20]: curveFitX = s_it.copy()
stdDeviationsList = []

def interpolatingFunctionSolver(x, a, b, c):
    return a * np.sin(b * x) + c
    #print(amplitude, frequency, phase)

print("defined")
```

defined

```
In [21]: for s in curveFitX: # Loop in states. Note s is the postal abbreviation here.
        if s not in ("AR", "RI", "AK", "FL", 0):
            # Python does not like Rhode Island, Alaska, Arkansas, or Florida. Does not c
            # Also getting rid of the Outside state with postal abbreviation " 0 ".
            s_i = curveFitX[s]
            sizeOf = s_i.size #in case we change interpolate distance later
            xVars = range(sizeOf)
            yVars = np.array(s_i)

            tuples, covarianceMatrix = sp.optimize.curve_fit(interpolatingFunctionSolver,
            # maxfev is the number of iterations until convergence is reached before halti
            # that there is no convergence in the data.
            stdDeviation = np.sqrt(np.diag(covarianceMatrix))

            #extract tuples
            amplitude, frequency, phase = tuples
            amplitude = abs(amplitude)

            print(s, "Amplitude:", amplitude, "Frequency:", frequency, "Phase:", phase)
            print(stdDeviation)
            stdDeviationsList.append(sum(stdDeviation) )
```

```
AL Amplitude: 593.3759046556825 Frequency: 1.549307871571894 Phase: 8319.24131964569
[1.60447574e+03 8.65124849e-02 1.12619087e+03]
AS Amplitude: 3.0184440937519395e-20 Frequency: 1.0000000000005007 Phase: 1.592417287
947139e-19
[3.22576864e-20 7.50761717e-13 2.26768726e-20]
AZ Amplitude: 872.7318200034628 Frequency: 5.459878925951252 Phase: 4420.402846111828
[1.10609758e+03 4.08859697e-02 7.77680135e+02]
CA Amplitude: 469.53647759918385 Frequency: 3.2097543158251676 Phase: 34276.976066814
845
[1.02358640e+04 5.69625811e-01 6.74558351e+03]
CO Amplitude: 591.9924666665868 Frequency: 9.422578453362302 Phase: 4949.345385297252
[1.01532080e+07 4.11233755e+01 9.29127435e+02]
CT Amplitude: 381.08408702191895 Frequency: 4.5605449599084515 Phase: 4585.6751206343
95
[1.13577507e+03 9.49630707e-02 7.96381415e+02]
DC Amplitude: 51.615688207640964 Frequency: 1.0621453356738495 Phase: 321.10924586234
46
[5.48485023e+01 3.40186919e-02 3.84930557e+01]
DE Amplitude: 27.091971055245754 Frequency: 2.8775651419227883 Phase: 1362.6390917366
434
[318.21153192 0.38217255 223.4467797 ]
FSM Amplitude: 0.03679282578513693 Frequency: 1.0166323757462619 Phase: 0.01751876591
4710455
[0.02648425 0.02284368 0.01855956]
GA Amplitude: 149.09219232356324 Frequency: -2.3090640296313443 Phase: 16257.13884803
7637
[3.38260415e+03 7.18240922e-01 2.36763540e+03]
GU Amplitude: 5.680602337062402 Frequency: 1.3007768756165907 Phase: 36.8692723512063
4
[10.44767143 0.05862229 7.32486727]
HI Amplitude: 18.312179673014974 Frequency: 1.7008214838719968 Phase: 154.84546595512
41
[31.94523173 0.05668957 22.50413292]
IA Amplitude: 406.1198923988358 Frequency: 9.241051631488979 Phase: 5175.826294312551
[1.22011134e+03 9.01555493e-02 8.41520982e+02]
ID Amplitude: 234.19266538858412 Frequency: 1.4373817924252172 Phase: 2468.2517772632
95
[5.23668886e+02 7.22396302e-02 3.68490824e+02]
```

IL Amplitude: 1489.1298343318747 Frequency: 4.704808720470669 Phase: 15410.8465976793
76
[3.28970578e+03 7.24332069e-02 2.32283725e+03]
IN Amplitude: 1144.2342786274737 Frequency: 7.592037756894067 Phase: 11432.2923832268
92
[2.79393746e+03 7.76368580e-02 1.95798151e+03]
KS Amplitude: 589.1091475285235 Frequency: 7.853790568550572 Phase: 5081.577167848025
[1.15928316e+03 6.49198833e-02 8.19947075e+02]
KY Amplitude: 2702.562630833312 Frequency: 12.271360762595185 Phase: 6375.1497140394
[1.62764219e+03 1.89578170e-02 1.14166328e+03]
LA Amplitude: 274.3704748181654 Frequency: 10.645459504800227 Phase: 4029.68523914753
5
[7.18595571e+02 8.64708670e-02 5.08321545e+02]
MA Amplitude: 374.5043851356571 Frequency: 2.321262995828477 Phase: 9436.391134930249
[2.33201288e+03 2.02685478e-01 1.64361535e+03]
MD Amplitude: 1110.310360427106 Frequency: 7.109649345223755 Phase: 5916.113408630476
[1.08207040e+03 3.11913679e-02 7.59336065e+02]
ME Amplitude: 108.53548812432823 Frequency: 1.3647756244465956 Phase: 672.98818681408
45
[2.13143850e+02 6.24414576e-02 1.49347134e+02]
MI Amplitude: 139.14895212422752 Frequency: 8.941352988735623 Phase: 6284.43764616016
1
[1.56320718e+03 3.49723930e-01 1.08933180e+03]
MN Amplitude: 161.76844563537364 Frequency: 14.778465816740608 Phase: 7739.9052383641
93
[2.09348479e+03 4.27820229e-01 1.48128714e+03]
MO Amplitude: 596.3156578770296 Frequency: 5.128855967968418 Phase: 9496.390214431965
[2.00660719e+03 1.10917898e-01 1.41924943e+03]
MP Amplitude: 0.5147131762346421 Frequency: 1.0499673692672558 Phase: 2.4438261367337
55
[0.49170359 0.03138997 0.34735833]
MS Amplitude: 152.3959375162408 Frequency: 1.748975591943349 Phase: 4320.302778758395
[7.94313799e+02 1.71982825e-01 5.61750817e+02]
MT Amplitude: 12.342267643826561 Frequency: 7.50163899570433 Phase: 1484.800127866175
2
[391.92811881 1.04875573 277.3243581]
NC Amplitude: 1081.2204592818807 Frequency: 5.630268630617744 Phase: 10946.0891893054
94
[2.39163003e+03 6.99402571e-02 1.67488507e+03]
ND Amplitude: 109.82896981615387 Frequency: 2.7010298848114562 Phase: 1331.7710758363
892
[3.70067648e+02 1.09306738e-01 2.60323170e+02]
NE Amplitude: 1005.7804298041634 Frequency: 5.963767080303897 Phase: 3225.86035735340
37
[7.44324780e+02 2.36467144e-02 5.26218285e+02]
NH Amplitude: 137.22072270469334 Frequency: 0.939207755963404 Phase: 681.097396461086
[2.06981349e+02 4.88642988e-02 1.45679663e+02]
NJ Amplitude: 657.1149657548731 Frequency: 2.9382722894175446 Phase: 12523.0093959504
14
[2.73596585e+03 1.32811573e-01 1.90953282e+03]
NM Amplitude: 74.47447918686092 Frequency: 15.667044919981326 Phase: 2916.38471504020
6
[6.91674182e+02 5.94494338e-01 5.34565513e+02]
NV Amplitude: 913.8162443953474 Frequency: 6.770707411499629 Phase: 5085.342147593719
[1.09839475e+03 3.76024844e-02 7.67742873e+02]
NY Amplitude: 192.17852140184976 Frequency: 7.774934532403679 Phase: 7980.80537528076
5
[2.09024916e+03 3.48550538e-01 1.46788785e+03]
NYC Amplitude: 92.72412193055976 Frequency: 2.3470409130004346 Phase: 1369.2085185901
756
[3.24567557e+02 1.13940222e-01 2.28671152e+02]
OH Amplitude: 442.1572045280467 Frequency: 1.9262861611415758 Phase: 16257.6018885057

82
 [4.25445532e+03 3.17557839e-01 3.00876723e+03]
 OK Amplitude: 447.341076659758 Frequency: 8.856480409829723 Phase: 7030.680550537367
 [1.60670385e+03 1.20086517e-01 1.13963354e+03]
 OR Amplitude: 50.7105571088771 Frequency: 7.916874664534869 Phase: 2593.863315133426
 [5.93058507e+02 3.85234140e-01 4.19219348e+02]
 PA Amplitude: 11741581.660781732 Frequency: 7.269754435343402e-05 Phase: -9160.02280148443
 [7.16322636e+11 4.46046475e+00 4.20408683e+03]
 PR Amplitude: 183.9475273454338 Frequency: -2.6405977450101346 Phase: 1711.537306375798
 [3.78982710e+02 6.72789408e-02 2.67105488e+02]
 PW Amplitude: 3.0184440937519395e-20 Frequency: 1.000000000005007 Phase: 1.592417287947139e-19
 [3.22576864e-20 7.50761717e-13 2.26768726e-20]
 RMI Amplitude: 0.08015318395195978 Frequency: 0.9887987062484072 Phase: 0.07681868322630851
 [0.08329162 0.034259 0.05891122]
 SC Amplitude: 6297.297822413428 Frequency: 0.08619876682517952 Phase: 6735.03286215261
 [1.04750662e+03 6.64162839e-03 9.46408230e+02]
 SD Amplitude: 21.381083213680714 Frequency: 2.0661704214497663 Phase: 761.7129376019268
 [193.65674619 0.2882305 135.64855841]
 TN Amplitude: 8420.451531620933 Frequency: -3.1405242497530597 Phase: 9974.991390976626
 [1.56092403e+08 2.08987991e+01 1.57913369e+03]
 TX Amplitude: 1012.281261004448 Frequency: 1.962031049262049 Phase: 40376.24766329864
 [8.34453164e+03 2.64142463e-01 5.85899140e+03]
 UT Amplitude: 402.72949880656137 Frequency: 10.849877177258838 Phase: 4878.423907542673
 [1.09303402e+03 8.62466174e-02 7.65846455e+02]
 VA Amplitude: 6209116.472001418 Frequency: 6.360695082183843e-05 Phase: -3684.1638988961504
 [4.02106496e+11 4.14215449e+00 1.57847396e+03]
 VI Amplitude: 2.6321304588600336 Frequency: 0.9399069933524776 Phase: 14.654731073651098
 [3.50941489 0.04311611 2.46894454]
 VT Amplitude: 44.5893606671943 Frequency: 1.421283208287651 Phase: 181.1700008268364
 [5.50654524e+01 3.92791769e-02 3.85881884e+01]
 WA Amplitude: 141.71065799010412 Frequency: 9.472406661079695 Phase: 5661.931966265776
 [1.11343795e+03 3.58739311e-01 8.28122626e+02]
 WI Amplitude: 6711.595545347998 Frequency: 6.101217488679808 Phase: 8222.70976069831
 [2.21726569e+03 9.68315693e-03 1.54472713e+03]
 WV Amplitude: 46.45182482663391 Frequency: 3.8214287802880595 Phase: 705.8151936382262
 [1.98194542e+02 1.40173274e-01 1.39943863e+02]
 WY Amplitude: 20.419263186101457 Frequency: 4.191692341793655 Phase: 658.0324859587399
 [192.12120168 0.30922427 135.74330061]

```
In [22]: avgError = sum(stdDeviationsList) / (len(stdDeviationsList) )
          print(avgError)
```

19974919782.733772

```
In [23]: y = 0

for x in stdDeviationsList:
    y = y+1
    if x > (2 * avgError):
        print(y, " : ", x)
```

```
41 : 716322640344.3839
50 : 402106497468.12103
```

```
In [24]: # 41 here = PA
# 50 here = VA
# Potential mutation. redo on these, halved.
```

```
In [25]: for s2 in curveFitX: # Loop in states. Note s is the postal abbreviation here.
    if s2 in ("VA", "PA"):
        s_i2 = curveFitX[s2]
        sizeOf2 = s_i.size / 2.0 #div 2
        xVars2 = range(int(sizeOf2) )
        yVars2 = np.array(s_i2[:int(sizeOf2)])

        tuples, covarianceMatrix = sp.optimize.curve_fit(interpolatingFunctionSolver,
            stdDeviation = np.sqrt(np.diag(covarianceMatrix)))

        #extract tuples
        amplitude, frequency, phase = tuples
        amplitude = abs(amplitude)

        print(s2, "Amplitude:", amplitude, "Frequency:", frequency, "Phase:", phase)
        print(stdDeviation)
```

```
PA Amplitude: 1076.8156059971875 Frequency: 19.788424907358817 Phase: 3498.1142180757
706
[8.83553897e+02 5.48489560e-02 6.22250116e+02]
VA Amplitude: 117.15661725974043 Frequency: 28.57954650939507 Phase: 2230.08914940454
22
[5.69661222e+02 3.40581992e-01 4.02758238e+02]
```

```
In [26]: # pre-half only has an amplitude of 117 and 1k. Interesting. Let's Look at post-half
```

```
In [27]: for s3 in curveFitX: # Loop in states. Note s is the postal abbreviation here.
    if s3 in ("VA", "PA"):
        s_i3 = curveFitX[s3]
        sizeOf3 = s_i.size / 2.0 #div 2
        xVars3 = range(int(sizeOf3), int(sizeOf3 * 2.0) )
        yVars3 = np.array(s_i3[:int(sizeOf2)])

        tuples, covarianceMatrix = sp.optimize.curve_fit(interpolatingFunctionSolver,
            stdDeviation = np.sqrt(np.diag(covarianceMatrix)))

        #extract tuples
        amplitude, frequency, phase = tuples
        amplitude = abs(amplitude)

        print(s2, "Amplitude:", amplitude, "Frequency:", frequency, "Phase:", phase)
        print(stdDeviation)
```

```
0 Amplitude: 108.90959173826906 Frequency: 8.95446934608311 Phase: 3501.6365029644026
[9.11417582e+02 2.03740152e-01 6.41706079e+02]
0 Amplitude: 504.9217207232555 Frequency: -0.5515007548316523 Phase: 2227.59025798185
5
[5.76067746e+02 2.70128424e-02 4.02548062e+02]
```

```
In [28]: # These two states have problems only because the amplitude is trivial; 108 cases or
# Similar to Alaska, but for different reasons. A mutation of impulse 108 can safely
```

```
In [29]: # Following code is no longer used:
```

```
for s3 in curveFitX: # loop in states. Note s is the postal abbreviation here. if s3 in ("VA", "PA"):
s_i3 = curveFitX[s] sizeOf3 = s_i.size / 4.0 #div 2 xVars3 = range(int(sizeOf 3.0), int(sizeOf 4.0) )
yVars3 = np.array(s_i)
```

```
    tuples, covarianceMatrix =
sp.optimize.curve_fit(interpolatingFunctionSolver, xVars3, yVars3,
maxfev=2000)
    stdDeviation = np.sqrt(np.diag(covarianceMatrix))

    #extract tuples
    amplitude, frequency, phase = tuples
    amplitude = abs(amplitude)

    print(s2, "Amplitude:", amplitude, "Frequency:", frequency,
"Phase:", phase)
    print(stdDeviation)
```

```
for s3 in curveFitX: # loop in states. Note s is the postal abbreviation here. if s3 in ("VA", "PA"):
s_i3 = curveFitX[s] sizeOf3 = s_i.size / 4.0 #div 2 xVars3 = range(int(sizeOf 2.0), int(sizeOf 3.0) )
yVars3 = np.array(s_i)
```

```
    tuples, covarianceMatrix =
sp.optimize.curve_fit(interpolatingFunctionSolver, xVars3, yVars3,
maxfev=2000)
    stdDeviation = np.sqrt(np.diag(covarianceMatrix))

    #extract tuples
    amplitude, frequency, phase = tuples
    amplitude = abs(amplitude)

    print(s2, "Amplitude:", amplitude, "Frequency:", frequency,
"Phase:", phase)
    print(stdDeviation)
```

```
In [30]: #Algorithm 3. REVERSE CHAOS
#Given: s_it for i = 1, ..., 51, t = 1, ..., 53 s // s states from SIMILAR WAVES
#1. errorBaseline = 2*Avergae( [error]_it)
#2. For i = 1 to 51 // loop over states
#3.     if ( [error]_i ) > errorbaseline )
#4.         perform a single SIMILAR_WAVES(s[i], t/2)
#5. Set [z_1,38,...,z_51,38]=[s_1,38,...,s_51,38]
# cut in half.
```

In []:

In [31]: *# The following 2 sections are no longer being used, but variables are being initialized*

In [32]: *restartParadigm = 0.01*
This is no longer used. Cleaning is now done after each step instead of a second round
other way could conceivably work too, but this way is logistically simpler due to the
of Jupyter Notebook.

```
X = actual.copy()
X = np.array(X)
delta = np.sum(X)
```

```
#Python is case sensitive
#transpose uses T
```

```
denominator = np.sum(np.array(states.copy() ) )
```

```
deltaNormed = delta / denominator
```

```
if deltaNormed >= restartParadigm:
    print("restart")
```

restart

In [33]: `curr = 100`
`first = 12`
`second = 77`
`third = 165`
`CDC = np.array(range(1, 3))`

`for j in range(3, first):`
 `curr = curr*1.05`
 `CDC = np.append(CDC, curr)`

`for j in range(first, second):`
 `curr = curr*1.0035`
 `CDC = np.append(CDC, curr)`

`for j in range(second, third):`
 `curr = curr*0.999`
 `CDC = np.append(CDC, curr)`

`print(CDC)`

```
[1.00000000e+00 2.00000000e+00 1.25892541e+02 1.60324539e+02
2.06656943e+02 2.69781708e+02 3.56913623e+02 4.78840947e+02
6.51929818e+02 9.01386164e+02 1.26664943e+03 1.29872060e+03
1.33172034e+03 1.36567852e+03 1.40062605e+03 1.43659492e+03
1.47361827e+03 1.51173040e+03 1.55096681e+03 1.59136431e+03
1.63296098e+03 1.67579628e+03 1.71991109e+03 1.76534775e+03
1.81215013e+03 1.86036369e+03 1.91003553e+03 1.96121448e+03
2.01395114e+03 2.06829795e+03 2.12430928e+03 2.18204151e+03
2.24155309e+03 2.30290462e+03 2.36615895e+03 2.43138129e+03
2.49863924e+03 2.56800295e+03 2.63954520e+03 2.71334148e+03
2.78947016e+03 2.86801254e+03 2.94905301e+03 3.03267917e+03
3.11898195e+03 3.20805575e+03 3.29999858e+03 3.39491223e+03
3.49290241e+03 3.59407888e+03 3.69855567e+03 3.80645126e+03
3.91788870e+03 4.03299586e+03 4.15190563e+03 4.27475609e+03]
```

```

4.40169077e+03 4.53285887e+03 4.66841548e+03 4.80852185e+03
4.95334565e+03 5.10306123e+03 5.25784994e+03 5.41790039e+03
5.58340877e+03 5.75457921e+03 5.93162408e+03 6.11476439e+03
6.30423011e+03 6.50026061e+03 6.70310506e+03 6.91302285e+03
7.13028404e+03 7.35516982e+03 7.58797304e+03 7.82899867e+03
7.75912079e+03 7.68993556e+03 7.62143549e+03 7.55361318e+03
7.48646134e+03 7.41997274e+03 7.35414024e+03 7.28895679e+03
7.22441540e+03 7.16050920e+03 7.09723137e+03 7.03457516e+03
6.97253393e+03 6.91110110e+03 6.85027015e+03 6.79003466e+03
6.73038827e+03 6.67132470e+03 6.61283774e+03 6.55492126e+03
6.49756917e+03 6.44077548e+03 6.38453427e+03 6.32883966e+03
6.27368587e+03 6.21906715e+03 6.16497786e+03 6.11141238e+03
6.05836518e+03 6.00583080e+03 5.95380381e+03 5.90227887e+03
5.85125069e+03 5.80071404e+03 5.75066376e+03 5.70109473e+03
5.65200189e+03 5.60338027e+03 5.55522491e+03 5.50753093e+03
5.46029350e+03 5.41350786e+03 5.36716928e+03 5.32127309e+03
5.27581468e+03 5.23078949e+03 5.18619301e+03 5.14202077e+03
5.09826837e+03 5.05493145e+03 5.01200568e+03 4.96948682e+03
4.92737064e+03 4.88565298e+03 4.84432971e+03 4.80339675e+03
4.76285008e+03 4.72268571e+03 4.68289970e+03 4.64348814e+03
4.60444719e+03 4.56577304e+03 4.52746191e+03 4.48951007e+03
4.45191384e+03 4.41466958e+03 4.37777368e+03 4.34122258e+03
4.30501274e+03 4.26914068e+03 4.23360296e+03 4.19839616e+03
4.16351690e+03 4.12896187e+03 4.09472774e+03 4.06081127e+03
4.02720923e+03 3.99391841e+03 3.96093568e+03 3.92825790e+03
3.89588198e+03 3.86380488e+03 3.83202357e+03 3.80053506e+03
3.76933640e+03 3.73842466e+03 3.70779697e+03 3.67745044e+03]

```

```

In [34]: curveFitX2 = states.copy()
curveFitX2 = curveFitX2.transpose()

```

```

def solver2(t, b):
    return constT * (b ** t)

print("init")

```

init

```

In [35]: startWeek = 40
# starting at 40 after the initial pulse for all states; otherwise we have a lot of 0s

for s in curveFitX2:
    yVars = pd.DataFrame(curveFitX2[s] )
    yVars = np.array(yVars).flatten()
    constT = yVars[startWeek]
    xVars = np.array(range(startWeek, len(yVars) + startWeek) )

    #print(xVars, yVars)
    tuples, covariance = sp.optimize.curve_fit(solver2, xVars, yVars, maxfev=2000)

    print(s, tuples, "covariance: ", covariance)

```

```

AK [0.99742655] covariance: [[6.82770461e-07]]
AL [0.99851998] covariance: [[5.61199041e-07]]
AR [0.99864187] covariance: [[6.54734789e-07]]
AS [1.] covariance: [[inf]]
AZ [1.00399865] covariance: [[6.75153245e-07]]
CA [1.00506895] covariance: [[7.71136656e-07]]

```

```

CO [0.99903979] covariance: [[7.19894827e-07]]
CT [1.0020155] covariance: [[6.20235319e-07]]
DC [1.00492157] covariance: [[1.03729129e-06]]
DE [1.0040935] covariance: [[6.44089471e-07]]
FL [1.00402015] covariance: [[5.73503729e-07]]
FSM [1.] covariance: [[inf]]
GA [1.00271241] covariance: [[5.94348335e-07]]
GU [0.99837739] covariance: [[1.0755265e-06]]
HI [1.00834903] covariance: [[9.00539325e-07]]
IA [0.9948715] covariance: [[5.97873325e-07]]
ID [0.99479509] covariance: [[5.06462971e-07]]
IL [0.99754509] covariance: [[5.51695198e-07]]
IN [0.99776516] covariance: [[5.652213e-07]]
KS [0.99818189] covariance: [[7.77298839e-07]]
KY [1.00012177] covariance: [[5.32185684e-07]]
LA [1.0041005] covariance: [[7.22878272e-07]]
MA [1.00322123] covariance: [[6.80795594e-07]]
MD [1.00293611] covariance: [[6.27299069e-07]]
ME [1.01001436] covariance: [[5.24493589e-07]]
MI [1.00025822] covariance: [[4.36343718e-07]]
MN [0.99872801] covariance: [[5.16070732e-07]]
MO [0.99704378] covariance: [[5.10007817e-07]]
MP [1.01709947] covariance: [[2.29218325e-06]]
MS [1.0004246] covariance: [[5.80322742e-07]]
MT [0.99200351] covariance: [[7.88962833e-07]]
NC [1.00193899] covariance: [[5.75741029e-07]]
ND [0.98927864] covariance: [[1.29172075e-06]]
NE [0.9949347] covariance: [[7.35088691e-07]]
NH [1.00688786] covariance: [[6.31735632e-07]]
NJ [1.00274553] covariance: [[5.96350762e-07]]
NM [0.998517] covariance: [[5.51667553e-07]]
NV [0.99973574] covariance: [[6.30784457e-07]]
NY [1.00610397] covariance: [[5.95693371e-07]]
NYC [1.00804744] covariance: [[9.43046916e-07]]
OH [1.00111568] covariance: [[4.92666278e-07]]
OK [0.99950115] covariance: [[6.3174937e-07]]
OR [1.00489266] covariance: [[5.27983928e-07]]
PA [1.00239623] covariance: [[4.88906358e-07]]
PR [1.00664855] covariance: [[4.31129013e-07]]
PW [1.] covariance: [[inf]]
RI [0.99995525] covariance: [[8.25567281e-07]]
RMI [1.02720012] covariance: [[9.09718373e-06]]
SC [1.00269407] covariance: [[6.57884944e-07]]
SD [0.98631936] covariance: [[1.5841277e-06]]
TN [0.99833908] covariance: [[5.48592126e-07]]
TX [1.0007573] covariance: [[5.42582855e-07]]
UT [0.99601722] covariance: [[8.51804399e-07]]
VA [1.00361311] covariance: [[4.32461744e-07]]
VI [1.01295321] covariance: [[1.11862496e-06]]
VT [1.01087571] covariance: [[9.38959423e-07]]
WA [1.00523572] covariance: [[5.7118272e-07]]
WI [0.99286093] covariance: [[9.8984376e-07]]
WV [1.00342283] covariance: [[4.51261712e-07]]
WY [0.99427495] covariance: [[7.79427197e-07]]
0 [1.] covariance: [[0.]]

```

```

C:\Users\admin\anaconda3\lib\site-packages\scipy\optimize\minpack.py:828: OptimizWarning: Covariance of the parameters could not be estimated
  warnings.warn('Covariance of the parameters could not be estimated',

```

In []:

In []:

In [36]: *# Graphing sections:*

In [37]: tempHold = np.array(states.loc["DC"])
CDC = tempHold[:53]
print(CDC)

```
tempHold = states.loc["DC"]  
curr = tempHold.loc[51]
```

```
for j in range(53, third):  
    curr = curr * 1.005  
    CDC = np.append(CDC, curr)
```

```
print(CDC)
```

```
[0.000e+00 0.000e+00 0.000e+00 0.000e+00 0.000e+00 0.000e+00 0.000e+00  
2.000e+00 3.700e+01 1.920e+02 3.550e+02 8.540e+02 7.570e+02 1.009e+03  
9.000e+02 1.355e+03 1.123e+03 9.670e+02 8.550e+02 6.100e+02 5.210e+02  
3.100e+02 2.810e+02 2.370e+02 2.770e+02 3.840e+02 5.030e+02 4.700e+02  
4.440e+02 5.160e+02 3.950e+02 3.680e+02 3.550e+02 3.100e+02 3.560e+02  
3.070e+02 2.760e+02 3.710e+02 4.350e+02 3.660e+02 4.750e+02 6.280e+02  
7.780e+02 1.086e+03 1.051e+03 1.326e+03 2.012e+03 1.748e+03 1.624e+03  
1.532e+03 1.724e+03 2.118e+03 1.803e+03]  
[0.00000000e+00 0.00000000e+00 0.00000000e+00 0.00000000e+00  
0.00000000e+00 0.00000000e+00 0.00000000e+00 2.00000000e+00  
3.70000000e+01 1.92000000e+02 3.55000000e+02 8.54000000e+02  
7.57000000e+02 1.00900000e+03 9.00000000e+02 1.35500000e+03  
1.12300000e+03 9.67000000e+02 8.55000000e+02 6.10000000e+02  
5.21000000e+02 3.10000000e+02 2.81000000e+02 2.37000000e+02  
2.77000000e+02 3.84000000e+02 5.03000000e+02 4.70000000e+02  
4.44000000e+02 5.16000000e+02 3.95000000e+02 3.68000000e+02  
3.55000000e+02 3.10000000e+02 3.56000000e+02 3.07000000e+02  
2.76000000e+02 3.71000000e+02 4.35000000e+02 3.66000000e+02  
4.75000000e+02 6.28000000e+02 7.78000000e+02 1.08600000e+03  
1.05100000e+03 1.32600000e+03 2.01200000e+03 1.74800000e+03  
1.62400000e+03 1.53200000e+03 1.72400000e+03 2.11800000e+03  
1.80300000e+03 2.12859000e+03 2.13923295e+03 2.14992911e+03  
2.16067876e+03 2.17148215e+03 2.18233956e+03 2.19325126e+03  
2.20421752e+03 2.21523861e+03 2.22631480e+03 2.23744637e+03  
2.24863361e+03 2.25987677e+03 2.27117616e+03 2.28253204e+03  
2.29394470e+03 2.30541442e+03 2.31694149e+03 2.32852620e+03  
2.34016883e+03 2.35186968e+03 2.36362903e+03 2.37544717e+03  
2.38732441e+03 2.39926103e+03 2.41125733e+03 2.42331362e+03  
2.43543019e+03 2.44760734e+03 2.45984538e+03 2.47214460e+03  
2.48450533e+03 2.49692785e+03 2.50941249e+03 2.52195955e+03  
2.53456935e+03 2.54724220e+03 2.55997841e+03 2.57277830e+03  
2.58564219e+03 2.59857040e+03 2.61156326e+03 2.62462107e+03  
2.63774418e+03 2.65093290e+03 2.66418756e+03 2.67750850e+03  
2.69089604e+03 2.70435052e+03 2.71787228e+03 2.73146164e+03  
2.74511895e+03 2.75884454e+03 2.77263876e+03 2.78650196e+03  
2.80043447e+03 2.81443664e+03 2.82850882e+03 2.84265137e+03  
2.85686462e+03 2.87114895e+03 2.88550469e+03 2.89993221e+03  
2.91443188e+03 2.92900403e+03 2.94364906e+03 2.95836730e+03  
2.97315914e+03 2.98802493e+03 3.00296506e+03 3.01797988e+03  
3.03306978e+03 3.04823513e+03 3.06347631e+03 3.07879369e+03  
3.09418766e+03 3.10965859e+03 3.12520689e+03 3.14083292e+03  
3.15653709e+03 3.17231977e+03 3.18818137e+03 3.20412228e+03  
3.22014289e+03 3.23624360e+03 3.25242482e+03 3.26868695e+03]
```

```

3.28503038e+03 3.30145553e+03 3.31796281e+03 3.33455262e+03
3.35122539e+03 3.36798151e+03 3.38482142e+03 3.40174553e+03
3.41875426e+03 3.43584803e+03 3.45302727e+03 3.47029240e+03
3.48764387e+03 3.50508209e+03 3.52260750e+03 3.54022053e+03
3.55792164e+03 3.57571124e+03 3.59358980e+03 3.61155775e+03
3.62961554e+03 3.64776362e+03 3.66600243e+03 3.68433245e+03
3.70275411e+03]

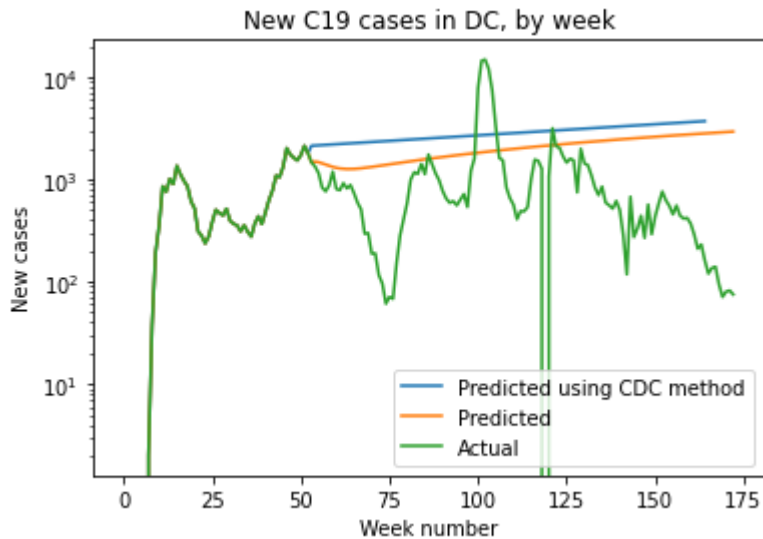
```

```

In [38]: fig = plt.figure()

plt.title("New C19 cases in DC, by week")
plt.plot(CDC, label = "Predicted using CDC method")
plt.plot(futureStates.loc[8], label = "Predicted")
plt.plot(states.loc["DC"], label = "Actual")
plt.yscale("log")
plt.ylabel("New cases")
plt.xlabel("Week number")
plt.legend()
plt.show()

```



```

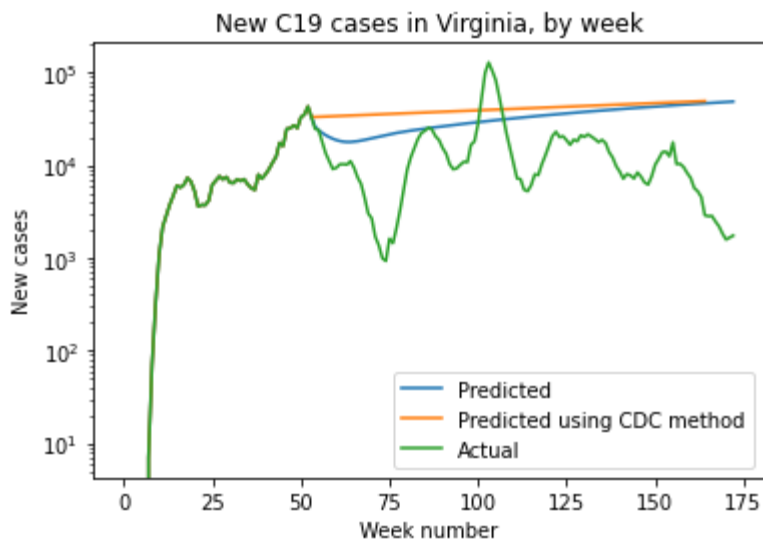
In [39]: fig = plt.figure()

tempHold = states.loc["VA"]
curr = tempHold.loc[53]
CDC = np.array(tempHold[:53] )

for j in range(53, third):
    curr = curr*1.0036
    CDC = np.append(CDC, curr)

plt.title("New C19 cases in Virginia, by week")
plt.plot(futureStates.loc[53], label = "Predicted")
plt.plot(CDC, label = "Predicted using CDC method")
plt.plot(states.loc["VA"], label = "Actual")
plt.yscale("log")
plt.ylabel("New cases")
plt.xlabel("Week number")
plt.legend()
plt.show()

```

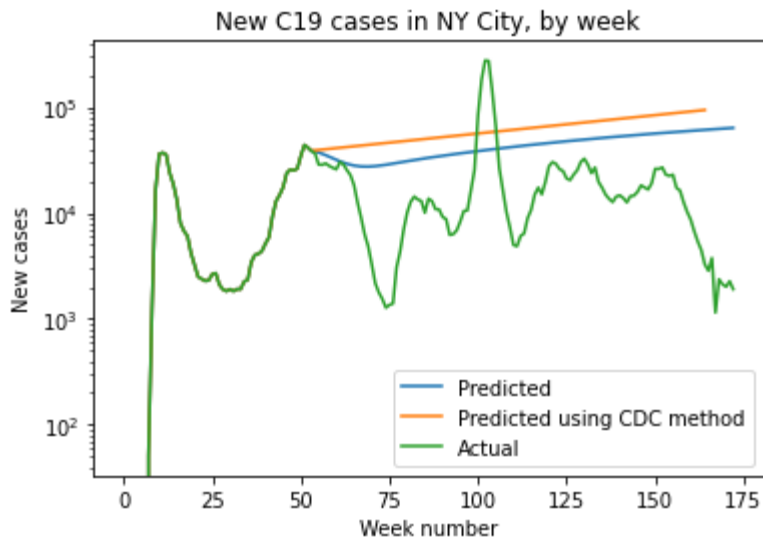



```
In [40]: fig = plt.figure()
prediction = futureStates.loc[39]
prediction = np.array(prediction)
t = 0

tempHold = states.loc["NYC"]
curr = tempHold.loc[53]
CDC = np.array(tempHold[:53] )

for j in range(53, third):
    curr = curr*1.008
    CDC = np.append(CDC, curr)

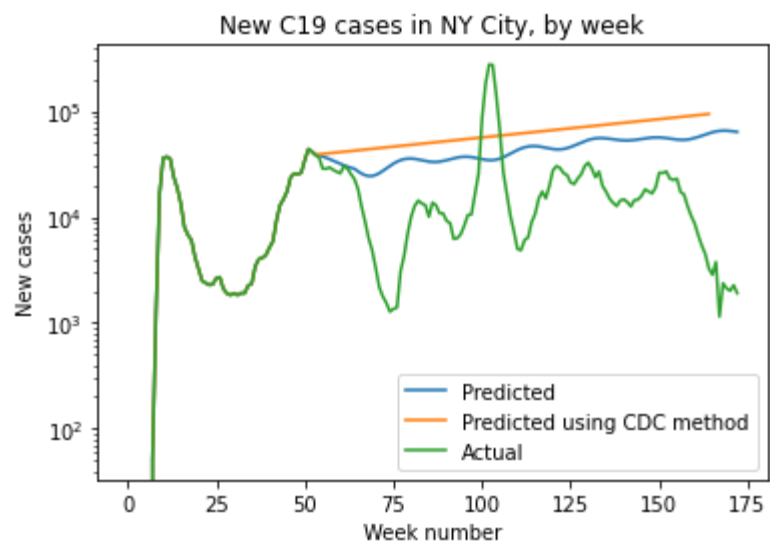
plt.title("New C19 cases in NY City, by week")
plt.plot(prediction, label = "Predicted")
plt.plot(CDC, label = "Predicted using CDC method")
plt.plot(states.loc["NYC"], label = "Actual")
plt.yscale("log")
plt.ylabel("New cases")
plt.xlabel("Week number")
plt.legend()
plt.show()
```



```
In [41]: fig = plt.figure()
prediction = futureStates.loc[39]
prediction = np.array(prediction)
t = 0

for j in prediction:
    t = t + 1
    if (t < 109): #interpolate forward an additional 109 weeks beyond 54.
        # amplitudes taken from table above, rounded to the nearest hundred
        addTo = 1100 * math.sin(2 * t * math.pi / 54.0)
        addTo = addTo - (800 * math.sin(2 * t * math.pi / 27.0) )
        addTo = addTo - (1400 * math.sin(2 * t * math.pi / 18.0) )
        addTo = addTo * 2
        # times two because a sine is both up and down, but here baseline is the trough
        prediction[64+t] = prediction[64+t] + addTo

plt.title("New C19 cases in NY City, by week")
plt.plot(prediction, label = "Predicted")
plt.plot(CDC, label = "Predicted using CDC method")
plt.plot(states.loc["NYC"], label = "Actual")
plt.yscale("log")
plt.ylabel("New cases")
plt.xlabel("Week number")
plt.legend()
plt.show()
```



```

In [53]: fig = plt.figure()
sumStates = np.array(1)
sumPredStates = np.array(1)

for t in futureStates:
    tempHold = np.sum(futureStates.iloc[:, t] )
    sumPredStates = np.append(sumPredStates, tempHold)

for t in states:
    tempHold = np.sum(states.iloc[:, t] )
    sumStates = np.append(sumStates, tempHold)

tempHold = sumStates
curr = sumStates[53]
CDC = np.array(tempHold[:53] )

for j in range(53, third):
    curr = curr * 1.00451355
    # this number is derived in the final cell of this workbook.
    CDC = np.append(CDC, curr)

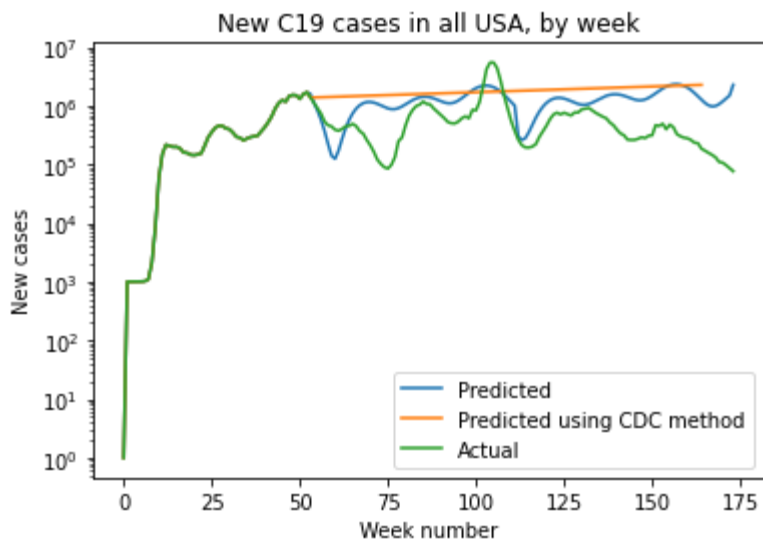
chaosNumb = sumPredStates.copy()

# accounting for waves
for t in range(53, 174): # sum of states' amplitudes, rounded to nearest thousand.
    addTo = -101000 * math.sin(2 * t * math.pi / 54.0)
    addTo = addTo - (150000 * math.sin(2 * t * math.pi / 27.0) )
    addTo = addTo - (184000 * math.sin(2 * t * math.pi / 18.0) )
    addTo = addTo * 2
    # times two because a sine is both up and down, but here baseline is the trough.
    chaosNumb[t] = chaosNumb[t] + addTo

# accounting for vaccination at t = 109
for t in range(112, maxTime):
    addTo = -10000
    durationStart = 112
    #vaccination of Omicron/Delta began at 112th week
    durationEnd = maxTime
    durationOfWithoutPulse = durationEnd - durationStart
    addTo = addTo * durationOfWithoutPulse
    # all at once as a pulse, instead of a cumulative duration effect because it's ec
    # still need the pulse active for the entire rest of t, anyway.
    chaosNumb[t] = chaosNumb[t] + addTo

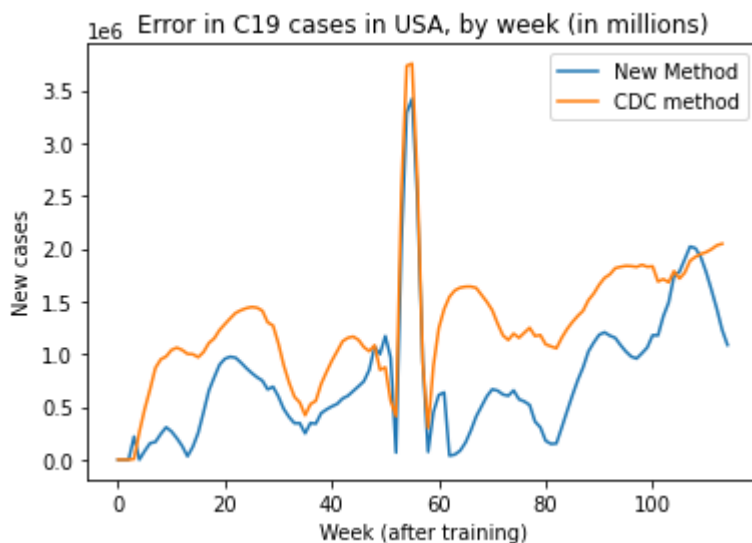
plt.title("New C19 cases in all USA, by week")
plt.plot(chaosNumb, label = "Predicted")
plt.plot(CDC, label = "Predicted using CDC method")
plt.plot(sumStates, label = "Actual")
plt.yscale("log")
plt.ylabel("New cases")
plt.xlabel("Week number")
plt.legend()
plt.show()

```



```
In [51]: fig = plt.figure()
tempHold = CDC[0:165] - sumStates[0:165]
CDCoff = tempHold[50:-1]
meOff = (chaosNumb - sumStates)[50:165]

plt.title("Error in C19 cases in USA, by week (in millions)")
plt.plot( abs(meOff), label = "New Method")
plt.plot( abs(CDCoff), label = "CDC method")
plt.ylabel("New cases")
plt.xlabel("Week (after training)")
plt.legend()
plt.show()
```



```
In [54]: million = 1000000

print("CDC error (in millions): ", sum( abs(CDCoff)[0:160])/million)
print("new method error (in millions): ", sum( abs(meOff)[0:160])/million)

CDC error (in millions): 146.93080645181885
new method error (in millions): 88.51721664252544
```

```
In [45]: print("End.")
```

End.

```
In [46]: # Bonus round
```

```
In [55]: startWeek = 40
stopWeek = 100
# giving it a stopweek of 100 so it still has 54 weeks of training

yVars = pd.DataFrame(sumStates[startWeek:stopWeek])
yVars = np.array(yVars).flatten()
constT = yVars[startWeek]
xVars = np.array(range(startWeek, stopWeek) )

tuples, covariance = sp.optimize.curve_fit(solver2, xVars, yVars, maxfev=2000)

print(s, tuples, "covariance: ", covariance)

0 [1.00451355] covariance: [[1.50433893e-06]]
```

```
In [ ]:
```

References:

1. Dettmer, P. (2021). Immune: A journey into the mysterious system that keeps you alive. Penguin Random House. New York. ISBN: 978-0-593-24131-8
2. Nohara, Y., & Manabe, T. (2022). Impact of human mobility and networking on spread of covid-19 at the time of the 1st and 2nd epidemic waves in Japan: An effective distance approach. PLOS ONE, 17(8). <https://doi.org/10.1371/journal.pone.0272996>
3. Brockmann, D., & Helbing, D. (2013). The hidden geometry of complex, network-driven contagion phenomena. Science, 342(6164), 1337–1342. <https://doi.org/10.1126/science.1245200>
4. Jacobs, R., Teunis, P., & van de Kasstele, J. (2020). Tracing the origin of food-borne disease outbreaks. Epidemiology, 31(3), 327–333. <https://doi.org/10.1097/ede.0000000000001169>
5. Pastore Y Piontti, A, Gomes Da Costa, M, Samay N, Perra N, Vespignani A, Ndro, A. (2014) the infection tree of global epidemics. Network Science, 2(1), 132–137.
<https://doi.org/10.1017/nws.2014.5>
http://journals.cambridge.org/article_S2050124214000058
6. Pinto, P. C., Thiran, P., & Vetterli, M. (2012). Locating the source of diffusion in large-scale networks. Physical Review Letters, 109(6). <https://doi.org/10.1103/physrevlett.109.068702>
7. Schlundt J, Toyofuku H, Jansen J, & Herbst S. A. (2004). Emerging food-borne zoonoses. Revue Scientifique Et Technique De L'OIE, 23(2), 513–533. <https://doi.org/10.20506/rst.23.2.1506>

8. May, R. M. (1976). Simple mathematical models with very complicated dynamics. *Nature*, 261(5560), 459–467. <https://doi.org/10.1038/261459a0>
9. Volterra, V. (1927). Fluctuations in the abundance of a species considered mathematically. *Nature*, 119(2983), 12–13. <https://doi.org/10.1038/119012b0>
10. Katie Gostic et al.; (2024). Technical Blog: Improving CDC’s Tools for Assessing Epidemic Growth. <https://www.cdc.gov/forecast-outbreak-analytics/about/technical-blog-rt.html>
11. Goncalves, B., Balcan, D., & Vespignani, A. (2013). Human mobility and the worldwide impact of intentional localized highly pathogenic virus release. *Sci Rep* 3, 810 (2013). <https://doi.org/10.1038/srep00810>
12. Miller, M. C., & Miller, J. M. (2015). The masses and spins of neutron stars and stellar-mass black holes. *Physics Reports*, 548, 1–34. <https://doi.org/10.1016/j.physrep.2014.09.003>
13. CDC, (2023) Ensemble model, <https://covid19forecasthub.org/doc/ensemble/>
14. Gleick, J. (1987). Chaos: Making a new science. Viking. ISBN: 0-670-81178-5
15. Ray, E. L., et al. (2023). Comparing trained and untrained probabilistic ensemble forecasts of covid-19 cases and deaths in the United States. *International Journal of Forecasting*, 39(3), 1366–1383. <https://doi.org/10.1016/j.ijforecast.2022.06.005>
16. Cramer, E. Y., Ray, et al. (2022). Evaluation of individual and ensemble probabilistic forecasts of covid-19 mortality in the United States. *Proceedings of the National Academy of Sciences*, 119(15). <https://doi.org/10.1073/pnas.2113561119>

17. Afzal, A., Saleel, C.A., Bhattacharyya, S. et al. (2022) Merits and Limitations of Mathematical Modeling and Computational Simulations in Mitigation of COVID-19 Pandemic: A Comprehensive Review. *Arch Computat Methods Eng* 29, 1311–1337 (2022). <https://doi.org/10.1007/s11831-021-09634-2>
18. Rahmandad, H., Xu, R., & Ghaffarzadegan, N. (2022). Enhancing long-term forecasting: Learning from covid-19 models. *PLOS Computational Biology*, 18(5).
<https://doi.org/10.1371/journal.pcbi.1010100>
19. Zhang, L., Tan, C., & Yu, F. (2017a). An improved rainbow table attack for long passwords. *Procedia Computer Science*, 107, 47–52. <https://doi.org/10.1016/j.procs.2017.03.054>